CHARACTERIZATION OF THE VACCINIA VIRUS ANKYRIN REPEAT PROTEIN K1 ON NF-KB INHIBITION AND ITS CONTRIBUTIONS TO VIRAL PATHOGENESIS

BY

ARIANA G. BRAVO

DISSERTATION

Submitted in partial fulfillment of the requirements
for the degree of Doctor of Philosophy in Microbiology
in the Graduate College of the
University of Illinois at Urbana-Champaign, 2017

Urbana, Illinois

Doctoral Committee:

Associate Professor Joanna Shisler, Chair
Professor Richard Tapping
Associate Professor Cari Vanderpool
Professor Steven Blanke

Abstract

All viruses strategically alter the anti-viral immune response to their benefit. The goal of this thesis was to examine how the vaccinia virus (VACV) K1 protein, which is encoded by the *K1L* gene, modulates the immune response *in vitro* and *in vivo*. *In vitro*, the K1 protein has multiple immunomodulatory effects in tissue culture models of infection. We have previously published that the K1 protein inhibits double-stranded RNA-dependent protein kinase (PKR) activation. A consequence of this function is that K1 inhibits PKR-induced NF-κB activation during VACV infection. However, transient expression of K1 also inhibits Toll-like receptor (TLR)-induced NF-κB activation. This suggested that K1 had a second NF-κB inhibitory mechanism that is PKR-independent. This possibility was explored by expressing K1 independently of infection and stimulating NF-κB under conditions that minimized or excluded PKR activation. Using these approaches, I found a second NF-κB inhibitory function for K1: K1 inhibited nuclear acetylation of the RelA (p65) subunit of NF-κB. Moreover, p65-CBP interactions were blocked in the presence of K1. However, K1 did not preclude NF-κB binding to oligonucleotides containing κB binding sites. This implies that NF-κB-promoter interactions still occurred in the presence of K1, but NF-κB cannot properly trigger transcriptional activation because K1 antagonizes acetylation of RelA. These data show that K1 has multiple mechanisms to inhibit NF-κB activation and, in comparison to all known VACV NF-κB inhibitory proteins, K1 acts at one of the most downstream events of NF-κB activation. A second goal of my thesis was to understand the contribution of K1 *in vivo*. I determined that a *K1L*-less vaccinia virus (vΔK1L) was less pathogenic than wild-type VACV in intranasal and intradermal models of infection. Decreased

pathogenicity correlated with diminished virus replication in intranasally-infected mice. However, in intradermally-inoculated ears, vΔK1L replicated to nearly identical levels as VACV, implying that the decreased immune response to vΔK1L infection, not virus replication, dictated lesion size. Several lines of evidence support this theory. First, vΔK1L induced slightly less edema than vK1L as revealed by histopathology and non-invasive quantitative ultrasound technology (QUS). Second, infiltrating immune cell populations were decreased in vΔK1L-infected ears. Third, cytokine and chemokine gene expression was decreased in vΔK1L-infected ears. While these results identified the biological basis for smaller lesions they remained puzzling: because K1 antagonizes NF-κB *in vitro*, anti-viral gene expression was expected to be higher during vΔK1L infection. Despite these diminished innate immune responses, vΔK1L vaccination induced a protective VACV-specific $CD8^+$ T cell response and protected against a lethal VACV challenge. Thus, vΔK1L is a unique construct that limits pathogenesis, yet still elicits protective immunity. We propose that continued studies of vΔK1L may uncover novel relationships between pathogenesis and immunity, information that has practical applications for vaccine design.

Acknowledgements

Throughout this journey, there were many individuals who contributed one way or another to help me obtain my doctorate and I would like to express my sincere gratitude.

First of all, I would like to thank my advisor, Dr. Joanna L. Shisler. I am extremely grateful for the opportunity to work in your laboratory. I would like to specifically thank you for your patience while teaching me how to design experiments, critically analyze data and relate my research to the bigger picture. At the same time, thank you for allowing me to be independent and to pursue my scientific interests. Thank you for all the afternoons of brainstorming, scientific conversations, conferences and your great enthusiasm, which was greatly needed when things were not going as planned. But most importantly, thank you for respecting my work-life balance.

To my lab mates, Lauren, Su, Melissa, Theresa, Aimee and Crystal. I am certain that I will never find such amazing coworkers. I cannot stress enough how crucial having such a great environment was to be able to finish my doctorate. You were the perfect balance between professionalism and friendship. Thank you for all the support and cheers. You brightened my days. When things were not going the best, you were my motivation to go to lab and be surrounded by such amazing and intelligent women. More than my labmates you became by best friends in Champaign and I take with me all the memories we made and hope that will continue to collect more.

To Dr. Ed Roy. You were always there to teach me everything about *in vivo* experiments. You became my second PI, as you were always available to help and answer questions. I would also like to thank Dr. Chris Brooke. In a little over a year I

learned a lot about how to be a good virologist and how to think outside of the box. You taught me how to trust my instincts and stick to what I think is correct. To Dr. Barbara Pilas from the flow cytometry facility; thank you for all your help designing and analyzing experiments. But also, thank you for encouraging me to pursue my career goals and for your empowerment as a successful woman in science.

To the Cena y Ciencias outreach program team and SACNAS; thank you for giving me the opportunity to serve as one of your leaders throughout so many years. It was a great experience for my professional development. Participating in such outreach helped me to discover my passion for science outreach and how I want to dedicate part of my scientific career to communicate science to the public.

To my Champaign family: Madeline, Manuel, María, Angela and Whitney; having a family away from home was fundamental. Thank you for all the fun and for being there for birthdays, holidays and all those nights when I needed to vent. Having such as support system always helped me to continue. I have no doubts that we will always have this special bond and I cannot wait to see all the great things you will achieve.

And last, but not least, to my family: Mami, Michelle, Abe, Titi and Madri. Gracias por siempre estar ahí aun en la distancia. Por todo el orgullo y el amor que siempre me han demostrado. Ese orgullo que sienten fue lo que muchas veces me motivó a seguir adelante para hacerlas sentir orgullosas una vez más. Esto es para ustedes.

Table of Contents

Chapter 1: Introduction

1.1 Viruses, evolution, and human health

Although excluded from the definition of life, viruses have and continue to influence the evolution of organisms from all domains of life. For example, viruses contributed to the development of the placenta; the mammalian *syncytin* gene is a retroviral *env* gene that was permanently recombined into the genome [71]. In addition, it is estimated that one-third of the adaptive mutations acquired by human proteins is a consequence of the arms race against viruses [27]. This demonstrates that viruses provide a constant pressure to their host. Despite this impact on diverse biological processes, viruses are mostly studied as causative agents of devastating diseases. One example is the variola virus (VARV), the causative agent of smallpox, which belongs to the *Poxviridae* family. Smallpox is the only human disease that has been declared eradicated. A myriad of viral diseases continue to be a threat to public health, and eradication of them by vaccination remains a grand challenge in human health. One key to combatting viruses is to understand how they evade the immune system. Our lab utilizes poxviruses as a model system to study virus-host interactions. Information gained from this system allows a better understanding of how viruses cause disease, which in turn aids in the development of vaccines and antivirals. The work in this thesis focuses on the modulation of the host immune system by the poxviral ankyrin repeat protein K1, which is encoded by vaccinia virus (VACV).

1.2 Poxviruses

Overview

The *Poxviridae* family consists of brick-shaped double-stranded DNA (dsDNA) viruses that infect a variety of hosts, from invertebrates to vertebrates [73]. Unique amongst DNA viruses, poxviruses replicate entirely in the cytoplasm of their host cell by encoding their own replication machinery. Although giant viruses such as Pandoravirus [81] and Pithovirus [2] have genomes of 2.5 megabase pairs (Mb) and 650 kilobase pairs (kb), respectively, poxviruses are still considered large viruses with genomes of approximately 200 kb and dumbbell shaped capsids of 360 x 270 x 250 nanometers (nm) [73].

Life cycle

The poxvirus life cycle is characterized by a cascade of gene expression: early, intermediate and late (Figure 1.1). The life cycle begins with the attachment of the virion to the host cell, followed by either direct fusion of the viral envelope with the plasma membrane [5] or by macropinocytosis [68], which allows the core to enter the cell. Although studies report that binding of the virion involves association with integrin β1 [50] and CD98 [91], a specific cell-host receptor that triggers fusion has not been yet identified [72]. Once the core is inside the cell, the class of early genes is transcribed and mRNA is synthesized within the core. The mRNAs are then translated into early proteins, including immune defense factors such as like the K1 protein (the focus of this thesis), enzymes needed for DNA replication, and transcription factors for intermediate gene transcription. Next, uncoating occurs, and the viral DNA is released and replicated in the

cytoplasm. The intermediate class of viral genes is then expressed and encodes for transcription factors that aid in the transcription of late genes [73]. Finally, the class of late genes is expressed which encodes early transcription factors and nonstructural proteins that will be encapsulated to form intracellular mature virions (IMVs). Some virions acquire a single Golgi or endoplasmic reticulum membrane and these are referred to as intracellular enveloped virions (IEVs) [74]). Then, they are transported by microtubules to the periphery where their membrane fuses with the plasma membrane resulting in exocytosis of extracellular enveloped virions (EEVs), which are efficient in cell-to-cell spread. In contrast, IMVs are released by cell lysis, are more stable and important for organism-to-organism transmission [73].

Poxviruses as human pathogens

There are several medically-relevant poxviruses. The most notorious poxvirus is the VARV, the causative agent of smallpox, which killed 300-500 million people worldwide [54]. Although smallpox was declared eradicated by the World Health Organization in 1980, other poxviruses are still relevant to the medical community. The molluscum contagiosum virus (MCV) is a poxvirus that infects children as well as sexually active adults [23]. MCV causes benign lesions (molluscum contagiosum; MC) that self-resolve within months after initial infection [83]. However, these lesions can persist for longer time periods in immunocompromised individuals, and this infection often develops into giant molluscum [60]. Monkeypox virus (MPXV) is closely related to VARV. MPXV can also infect humans and it can be transmitted from monkeys or other animal reservoirs to humans. MPXV causes a smallpox-like disease and is endemic in

several African countries [63]. It also caused an outbreak in the USA in 2003, when MPXV-infected prairie dogs were shipped from Africa to the USA, and infected prairie dogs bit and transmitted MPXV to 53 people [62]. Since human-to-human transmission of MPXV is not efficient, the outbreak was contained. However, close attention must be paid to MPXV as a continued potential threat to public health. The work of this thesis focuses on the VACV K1 protein. Interestingly, while MPXV expresses the K1 protein, neither VARV nor MCV does [22] [93]. This exemplifies that each poxvirus likely faces different immune system challenges, and as a result each poxvirus expresses its own arsenal of proteins to battle these challenges. Studying proteins such as K1 aids to understand the diverse challenges encountered by and countermeasures used by these closely-related viruses.

1.3 Vaccinia virus modulation of host innate immune responses

Vaccinia virus overview

Work in this thesis project characterizes the VACV K1 protein. VACV is the best-studied poxvirus. It was the first virus to be observed under the microscope, to be grown in cell culture, to be appropriately tittered, and to be purified and chemically analyzed [73]. In addition, VACV was used as the vaccine during the smallpox eradication campaign [54]. Originally, it was thought that cowpox virus (CPXV) was used as the smallpox vaccine and that VACV originated from CPXV. However, more recent studies now show that VACV origins trace back to horsepox virus (HSXV) instead of CPXV [82].

Despite the eradication of smallpox, VACV continues to be medically important for several reasons. First, the current smallpox vaccine, which is still delivered to military personnel due to the potential use of smallpox as a bioweapon, is sub-optimal. The current vaccine has an unacceptably high rate of morbidity and mortality, and can cause severe adverse effects in immunocompromised individuals. Second, due to its success as a vaccine, VACV is studied as a potential vaccine vector to protect against infectious diseases such as AIDS and as an oncolytic therapy for several cancers [88]. Moreover, VACV is used as a model organism to study host-pathogen interactions [96].

Approximately 20% of a poxvirus genome is devoted to coding for immune evasion proteins. VACV is no exception as it encodes multiple inhibitors of the host immune response. Examples of extracellular defense proteins that it encodes include: inhibitors of complement, chemokine and cytokine binding proteins, as well as secreted inhibitors of Natural Killer (NK) cells. VACV also encodes for intracellular inhibitors that target: pathogen recognition receptors, Nuclear Factor kappa B (NF-κB), Interferon Regulated Factors (IRFs), apoptosis and antigen presentation [96]. Interestingly, VACV not only encodes inhibitors for multiple cellular immune pathways, but it also encodes multiple proteins that target the same pathway. For example, two main cellular anti-viral responses are Protein Kinase R (PKR) and NF-κB activation. VACV encodes at least 3 and 10 proteins, respectively, to inhibit PKR and NF-κB [96]. These are discussed below. As described the VACV K1 protein inhibits both signaling pathways.

PKR

It is important to discuss PKR here because i) the K1 protein inhibits PKR activation [107, 108] and ii) PKR also activates NF-κB (Figure 1.2). The second chapter of this thesis uses multiple approaches to show that K1 inhibition of NF-κB is not due to K1 inhibition of PKR. Thus, to appreciate this work, one must understand PKR activation.

PKR is a serine/threonine kinase activated by dsRNA, a byproduct of poxvirus infection, [32]. The dsDNA genome of a poxvirus encodes genes on both the top and bottom strands of DNA. Transcripts of the top strand are described as going leftward to rightward, while transcription from the bottom strand is described as going rightward to leftward. During the transcription of poxvirus DNA, double-stranded RNAs (dsRNAs) are formed [20] when rightward and leftward transcripts overlap, and these dsRNAs could activate anti-viral cellular responses such as PKR [32]. PKR detects and binds to 30 bp dsRNA, and then PKR undergoes homodimerization and autophosphorylation at residues T446 and T451. Once activated, PKR phosphorylates eukaryotic translation initiator factor alpha 2 (eIF2α). As a result, host cell translation is halted as a mechanism to control viral replication [105]. It was originally thought that dsRNA was only formed during transcription of intermediate and late genes. However, work from our lab demonstrated that dsRNAs are also generated during transcription of early genes [107].

Interestingly, PKR was discovered due to the observation that IFN treatment of VACV-infected cells blocked virus mRNA translation. At the time it was known that dsRNAs are produced during VACV infection and prevent protein synthesis [31, 70]. It was hypothesized that a kinase was responsible for this response, which led to the search

and discovery of PKR [32]. This is an example of how the study of VACV allows the discovery of new aspects the of anti-viral immune response.

NF-κB

NF-κB is a transcription factor, initially identified as a nuclear protein bound to an enhancer element of the gene that encodes the kappa light chain of an immunoglobulin [92]. It is a master regulator of genes that control innate immune responses, apoptosis, inflammation, and oncogenesis [77]. NF-κB stimulates the inflammatory response by inducing pro-inflammatory gene expression and mediating the classical signs of inflammation: rubor, calor and dolor [9]. Five proteins belong to the NF-κB family: RelA (p65), NF-κB1 (p50), NF-κB2 (p52) c-Rel and RelB. These proteins form homodimers and heterodimers within the cell, and the best studied is the p65-p50 heterodimer. Inactive NF-κB is in the cytoplasm of every unstimulated cell because it is associated with one of its inhibitory factors: IκBα, IκBβ or IκBε [46]. The IκB proteins possess ankyrin repeat domains (ARDs), domains known for protein-protein interactions, and which mediate NF-κB-IκB interactions [49]. These interactions mask the nuclear localization signal of NF-κB, which keeps NF-κB in the cytoplasm during resting state [44].

In chapter 2 I evaluate how the K1 protein inhibits NF-κB activation. Here I describe the NF-κB signal transduction pathway, which can be stimulated by a variety of ligand-receptor interactions such as pathogen recognition receptor (e.g. LPS-Toll-like receptor (TLR) 4) and cytokine-receptor interactions such as TNF-TNFR [43]. Regardless of the stimuli, all signaling converges at the I kappa kinase (IKK) complex

[47]. Upon stimulation, the IKK complex phosphorylates IκBα, which leads to its polyubiquitination by the β–TrCP E3 ubiquitin ligase and subsequent proteasomal degradation [89]. As a result of IκBα degradation, the nuclear localization signal of NF-κB is exposed, and NF-κB translocates to the nucleus and activates the transcription of its target genes [44] (Figure 1.3).

NF-κB is present in every cell type, and it controls the expression of hundreds of genes. Thus, NF-κB activation needs to be tightly regulated. In addition to the regulation provided by members of the IκB family, post-translational modifications of NF-κB play a fundamental role in controlling the transcriptional activity. Acetylation, phosphorylation, methylation, and ubiquitination are examples of RelA post-translational modifications. The effect of each post-translational modification on the transcriptional activity of NF-κB is dependent on (i) the modification, (ii) the RelA residue affected (iii) and the source of stimulus [48]. For example, acetylation of residue K310 on RelA enhances the transcriptional activity of NF-κB by recruiting coactivators such as CBP/p300 [36]. In contrast, acetylation of K122 and K123 on RelA reduces transcriptional activity of NF-κB [52]. As discussed in chapter 2, I have found that the K1 protein prevents acetylation of RelA.

Vaccinia virus modulation of NF-κB

As with many viruses [56], poxviruses inhibit NF-κB activation [78]. The focus of this thesis was to determine how the K1 protein inhibits NF-κB activation. In addition to K1, VACV encodes at least nine other inhibitors of NF-κB: A46, A52, K7, B14, N1, C4, A49, M2, and E3 [11] [90] [18] [24] [26] [61] [34] [75] [94] (Figure 1.3). Each

protein uses a different mechanism to inhibit different NF-κB activation pathways. For example, A46 interacts with Toll-IL-1 receptor (TIR) domain-containing proteins to inhibit NF-κB from multiple inducers that trigger TLR-induced NF-κB activation [97]. A52 and K7 inhibit downstream of TLRs and IL-1 because they interact with IL-1 receptor-associated kinase (IRAK) 2 and tumor necrosis factor receptor-associated factor (TRAF) 6 [11, 76]. In contrast, B14 and N1 target the IKK complex [18] [24]. C4 inhibits at or downstream of IKK, but before p65 translocation [26]. M2 prevents NF-κB activation via an ERK2 pathway [34]. A49 employs molecular mimicry to β–TrCP substrates and sequesters the E3 ligase β–TrCP responsible for cellular IκBα ubiquitination [61]. In addition, it has been reported that E3 inhibits the expression of IL-6, TNF, IFN and inhibitin beta A (INHBA) via the NF-κB pathway [75]. Each of these poxviral inhibitors target NF-κB prior to nuclear translocation. In contrast, here I found that the K1 protein targets NF-κB in the nucleus. Recently, Summer *et al*. suggested that there is at least one more uncharacterized NF-κB inhibitor, demonstrating the complexity and importance of targeting this signaling pathway [99]. One would hypothesize that these protein inhibitors are redundant. However, as it will be discussed later in detail, deletion of any of these inhibitors results in a virus that is now attenuated in animal models of infection. I show here that this is also the case for the *K1L* gene: deletion of the *K1L* gene from a VACV results in a less virulent virus. This implies that each viral NF-κB inhibitory protein has unique functions that may be important for different host cell types.

1.4 The K1 protein

The K1 protein is encoded by the *K1L* gene. It is also referred as WR032 according to new poxvirus nomenclature. In this thesis, the traditional terminology will be employed. Thus *K1L* will be used. It is expressed as an early and intermediate gene during a VACV infection, and is a 32.5 kDa product [38]. The *K1L* gene is conserved within members of the Orthopoxvirus genus except that *K1L* is not present in camelpox virus and VARV [22, 41]. For VARV, the *K1L* gene contains a premature stop codon.

The K1 crystal structure was elucidated and revealed that it consists of nine ankyrin repeat domains (ARDs). While there are many other ARD-containing proteins expressed by poxviruses, K1 is unique amongst other orthologs because K1 lacks an F-box motif, a domain that other ARDs use to bind to E3 ligase complexes to execute their functions. Additionally, while most cellular ARD-containing proteins interact with functional binding partners by their concave surface, critical residues for the host range function of K1 (discussed later) are located on the convex surface of its structure [57], solidifying K1 as a unique ARD-containing protein.

K1's host range function

There are a family of poxvirus genes that are classified as host range genes. These are defined as genes that are required for virus replication [79]. The *K1L* gene is one such host range gene. This function of *K1L* was discovered in 1981, when Drillien *et al*. reported a VACV mutant that, unlike wild-type VACV, is unable to replicate in most human cell lines [25]. This mutant virus has an 18 kb deletion. Later, Gillard *et al*. identified that the *K1L* gene is the minimal region to rescue the replication of this virus

[38]. Thus, *K1L* is a host range gene. The *K1L* host range is slightly different for human versus rabbit cell lines. While the restriction is characterized by a shutdown of both early viral and cellular protein synthesis during infection in rabbit cell lines, this restriction occurs during intermediate protein synthesis in human cell lines. [79]. In addition, in human cell lines, insertion of *C7L* can rescue virus replication of a VACV lacking the *K1L* gene (vΔK1L), indicating that the K1 and C7 proteins have homologous host range function. However, in rabbit cell lines, insertion of the *C7L* gene can not rescue viral replication of vΔK1L, thus the *K1L* gene is required for virus replication [80]. In this thesis, I evaluated the host range phenotype in murine cells of VACV lacking just the *K1L* gene or both *K1L* and *C7L* genes (ΔK1LΔC7L) as both animal models of infection are in mice.

There is great interest in understanding the host range mechanism for K1: solving this puzzle provides potential means to control virus replication and perhaps control poxvirus pathogenesis. In a cellular genome-wide siRNA screening, sterile alpha motif domain containing 9 (SAMD9) was found to have a role in preventing ΔK1LΔC7L replication in human cells [95]. Liu and McFadden reported that SAMD9 is an anti-viral stress response element that aids in the formation of anti-viral granules [58]. While wild-type myxoma virus (MYXM) or VACV blocks formation of SAMD9-mediated granules, MYXM lacking the *M062R* gene (ΔM062) or ΔK1LΔC7L induce anti-viral granules during infection. Moreover, viral replication of ΔM062 and ΔK1LΔC7L was rescued in SAMD9 knockdown cell lines and no anti-viral granules were formed. While M062 antagonizes SAMD9 by direct interaction which results in sequestration and redistribution of SAMD9, the mechanism employed by K1 or C7 to antagonize SAMD9

and promote viral replication remains to be determined. It has been shown that both K1 and C7 proteins interact with SAMD9 [95], however, the relevance of these interactions remains unclear. Interestingly, SAMD9 can be induced by interferon (IFN) and interferon-regulated factor 1 (IRF-1), and the K1 protein inhibits IFN and IRF-1 mediated genes [66]. One hypothesis is that K1 antagonistic function of SAMD9 is dependent on its INF or IRF-1 inhibitory function.

Interestingly, ΔK1LΔC7L is also replication-deficient in mouse cells [65]. However, SAMD9 is not expressed in mouse cells, suggesting that there are additional cellular factors involved in this host-range restriction. Indeed, the siRNA screening also revealed that WD repeat-containing protein 6 (WDR6) and the methyltransferase FTSJ1 also have roles in restricting replication of ΔK1LΔC7L [95].

Binding partners of K1

ARDs are motifs that allow protein-protein interactions. Thus, one hypothesis is that K1 mediates its effects (e.g. host range function or NF-κB inhibition) by binding to viral or cellular partners. In addition to SAMD9 [95], K1 has been found to interact with VACV protein C10 [64]. K1 has also been found to co-immunoprecipitate with cellular GTPase ACAP2 [12]. However, K1's host range function is independent of its interactions with ACAP2 as K1 mutants unable to bind to ACAP have no effect on VACV replication and vice versa [67]. The biological relevance of these K1-mediated interactions remains to be elucidated. I also show here that K1 binds to the RelA subunit of NF-κB. However, whether this interaction is relevant for host range or for NF-κB inhibition remains to be determined.

PKR inhibition by the K1 protein

In our lab, it was discovered that the K1 protein inhibits PKR activation [107, 108]. First, it was observed that in the presence of K1, VACV inhibited phosphorylation of both PKR and eIF2α [108]. In further studies, our lab also found that the K1 protein prevented early and intermediate dsRNA formation in RK13 and HeLa cells, respectively [107]. Thus during VACV infection K1 prevents the formation of dsRNA to prevent PKR activation. Originally it was hypothesized that PKR inhibition was K1's host range function as K1 mutants that no longer support viral replication are also defective on inhibiting PKR activation. However, knockdown of PKR does not rescue viral replication of ΔK1LΔC7L. Thus inhibition of PKR is not K1's host range function [108].

The mechanism by which the K1 protein inhibits dsRNA formation remains unclear. One hypothesis is that the K1 protein acts as a facilitator of translation; as a consequence, when the K1 protein is absent, an abundant amount of mRNA is present. Several studies support this hypothesis: i) in RK13 or HeLa cells infected with ΔK1L, only early or intermediate gene transcription occurs and ii) these early gene transcripts are detected for longer time periods in ΔK1L-infected cells compared to wild-type VACV. This accumulation of mRNAs could trigger the formation of dsRNA that could activate PKR [107]. Further studies are required to elucidate how the K1 protein could promote mRNA translation.

Inhibition of NF-κB by the K1 protein

In 2004, our lab published that K1 protein inhibits IκBα degradation during virus infection [94]. First, in RK13 and HeLa cells, Modified Vaccinia virus Ankara (MVA),

which lacks *K1L*, induces NF-κB driven luciferase transcription and IκBα degradation, while MVA/K1L does not. Also, RK13 ΔK1L-infected cells show IκBα degradation. Later studies identified that one mechanism for the K1 protein to inhibit NF-κB activation was by preventing PKR activation since mutants that no longer inhibit PKR are also unable to inhibit NF-κB [107]. In addition, NF-κB activation does not occur in PKR^{KD} cells, indicating that during VACV infection, PKR is an activator of NF-κB [107]. PKR has been shown to activate NF-κB by interacting with the IKK complex [109], the kinase responsible for IκBα degradation. Thus the degradation of IκBα in ΔK1L infected cells is due to activation of the IKK complex by PKR (Figure 1.2). However, data from our lab and others [4] suggested that K1 possesses a PKR-independent mechanism to inhibit NF-κB activation. Work in this thesis evaluated this hypothesis, which proved correct and data are shown in chapter 2.

1.5 Vaccinia virus animal models of infection

As mentioned earlier, VACV encodes multiple immune evasion proteins that target a myriad of cellular signaling pathways [96]. Studying these proteins and their molecular mechanisms of action is important for understanding viral pathogenesis and developing therapeutics. While cell culture systems are facile means to discover and study these viral immunomodulators, they cannot be used to understand how immune evasion molecules dictate severity of infection. There are several VACV animal models of infection that allow such questions to be answered. The poxvirus field utilizes different routes of inoculation: intranasal, intradermal, intracranial, footpad, intraperitoneal, intravenous and subcutaneous. Each route has advantages and

disadvantages. Here I will describe two of these inoculation routes, intradermal and intranasal, which were used to study the role of the K1 protein *in vivo*. They were chosen for several reasons. First, these are the two most widely used VACV animal models to study the contribution of VACV proteins to pathogenesis. Second, these models utilize the most natural routes of inoculation with ectromelia virus and VACV or during human vaccination. Third, the intranasal and intradermal routes mimic a systemic disease (like smallpox) and a dermal vaccination, respectively. This will allow us to better understand the pathogenesis of smallpox-like diseases as well as the immune response to vaccination with VACV, which is a potential vaccine vector for several diseases.

Intranasal model

Intranasal inoculation (IN) of mice with VACV results in an acute infection of the lower respiratory tract [86] [106]. Although this route of inoculation does not cause skin lesions like smallpox, IN infection with VACV mimics a smallpox infection in that it also causes a systemic disease. After an IN inoculation, the primary site of viral replication is the lungs. Since VACV western reserve (WR) strain is neurovirulent, VACV next spreads to the brain of infected mice [15]. Then, the virus disseminates to other organs such as the liver, kidney, spleens and ovaries [84]. The disease progression is monitored by assessing: i) weight changes, ii) clinical signs of illness such as conjunctivitis, fur ruffling, arched backs, difficulty breathing, moving and socializing and iii) virus titers of organs including lungs, brains, livers, spleens and ovaries [106].

The immune response during IN infection is well-characterized. As early as 24 hours post-infection, cytokines and chemokines such as IL-2, IL-6, TNFα, CXCL9, and

CXCL10 are expressed in the lungs [98]. By 48 hours post-infection, there is a significant increase in the number of cells in bronchoalveolar lavage fluids. These cells include macrophages, neutrophils, natural killer (NK) cells, and lymphocytes such as CD8+ and CD4+ T cells [84]. Macrophages and dendritic cells have been shown to drive the early innate response against VACV [10, 87]. Ultimately, $CD8^+$ T cells protect against death via the secretion of IFN-γ [39, 40]. This response is sufficient to protect mice in the absence of $CD4^+$ T cells and B cells [39]. More recently, NK cells have been reported to be the primary producers of IFN-γ in the lungs prior to the infiltration of $CD8^+$ T cells and also contribute to protection against a respiratory infection with VACV [1].

Intradermal model

The intradermal model (ID) of infection was developed as an alternative to the IN route of infection [102]. This model is characterized by a highly localized infection, where lesions in the ears are formed and no signs of systemic illness are observed. As such, ID infection is a model that more closely represents smallpox vaccination or lesion formation that occurs during smallpox infection. It consists of inoculating mice in the ear pinna with VACV. An ear lesion develops about 5-7 days post-infection and the lesion grows in size until 12 days post infection. The lesion size decreases during the next 12-14 days and scabbing forms.

Mice are routinely inoculated with 10^2 or 10^4 PFU of virus. Interestingly, the amount of inoculum correlates with the lesion size: the lower the inoculum size, the smaller the lesion. Regardless, virus replication kinetics are similar for both doses, and the peak in virus titers in the ear is observed at day 5, regardless of the inoculum dose.

One explanation for this phenomenon could be that the number of host cells available for infection in the dermal layer of the ear is limited. Thus, a low dose of virus reaches this limit [101]. Regardless of the dose, viral titers peak at five days post-infection, plateau and then viral titers start to decrease approximately 11-12 days post-infection.

The localized immune response to an ID infection with VACV virus is well-known. This characterization was performed by examining the inflammatory response and infiltration of immune cells to the ear pinna longitudinally after infection. There is minimal inflammation and cellular infiltration three days post-infection. Then, there is an influx of classical inflammatory monocytes ($CD11c^{-}$ $Ly6c^{HI}$ $Ly6g^{-}$) and this population peaks at day five post infection [29]. Macrophages are also recruited by day 3 post-infection. A variety of cytokines and chemokines are induced, with CXCL9 and CXCL10 being the most predominant at day 5 post-infection [45]. Then, the development of lesions is observed as well as the entry of tissue-protective unconventional neutrophils ($CD11b^{+}$ $Lyg6^{+}$), which are attracted by unknown mechanisms. These cells outnumber the inflammatory monocytes by day seven and produce large amounts of Type I IFNs and reactive oxygen species (ROS). Depletion of these cells results in an increase in tissue damage, showing that these cells are tissue protective [29]. The number of lymphocytes gradually increases up to 17 days post infection, with peaks around days 9-11 post-infection. The spread and replication of VACV in this model is controlled by phagocytes [29] [84] [51].

Vaccinia virus virulence factors

The use of the IN and ID models of infection has allowed the identification of dozens of VACV proteins that play a role in virus virulence [96]. Curiously, the deletion of some genes (e.g. *B18R*, *C6L*, *F1L*) [35, 100, 103] decreases the virulence of a virus compared to wild-type VACV, while the deletion of other genes (e.g. *A41L*, *B15R*, *169R*) [3, 19, 98] increases the virulence of the virus during IN infection. Similar unpredictability occurs in the ID model of infection. To date, the field does not understand the reason for these different outcomes. In an attempt to understand this, studies have examined if there are differences in viral titer or cell recruitment to an area of infection when a gene of interest is present or absent from the virus. Below is a summary of virulence factors found during VACV intranasal and intradermal infections, focusing on those that inhibit the NF-κB signal transduction pathway (Table 1.1).

Vaccinia virus NF-κB inhibitors as virulence factors during intranasal infection

As mentioned earlier, VACV encodes at least ten intracellular inhibitors of NF-κB and these inhibitors have non-redundant functions *in vivo* [96]. With the exception of K1 and M2, the effects of removing each of these proteins have been examined *in vivo*. Deletion of *A46R*, *A49R, A52R*, *C4L*, *K7R*, *E3L* or *N1L* results in a virus that has decreased virulence, as measured by decreased weight loss and signs of illness when using the IN route of infection. In contrast, deletion of *B14R* has no effect on virus virulence in this IN model of infection [61, 97] [42] [26] [8, 13] [6].

When examining viral replication in the primary site of infection (lungs), wild-type VACV and mutant viruses ΔA49R, ΔC4L, and ΔK7R replicate to equal levels at

early times (2 days) post-infection. However, by day 5 post infection, the titers of mutants viruses are much lower than that of wild-type VACV [61] [26] [8]. In the case of ΔC4L infection, this decrease in virus replication correlates with an increase in the number of total immune cells in the bronchoalveolar fluids (BAL) at day 5 post-infection [26]. These data suggest that deletion of a VACV NF-κB inhibitor results in an increase in the number of immune cells to the site of infection, which may result in the decrease in viral titers at later time post-infection.

Different results were observed when examining the lungs of ΔK7R-infected mice, which implies that each viral NF-κB inhibitory protein has unique physiological roles. During ΔK7R infection, there is no significant difference in the number of total immune cells infiltrating the lungs [8]. However, there is a higher proportion of cells expressing CD45, a leukocyte marker, as compared to cells observed in lungs from VACV-infected mice. The percentage of NK cells, $CD8^+$ T cells, and $CD4^+$ T cells is also higher during ΔK7R infection than wild-type VACV infection. Although infection with ΔK7R results in less recruitment of neutrophils compared to wild-type VACV, there is an enhanced MHC class II expression by macrophages. Moreover, NK cells and VACV specific CD8+ T cells from the lungs ΔK7R-infected mice have enhanced cytolytic properties as compared to those from VACV-infected mice.

Although the VACV proteins discussed above inhibit NF-κB in cell culture, little is known about the link between their NF-κB inhibitory function and their contributions to VACV pathogenesis. Only one study has linked these two subject areas. The VACV N1 protein inhibits both apoptosis and NF-κB [24] [21]. Maluquer de Montes *et al*. created a panel of mutant N1 proteins that inhibited either apoptosis or NF-κB, and

reported that an infection with viruses expressing an N1 impaired from inhibiting NF-κB activation results in an attenuated infection, while a mutant N1 unable to inhibit apoptosis remains as virulent as wild-type VACV [59]. This shows that the NF-κB inhibitory function is critical for VACV pathogenesis. More studies are needed to understand the effects of removing a VACV NF-κB inhibitor regarding virulence. In this thesis project, I characterized the effects of removing one VACV inhibitor of NF-κB, K1, during an *in vivo* infection. Studying the effects of removing each of these proteins will shed light on why VACV encodes multiple inhibitors of the same signaling pathway.

Vaccinia virus PKR inhibitors as virulence factors during intranasal infection

Although the K1 protein inhibits NF-κB activation, it also inhibits PKR [107, 108]. The VACV *E3L* and *K3L* genes also encode for proteins that inhibit PKR in tissue culture [7, 16]. A group of studies asked how each PKR inhibitory gene affects virus virulence. It was interesting to observe that each virus had different properties with respect to virulence, suggesting that the E3 and K3 proteins are not redundant *in vivo*. For example, ΔE3L is attenuated in both intracranial and intranasal models of infection. This attenuation is partially resolved by deleting both PKR and RNAseL from the host, but very little when only PKR is absent [86]. In contrast, intranasal ΔK3L infection retains virulence because mice infected with ΔK3L have a similar weight loss as VACV infection. ΔK3L replicates in the lungs to levels similar to VACV, and this is likely one reason for the observed weight loss. However, unlike VACV, ΔK3L infection does not spread to other organs. Interestingly, the *K3L* mediated viral dissemination was independent of PKR [86]. Thus, K3 and E3 likely target different host cell types or

modulate PKR activation at different times post-infection. K1 is the third VACV protein shown to inhibit PKR *in vitro*. However, the role of K1 in virus virulence remains unknown, and this was the goal of chapter 3.

Vaccinia virus NF-κB inhibitors as virulence factors during intradermal infection

Several studies have examined the effects of removing a single VACV NF-κB antagonist on viral pathogenesis, using the ID inoculation route. IN and ID inoculations are not equivalent systems because some VACV mutants are attenuated in the IN model but not in the ID model. This is the case for the ΔC4L and ΔA49R viruses; while deletion of each of these genes results in fewer signs of illness in the intranasal infection, no differences are observed in lesions sizes compared to wild-type VACV [26, 61]. Conversely, there are some mutant VACV viruses that (ΔB14) in which the mutant virus is equally pathogenic as VACV via the IN route of inoculation, but induce smaller lesions during ID infection.

When the number of immune cells was investigated, macrophages and T cells are higher in ears infected with ΔB14R at eight days post infection. Similar to what has been observed with other inhibitors of NF-κB in the IN model, there are no differences in viral titers at early time post infections. However, at day 11 post-infection, there is less viral replication of ΔB14R in the ears of infected mice. In addition, the number of total cells during ΔB14R infection is higher. The percentage of neutrophils is lower at eight days post-infection in ΔB14R infected ears, while the percentage of macrophages and lymphocytes were slightly higher [17].

Several inhibitors of NF-κB contribute to VACV pathogenesis in both models of infection. For example, deletion of either *K7L* or *N1L* results in decreased clinical signs of illness during IN infection and smaller ear lesions during ID infection compared to wild-type VACV [8] [6].

1.6 Vaccinia virus as a vaccine

As mentioned previously, besides being an excellent model to study host-viral interactions, VACV is well known for its immunogenicity. The success of the smallpox eradication campaign is partly attributed to the use of VACV as a vaccine [28]. Although VACV is immunogenic, vaccination with VACV can result in several adverse effects such as generalized vaccinia, eczema vaccinatum, vaccinia keratitis, progressive vaccinia, and post-vaccinia encephalitis [55]. These side effects are more common in immunocompromised individuals. Despite smallpox eradication in 1980, smallpox is still a concern as it could be used as a bioweapon. Thus, military personnel are required to get a smallpox vaccination. The unacceptably high levels of morbidity and mortality in the armed forces who receive this vaccine is one reason to improve on the current smallpox vaccine.

In addition to its use as the smallpox vaccine, VACV is being exploited as a potential vaccine vector to protect against other types of infectious diseases such as HIV and other viral, bacterial and parasitic infectious diseases. To this end, VACV is engineered to express antigenic genes from pathogens and the benefit to this approach is that heterologous gene products are expressed intracellularly, increasing the likelihood

that the heterologous protein will be expressed and presented by MHC I and MHC II molecules [88].

Finally, several labs use VACV as an oncolytic therapeutic. VACV is modified in a manner that infects and lyses tumor cells but not healthy cells. This approach has been used to target several types of cancer including liver, skin and colorectal cancers [53].

Modifications to vaccinia virus to increase safety and immunogenicity

As mentioned earlier, VACV vaccination has detrimental effects. Thus a safer, but equally immunogenic VACV is needed for vaccines and oncolytic viruses. Multiple labs have developed VACV that are attenuated, including MVA [37, 104]. These viruses lack multiple immune evasion genes that are otherwise present in wild-type VACV. Unfortunately, while these third-generation vaccines are safe, they are not appropriately immunogenic, and several boosters are required to get appropriate levels of protective immunization [30, 69]. Several labs have attempted to increase the immunogenicity of MVA by re-inserting genes from wild-type poxviruses into MVA to increase immunogenicity or deleting genes from wild-type poxviruses, such as VACV, to make them safer [33]. One example of removing a protein from VACV to increase its safety and immunogenicity is the deletion of N1, an inhibitor of NF-κB. Deletion of N1 resulted not only in an attenuated virus in both intranasal and intradermal models of infection, but also there was enhanced $CD8^+$ T cell memory. These effects were dependent on N1's NF-κB inhibitory function [85].

A constant debate in the poxvirus field is to determine what is the nature of VACV virus immunogenicity. Some attribute VACV immunogenicity to its modulation

of the immune system while others attribute it to its replication competency. Work in this thesis evaluated the effects of removing K1 in VACV immunogenicity while aiming to clarify which attribute of VACV is crucial for its success as a vaccine.

1.7 Thesis outline

The goal of this thesis project was to characterize the mechanism by which the K1 protein inhibits NF-κB activation as well as to determine its contributions to VACV pathogenesis. I hypothesized that K1 possessed the ability to inhibit the NF-κB pathway directly and that it acts as a virulence factor.

Chapter 2 describes a novel mechanism by which the K1 protein inhibits NF-κB activation [14]. Initially, it was believed that K1 inhibited NF-κB solely by inhibiting PKR activation [107], which is upstream of IκBα degradation [109]. However, I found evidence that indicates that the K1 protein has a PKR-independent mechanism where it allows IκBα degradation, RelA nuclear translocation, and RelA-DNA interactions [14]. However, acetylation of RelA at lysine 310 was inhibited by K1. In addition, RelA-CBP interactions were impaired in the presence of the K1 protein [14]. The identification of this novel mechanism was possible when the K1 protein was studied independently of viral infection.

Although the K1 protein was discovered over 30 years ago, the contributions of K1 to VACV pathogenesis was not known. In Chapter 3 I characterized the effects of removing K1 on virulence utilizing the intranasal and intradermal models of infection. I found that the K1 protein is a virulence factor. I discovered that, while removing K1 had no effect on viral replication *in vitro*, mice showed fewer signs of illness compared to

wild-type VACV when introduced via the IN route. In addition, ΔK1L had decreased replication in the lungs and other visceral organs. In the ID model, mice infected with ΔK1L showed smaller ear lesions. ΔK1L showed similar titers but a decrease in the inflammatory response. Despite this, ΔK1L provided equal protection as wild-type VACV to a lethal challenge suggesting that VACV immunogenicity is due to its replication competency.

Chapter 4 describes the efforts to elucidate the contributions of K1's ARDs on NF-κB inhibition. This was the original scope of this thesis project. I have found that K1 is not only structurally similar to IκBα, but it also co-immunoprecipitates with NF-κB. *K1L* mutants lacking one or two ARDs were cloned from viruses into a mammalian vector to study the contribution, if any, of each ARD. Although the mutants have yet to be tested, work on this chapter made available the tools to determine if NF-κB-K1 interactions are relevant to NF-κB inhibition.

Chapter 5 includes a summation of the findings in this thesis project as well as future directions that should be approached. While the initial goal of my project was to determine the relevance of K1's ARDs on NF-κB inhibition, the outcome of my studies revealed a previously uncharacterized mechanism for NF-κB inhibition. In addition, these are the first studies that investigate K1 *in vivo* and revealed that a VACV lacking K1 has a unique phenotype compared to other mutant VACVs lacking NF-κB or PKR inhibitors. This shows that each of these proteins is crucial for VACV pathogenesis and re-emphasizes the complexity of host-viral interactions. These findings open a new window for how VACV and other viruses modulate the host immune response and help to understand viral pathogenesis as well as to develop novel therapeutics.

1.8 Figures and Table

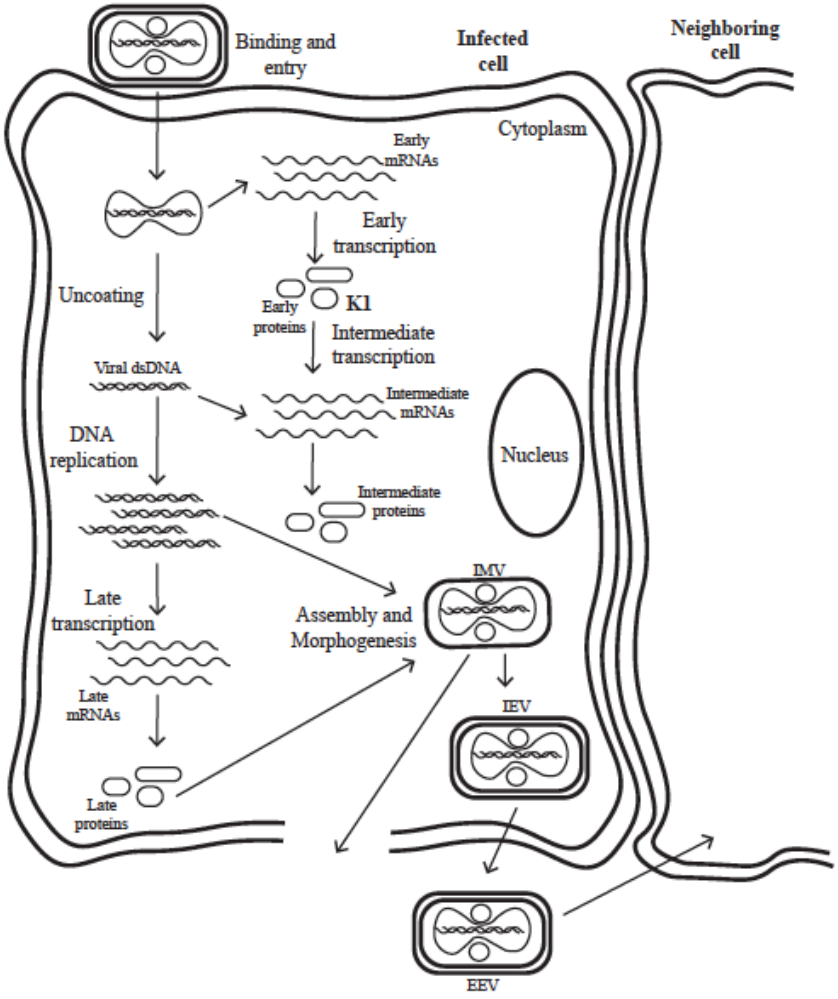

Figure 1.1 Poxvirus life cycle. Poxviruses bind and enter the host cell, then early mRNAs and proteins are made. Next, uncoating occurs followed by viral genome replication. Then transcription and translation of intermediate and late proteins occur followed by assembly and morphogenesis of intracellular mature virions (IMV). Intracellular enveloped virions (IEV) acquire an additional membrane and release of extracellular mature virions (EEV) occur, which can infect neighboring cells.

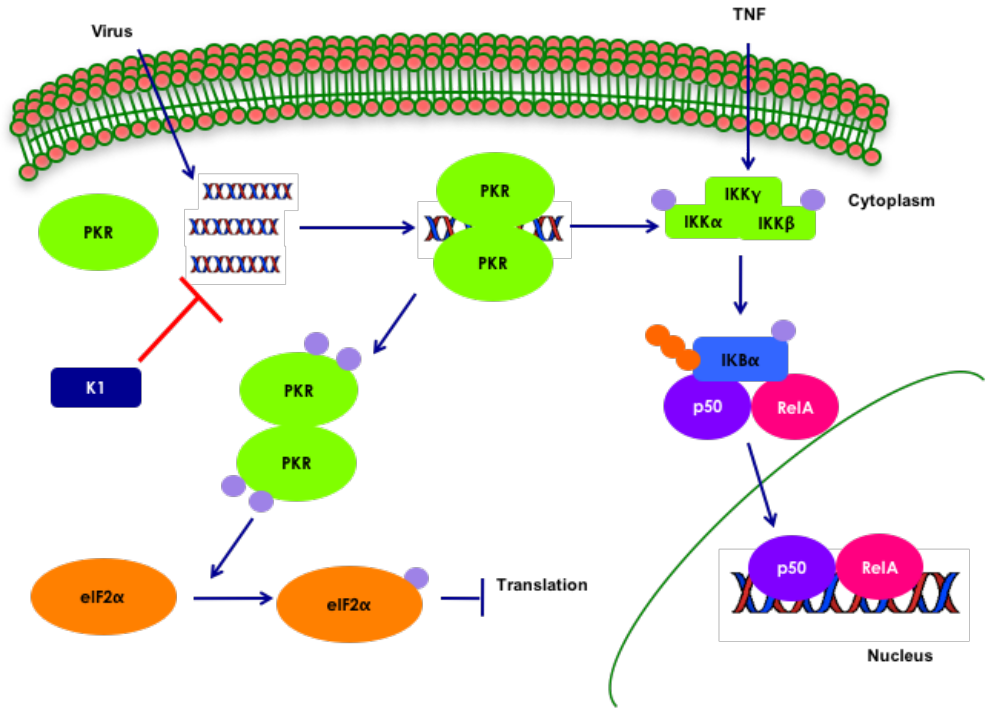

Figure 1.2 PKR mediated activation of NF-κB during vaccinia virus infection. Transcription of vaccinia virus' mRNAs results in dsRNA formation. Monomeric protein kinase R (PKR) binds to dsRNAs, which triggers its dimerization and autophosphorylation. Once phosphorylated, PKR phosphorylates eukaryotic initiation factor 2 alpha (eIF2α), which results in a halt of protein translation. In addition, PKR can activate nuclear factor kappa b (NF-κB) via interactions with the I kappa kinase (IKK) complex. Activation of NF-κB results in the transcription of pro-inflammatory genes.

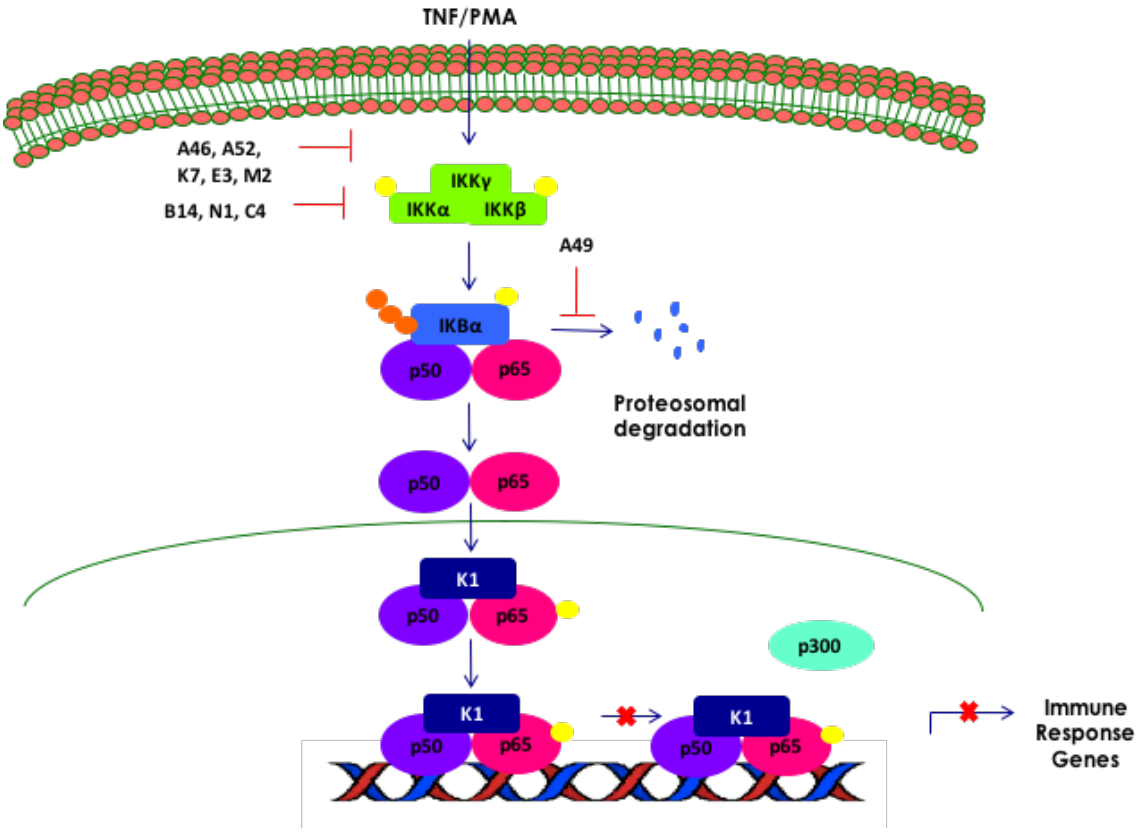

Figure 1.3 NF-κB signaling pathway is modulated by vaccinia virus proteins. Upon stimulation, the IKK complex phosphorylates IκBα, which leads to its polyubiquitination and subsequent proteasomal degradation. As a result of IκBα degradation, the nuclear localization signal of NF-κB (p65 and p50) is exposed, and NF-κB translocates to the nucleus. In the nucleus, NF-κB interacts with CBP/p300 and undergoes acetylation. Then, transcriptionally active NF-κB drives the transcription of immune response genes. Vaccinia virus encodes 10 inhibitors of NF-κB: A46, A49, A52, B14, C4, E3, K1, K7, M2, and N1.

Table 1.1 Effects of individually removing each of the ten VACV NF-κB inhibitors.

NF-κB Inhibitor	Intranasal Model (IN)	Intradermal Model (ID)	Effects of deleting NF-κB inhibitor
A46 (Also inhibits IRF3)	Attenuated	ND	• More total cells are recruited to the lungs at day 2 post-infection, while less total cells are found at days 5 and 8 post-infection. • Increased immunogenicity.
A49	Attenuated	No phenotype	• No differences in viral titers at day 2 post infection. Decreased replication at days 5 and 7 post-infection.
A52	Attenuated	ND	ND
B14	No phenotype	Attenuated	• No differences in viral titers at day 2 post infection. Decreased replication at days 5, 7, and 11 post-infection. • More total cells recruited at day 11 post-infection. • Decreased percentage of neutrophils at day 8 post-infection, but macrophages and lymphocytes have slightly higher percentage. • No differences in the absolute number of neutrophils, $CD4^+$, $CD8^+$, and γδ T cells, but increased number of macrophages and lymphocytes.
C4	Attenuated	No phenotype	• No differences in viral titers at day 2 post-infection. Decreased replication at days 5 and 8 post-infection. • Significantly more cells in BALs at day 5 post-infection.
E3 (Also inhibits PKR)	Attenuated	ND	• Less virus titers in all organs (nasal turbinates, lung, brain and spleen) at all time points tested (2, 4, 6 and 8 days post-infection). • Both C- and N-terminus of E3 protein are required for pathogenesis.
K1	Attenuated (Chapter 3)	Attenuated (Chapter 3)	IN: • Less virus titers in all organs (lung, spleen, brain) and time points (2, 4, and 6 days post-infection). ID: • No differences in virus replication. • Decreased edema and immune gene expression. • Provides equal protection.
K7 (Also inhibits IRF-3)	Attenuated	Attenuated	IN: • No differences in viral titers at day 2 post-infection. Decreased replication at days 5 and 7 post-infection.

Table 1.1 (cont.)

			• No significant difference in overall number of cells. • Decreased percentage of neutrophils at days 3 and 6 post-infection. • Increased number of total leukocytes at 4, 6, and 8 days post-infection. • Higher percentage of MHC class II, T cells, NK cells, $CD8^+$ cells. • Lower percentage of $CD4^+$ T cells. • Enhanced cytotoxicity by NK cells and $CD8^+$ T cells.
M2	ND	ND	ND
N1 (Also inhibits apoptosis)	Attenuated	Attenuated	IN: • No difference in viral titers at days 3. Decreased replication at days 6 and 11 post-infection. • Immunogenecity: Increased number of central and memory $CD8^+$ T-cell populations in spleens. Increased $CD8^+$ T cell cytotoxicity and lower virus titres after challenge. $CD8^+$ memory T-cell function was increased with more IFN production. • Attenuation and immunogenicity depends on N1's NF-κB inhibitory function.

ND: Not determined.

1.9 References

1. Abboud, G., et al., *Natural Killer Cells and Innate Interferon Gamma Participate in the Host Defense against Respiratory Vaccinia Virus Infection.* J Virol, 2015. **90**(1): p. 129-41.

2. Abergel, C. and J.M. Claverie, *[Pithovirus sibericum: awakening of a giant virus of more than 30,000 years].* Med Sci (Paris), 2014. **30**(3): p. 329-31.

3. Alcami, A. and G.L. Smith, *A Soluble Receptor for Interleukin-1-Beta Encoded by Vaccinia Virus - a Novel Mechanism of Virus Modulation of the Host Response to Infection.* Cell, 1992. **71**(1): p. 153-167.

4. Aravalli, R.N., S. Hu, and J.R. Lokensgard, *Inhibition of toll-like receptor signaling in primary murine microglia.* J Neuroimmune Pharmacol, 2008. **3**(1): p. 5-11.

5. Armstrong, J.A., D.H. Metz, and M.R. Young, *The mode of entry of vaccinia virus into L cells.* J Gen Virol, 1973. **21**(3): p. 533-7.

6. Bartlett, N., et al., *The vaccinia virus N1L protein is an intracellular homodimer that promotes virulence.* J Gen Virol, 2002. **83**(Pt 8): p. 1965-76.

7. Beattie, E., J. Tartaglia, and E. Paoletti, *Vaccinia virus-encoded eIF-2 alpha homolog abrogates the antiviral effect of interferon.* Virology, 1991. **183**(1): p. 419-22.

8. Benfield, C.T., et al., *Vaccinia virus protein K7 is a virulence factor that alters the acute immune response to infection.* J Gen Virol, 2013. **94**(Pt 7): p. 1647-57.

9. Bhatt, D. and S. Ghosh, *Regulation of the NF-kappaB-Mediated Transcription of Inflammatory Genes.* Front Immunol, 2014. **5**: p. 71.

10. Bonduelle, O., et al., *Cutting edge: Protective effect of CX3CR1+ dendritic cells in a vaccinia virus pulmonary infection model.* J Immunol, 2012. **188**(3): p. 952-6.

11. Bowie, A., et al., *A46R and A52R from vaccinia virus are antagonists of host IL-1 and toll-like receptor signaling.* Proc Natl Acad Sci U S A, 2000. **97**(18): p. 10162-7.

12. Bradley, R.R. and M. Terajima, *Vaccinia virus K1L protein mediates host-range function in RK-13 cells via ankyrin repeat and may interact with a cellular GTPase-activating protein.* Virus Res, 2005. **114**(1-2): p. 104-12.

13. Brandt, T.A. and B.L. Jacobs, *Both carboxy- and amino-terminal domains of the vaccinia virus interferon resistance gene, E3L, are required for pathogenesis in a mouse model.* J Virol, 2001. **75**(2): p. 850-6.

14. Bravo Cruz, A.G. and J.L. Shisler, *The vaccinia virus K1 ankyrin repeat protein inhibits NF-kB activation by preventing RelA acetylation.* J Gen Virol, 2016. **97**: p. 2691-2702.

15. Bronson, L.H.P., R. F., *The neutralization of vaccine virus by immune serum: titration by the intracerebral inoculation of mice.* Journal of Bacteriology, 1941. **41**: p. 56-57.

16. Chang, H.W., J.C. Watson, and B.L. Jacobs, *The E3L gene of vaccinia virus encodes an inhibitor of the interferon-induced, double-stranded RNA-dependent protein kinase.* Proc Natl Acad Sci U S A, 1992. **89**(11): p. 4825-9.

17. Chen, R.A., N. Jacobs, and G.L. Smith, *Vaccinia virus strain Western Reserve protein B14 is an intracellular virulence factor.* J Gen Virol, 2006. **87**(Pt 6): p. 1451-8.

18. Chen, R.A., et al., *Inhibition of IkappaB kinase by vaccinia virus virulence factor B14.* PLoS Pathog, 2008. **4**(2): p. e22.

19. Clark, R.H., et al., *Deletion of gene A41L enhances vaccinia virus immunogenicity and vaccine efficacy.* J Gen Virol, 2006. **87**(Pt 1): p. 29-38.

20. Colby, C. and P.H. Duesberg, *Double-stranded RNA in vaccinia virus infected cells.* Nature, 1969. **222**(5197): p. 940-4.

21. Cooray, S., et al., *Functional and structural studies of the vaccinia virus virulence factor N1 reveal a Bcl-2-like anti-apoptotic protein.* J Gen Virol, 2007. **88**(Pt 6): p. 1656-66.

22. Cowley, R. and P.J. Greenaway, *Nucleotide sequence comparison of homologous genomic regions from variola, monkeypox, and vaccinia viruses.* J Med Virol, 1990. **31**(4): p. 267-71.

23. Damon, I.K., *Poxviruses*. 6th ed. Fields Virology, ed. P.M.H. David M. Knipe. Vol. 2. 2013: Lippincott williams & Wilkins.

24. DiPerna, G., et al., *Poxvirus protein N1L targets the I-kappaB kinase complex, inhibits signaling to NF-kappaB by the tumor necrosis factor superfamily of receptors, and inhibits NF-kappaB and IRF3 signaling by toll-like receptors.* J Biol Chem, 2004. **279**(35): p. 36570-8.

25. Drillien, R., F. Koehren, and A. Kirn, *Host range deletion mutant of vaccinia virus defective in human cells.* Virology, 1981. **111**(2): p. 488-99.

26. Ember, S.W., et al., *Vaccinia virus protein C4 inhibits NF-kappaB activation and promotes virus virulence.* J Gen Virol, 2012. **93**(Pt 10): p. 2098-108.

27. Enard, D., et al., *Viruses are a dominant driver of protein adaptation in mammals.* Elife, 2016. **5**.

28. Fenner, F., *The eradication of smallpox.* Prog Med Virol, 1977. **23**: p. 1-21.

29. Fischer, M.A., et al., *CD11b(+), Ly6G(+) cells produce type I interferon and exhibit tissue protective properties following peripheral virus infection.* PLoS Pathog, 2011. **7**(11): p. e1002374.

30. Frey, S.E., et al., *Clinical and immunologic responses to multiple doses of IMVAMUNE (Modified Vaccinia Ankara) followed by Dryvax challenge.* Vaccine, 2007. **25**(51): p. 8562-73.

31. Friedman, R.M., et al., *Mechanism of interferon action: inhibition of viral messenger ribonucleic acid translation in L-cell extracts.* J Virol, 1972. **10**(6): p. 1184-98.

32. Garcia, M.A., E.F. Meurs, and M. Esteban, *The dsRNA protein kinase PKR: virus and cell control.* Biochimie, 2007. **89**(6-7): p. 799-811.

33. Garcia-Arriaza, J. and M. Esteban, *Enhancing poxvirus vectors vaccine immunogenicity.* Hum Vaccin Immunother, 2014. **10**(8): p. 2235-44.

34. Gedey, R., et al., *Poxviral regulation of the host NF-kappaB response: the vaccinia virus M2L protein inhibits induction of NF-kappaB activation via an ERK2 pathway in virus-infected human embryonic kidney cells.* J Virol, 2006. **80**(17): p. 8676-85.

35. Gerlic, M., et al., *Vaccinia virus F1L protein promotes virulence by inhibiting inflammasome activation.* Proceedings of the National Academy of Sciences of the United States of America, 2013. **110**(19): p. 7808-7813.

36. Gerritsen, M.E., et al., *CREB-binding protein/p300 are transcriptional coactivators of p65.* Proc Natl Acad Sci U S A, 1997. **94**(7): p. 2927-32.

37. Gilbert, S.C., *Clinical development of Modified Vaccinia virus Ankara vaccines.* Vaccine, 2013. **31**(39): p. 4241-6.

38. Gillard, S., et al., *Localization and sequence of a vaccinia virus gene required for multiplication in human cells.* Proc Natl Acad Sci U S A, 1986. **83**(15): p. 5573-7.

39. Goulding, J., et al., *CD8 T cells use IFN-gamma to protect against the lethal effects of a respiratory poxvirus infection.* J Immunol, 2014. **192**(11): p. 5415-25.

40. Goulding, J., et al., *CD8 T cells are essential for recovery from a respiratory vaccinia virus infection.* J Immunol, 2012. **189**(5): p. 2432-40.

41. Gubser, C. and G.L. Smith, *The sequence of camelpox virus shows it is most closely related to variola virus, the cause of smallpox.* J Gen Virol, 2002. **83**(Pt 4): p. 855-72.

42. Harte, M.T., et al., *The Poxvirus Protein A52R Targets Toll-like Receptor Signaling Complexes to Suppress Host Defense.* Journal of Experimental Medicine, 2003. **197**(3): p. 343-351.

43. Hayden, M.S. and S. Ghosh, *Regulation of NF-kappaB by TNF family cytokines.* Semin Immunol, 2014. **26**(3): p. 253-66.

44. Hayden, M.S. and S. Ghosh, *Shared principles in NF-kappaB signaling.* Cell, 2008. **132**(3): p. 344-62.

45. Hickman, H.D., et al., *CXCR3 chemokine receptor enables local CD8(+) T cell migration for the destruction of virus-infected cells.* Immunity, 2015. **42**(3): p. 524-37.

46. Hinz, M., S.C. Arslan, and C. Scheidereit, *It takes two to tango: IkappaBs, the multifunctional partners of NF-kappaB.* Immunol Rev, 2012. **246**(1): p. 59-76.

47. Hinz, M. and C. Scheidereit, *The IkappaB kinase complex in NF-kappaB regulation and beyond.* EMBO Rep, 2014. **15**(1): p. 46-61.

48. Huang, B., et al., *Posttranslational modifications of NF-kappaB: another layer of regulation for NF-kappaB signaling pathway.* Cell Signal, 2010. **22**(9): p. 1282-90.

49. Huxford, T., et al., *The crystal structure of the IkappaBalpha/NF-kappaB complex reveals mechanisms of NF-kappaB inactivation.* Cell, 1998. **95**(6): p. 759-70.

50. Izmailyan, R., et al., *Integrin beta1 mediates vaccinia virus entry through activation of PI3K/Akt signaling.* J Virol, 2012. **86**(12): p. 6677-87.

51. Jacobs, N., et al., *Intradermal immune response after infection with Vaccinia virus.* J Gen Virol, 2006. **87**(Pt 5): p. 1157-61.

52. Kiernan, R., et al., *Post-activation turn-off of NF-kappa B-dependent transcription is regulated by acetylation of p65.* J Biol Chem, 2003. **278**(4): p. 2758-66.

53. Kim, M., *Replicating poxviruses for human cancer therapy.* J Microbiol, 2015. **53**(4): p. 209-18.

54. Koplow, D.A., *Smallpox: The Fight to Eradicate a Global Scourge*. 2004: University of California Press.

55. Lane, J.M., et al., *Complications of smallpox vaccination, 1968: results of ten statewide surveys.* J Infect Dis, 1970. **122**(4): p. 303-9.

56. Le Negrate, G., *Viral interference with innate immunity by preventing NF-kappaB activity.* Cell Microbiol, 2012. **14**(2): p. 168-81.

57. Li, Y., et al., *Structure function studies of vaccinia virus host range protein k1 reveal a novel functional surface for ankyrin repeat proteins.* J Virol, 2010. **84**(7): p. 3331-8.

58. Liu, J. and G. McFadden, *SAMD9 is an innate antiviral host factor with stress response properties that can be antagonized by poxviruses.* J Virol, 2015. **89**(3): p. 1925-31.

59. Maluquer de Motes, C., et al., *Inhibition of apoptosis and NF-kappaB activation by vaccinia protein N1 occur via distinct binding surfaces and make different contributions to virulence.* PLoS Pathog, 2011. **7**(12): p. e1002430.

60. Mansur, A.T., et al., *Multiple giant molluscum contagiosum in a renal transplant recipient.* Transpl Infect Dis, 2004. **6**(3): p. 120-3.

61. Mansur, D.S., et al., *Poxvirus targeting of E3 ligase beta-TrCP by molecular mimicry: a mechanism to inhibit NF-kappaB activation and promote immune evasion and virulence.* PLoS Pathog, 2013. **9**(2): p. e1003183.

62. Maskalyk, J., *Monkeypox outbreak among pet owners.* Cmaj, 2003. **169**(1): p. 44-5.

63. McCollum, A.M. and I.K. Damon, *Human monkeypox.* Clin Infect Dis, 2014. **58**(2): p. 260-7.

64. McCraith, S., et al., *Genome-wide analysis of vaccinia virus protein-protein interactions.* Proc Natl Acad Sci U S A, 2000. **97**(9): p. 4879-84.

65. Meng, X., J. Chao, and Y. Xiang, *Identification from diverse mammalian poxviruses of host-range regulatory genes functioning equivalently to vaccinia virus C7L.* Virology, 2008. **372**(2): p. 372-83.

66. Meng, X., et al., *C7L family of poxvirus host range genes inhibits antiviral activities induced by type I interferons and interferon regulatory factor 1.* J Virol, 2012. **86**(8): p. 4538-47.

67. Meng, X. and Y. Xiang, *Vaccinia virus K1L protein supports viral replication in human and rabbit cells through a cell-type-specific set of its ankyrin repeat residues that are distinct from its binding site for ACAP2.* Virology, 2006. **353**(1): p. 220-33.

68. Mercer, J. and A. Helenius, *Vaccinia virus uses macropinocytosis and apoptotic mimicry to enter host cells.* Science, 2008. **320**(5875): p. 531-5.

69. Meseda, C.A., et al., *Enhanced immunogenicity and protective effect conferred by vaccination with combinations of modified vaccinia virus Ankara and licensed smallpox vaccine Dryvax in a mouse model.* Virology, 2005. **339**(2): p. 164-75.

70. Metz, D.H. and M. Esteban, *Interferon inhibits viral protein synthesis in L cells infected with vaccinia virus.* Nature, 1972. **238**(5364): p. 385-8.

71. Mi, S., et al., *Syncytin is a captive retroviral envelope protein involved in human placental morphogenesis.* Nature, 2000. **403**(6771): p. 785-9.

72. Moss, B., *Membrane fusion during poxvirus entry.* Semin Cell Dev Biol, 2016.

73. Moss, B., *Poxviridae* 6th ed. Fields Virology, ed. P.M.H. David M. Knipe. Vol. 2. 2013: Lippincott williams & Wilkins.

74. Moss, B., *Poxvirus membrane biogenesis.* Virology, 2015. **479-480**: p. 619-26.

75. Myskiw, C., et al., *Vaccinia virus E3 suppresses expression of diverse cytokines through inhibition of the PKR, NF-kappaB, and IRF3 pathways.* J Virol, 2009. **83**(13): p. 6757-68.

76. Oda, S., M. Schroder, and A.R. Khan, *Structural basis for targeting of human RNA helicase DDX3 by poxvirus protein K7.* Structure, 2009. **17**(11): p. 1528-37.

77. Oeckinghaus, A. and S. Ghosh, *The NF-kappaB family of transcription factors and its regulation.* Cold Spring Harb Perspect Biol, 2009. **1**(4): p. a000034.

78. Oie, K.L. and D.J. Pickup, *Cowpox virus and other members of the orthopoxvirus genus interfere with the regulation of NF-kappaB activation.* Virology, 2001. **288**(1): p. 175-87.

79. Perkus, M.E., et al., *Vaccinia virus host range genes.* Virology, 1990. **179**(1): p. 276-86.

80. Perkus, M.E., et al., *Insertion and deletion mutants of vaccinia virus.* Virology, 1986. **152**(2): p. 285-97.

81. Philippe, N., et al., *Pandoraviruses: amoeba viruses with genomes up to 2.5 Mb reaching that of parasitic eukaryotes.* Science, 2013. **341**(6143): p. 281-6.

82. Qin, L., et al., *Genomic analysis of the vaccinia virus strain variants found in Dryvax vaccine.* J Virol, 2011. **85**(24): p. 13049-60.

83. Randall, C.M.H. and J. Shisler, *Molluscum contagiosum virus: persistence pays off.* Future Virology, 2013. **8**(6): p. 561-573.

84. Reading, P.C. and G.L. Smith, *A kinetic analysis of immune mediators in the lungs of mice infected with vaccinia virus and comparison with intradermal infection.* J Gen Virol, 2003. **84**(Pt 8): p. 1973-83.

85. Ren, H., et al., *Enhancement of CD8(+) T-cell memory by removal of a vaccinia virus nuclear factor-kappaB inhibitor.* Immunology, 2015. **145**(1): p. 34-49.

86. Rice, A.D., et al., *Roles of vaccinia virus genes E3L and K3L and host genes PKR and RNase L during intratracheal infection of C57BL/6 mice.* J Virol, 2011. **85**(1): p. 550-67.

87. Rivera, R., et al., *Murine alveolar macrophages limit replication of vaccinia virus.* Virology, 2007. **363**(1): p. 48-58.

88. Sanchez-Sampedro, L., et al., *The evolution of poxvirus vaccines.* Viruses, 2015. **7**(4): p. 1726-803.

89. Scherer, D.C., et al., *Signal-induced degradation of I kappa B alpha requires site-specific ubiquitination.* Proc Natl Acad Sci U S A, 1995. **92**(24): p. 11259-63.

90. Schroder, M., M. Baran, and A.G. Bowie, *Viral targeting of DEAD box protein 3 reveals its role in TBK1/IKKepsilon-mediated IRF activation.* Embo j, 2008. **27**(15): p. 2147-57.

91. Schroeder, N., et al., *The lipid raft-associated protein CD98 is required for vaccinia virus endocytosis.* J Virol, 2012. **86**(9): p. 4868-82.

92. Sen, R. and D. Baltimore, *Multiple nuclear factors interact with the immunoglobulin enhancer sequences.* Cell, 1986. **46**(5): p. 705-16.

93. Senkevich, T.G., et al., *The genome of molluscum contagiosum virus: analysis and comparison with other poxviruses.* Virology, 1997. **233**(1): p. 19-42.

94. Shisler, J.L. and X.L. Jin, *The vaccinia virus K1L gene product inhibits host NF-kappaB activation by preventing IkappaBalpha degradation.* J Virol, 2004. **78**(7): p. 3553-60.

95. Sivan, G., et al., *Identification of Restriction Factors by Human Genome-Wide RNA Interference Screening of Viral Host Range Mutants Exemplified by Discovery of SAMD9 and WDR6 as Inhibitors of the Vaccinia Virus K1L-C7L-Mutant.* MBio, 2015. **6**(4): p. e01122.

96. Smith, G.L., et al., *Vaccinia virus immune evasion: mechanisms, virulence and immunogenicity.* J Gen Virol, 2013. **94**(Pt 11): p. 2367-92.

97. Stack, J., et al., *Vaccinia virus protein A46R targets multiple Toll-like-interleukin-1 receptor adaptors and contributes to virulence.* J Exp Med, 2005. **201**(6): p. 1007-18.

98. Strnadova, P., et al., *Inhibition of Translation Initiation by Protein 169: A Vaccinia Virus Strategy to Suppress Innate and Adaptive Immunity and Alter Virus Virulence.* PLoS Pathog, 2015. **11**(9): p. e1005151.

99. Sumner, R.P., et al., *Vaccinia virus inhibits NF-kappaB-dependent gene expression downstream of p65 translocation.* J Virol, 2013.

100. Symons, J.A., A. Alcami, and G.L. Smith, *Vaccinia virus encodes a soluble type I interferon receptor of novel structure and broad species specificity.* Cell, 1995. **81**(4): p. 551-60.

101. Tscharke, D.C., P.C. Reading, and G.L. Smith, *Dermal infection with vaccinia virus reveals roles for virus proteins not seen using other inoculation routes.* J Gen Virol, 2002. **83**(Pt 8): p. 1977-86.

102. Tscharke, D.C. and G.L. Smith, *A model for vaccinia virus pathogenesis and immunity based on intradermal injection of mouse ear pinnae.* J Gen Virol, 1999. **80**: p. 2751-5.

103. Unterholzner, L., et al., *Vaccinia virus protein C6 is a virulence factor that binds TBK-1 adaptor proteins and inhibits activation of IRF3 and IRF7.* PLoS Pathog, 2011. **7**(9): p. e1002247.

104. Volz, A. and G. Sutter, *Protective efficacy of Modified Vaccinia virus Ankara in preclinical studies.* Vaccine, 2013. **31**(39): p. 4235-40.

105. Williams, B.R., *PKR; a sentinel kinase for cellular stress.* Oncogene, 1999. **18**(45): p. 6112-20.

106. Williamson, J.D., et al., *Biological characterization of recombinant vaccinia viruses in mice infected by the respiratory route.* J Gen Virol, 1990. **71**: p. 2761-7.

107. Willis, K.L., J.O. Langland, and J.L. Shisler, *Viral double-stranded RNAs from vaccinia virus early or intermediate gene transcripts possess PKR activating function, resulting in NF-kappaB activation, when the K1 protein is absent or mutated.* J Biol Chem, 2011. **286**(10): p. 7765-78.

108. Willis, K.L., et al., *The effect of the vaccinia K1 protein on the PKR-eIF2alpha pathway in RK13 and HeLa cells.* Virology, 2009. **394**(1): p. 73-81.

109. Zamanian-Daryoush, M., et al., *NF-kappaB activation by double-stranded-RNA-activated protein kinase (PKR) is mediated through NF-kappaB-inducing kinase and IkappaB kinase.* Mol Cell Biol, 2000. **20**(4): p. 1278-90.

Chapter 2: Vaccinia virus K1 protein inhibits NF-κB activation by preventing RelA acetylation

Originally published in the *Journal of General Virology*. Bravo Cruz A and Shisler J. 97(10):2691-2702 doi:10.1099/jgv.0.000576. Published in partial fulfillment of the requirements for the degree of doctor of philosophy in Microbiology.

2.1 Introduction

Vaccinia virus (VACV) was used as a vaccine against variola virus (smallpox) infection [41]. Despite the elimination of smallpox in 1980, VACV remains important to the medical community. It is now being used as a vector for vaccines against other infectious diseases and as an oncolytic virus [24, 51]. In addition, VACV remains an excellent model for understanding immune responses to complex pathogens [55]. As such, the continued study of VACV identifies key virus-host interactions that can be exploited to the benefit of human health.

The NF-κB transcription factor is critical for the host anti-viral defense because it activates genes involved in immunity and inflammation [2]. The RelA (p65) and NF-κB1 (p50) heterodimer is the best-studied member of this family [2]. NF-κB is sequestered in the cytoplasm by IκBα [28]. Upstream proteins (e.g. TNF receptor-1) activate the IκB kinase (IKK) complex [25], and IKK phosphorylates IκBα [29]. As a consequence, IκBα is polyubiquitinated by the $SCF^{\beta TrCP}$ E3 ubiquitin ligase complex and degraded by the 26S proteasome [28]. The freed NF-κB then migrates to the nucleus [26], where it undergoes several post-translational modifications that are required for its transcriptional activity, such as acetylation of RelA [30]. Originally, it was thought that RelA must be acetylated by CBP/p300 prior to NF-κB binding to its promoter. However, recent publications demonstrate that, for some genes, RelA migrates to a promoter already

bound by CBP/p300 [42]. In these cases, RelA is acetylated after it binds to the DNA-CBP/p300 complex [42]. Regardless, once the promoter is occupied by NF-κB, transcription is initiated when the adjacent transcriptional start site is occupied by RNA polymerase II and a set of general transcription factors [46].

The VACV K1 protein is a 31-kDa protein that possesses nine ankyrin repeat domains (ARDs) [33]. During virus infection, the presence of K1 correlates with the presence of IκBα and absence of NF-κB activation [56]. This implies that K1 acts at or upstream of IκBα [56]. K1 also inhibits PKR [69], a multifunctional cellular protein that activates NF-κB [71] in addition to PKR's main role of inhibiting host cell translation [70]. Willis et al. went on to show that, during virus infection, PKR activation is the cause of NF-κB activation [68]. Thus, in the infected cell environment, K1 antagonizes PKR activation, and this upstream event is responsible for K1's inhibition of NF-κB [68].

Aravalli et al. show that ectopic K1 inhibits Toll-like receptor 2 (TLR2)-induced NF-κB activation [1] in primary murine macrophages. Although this may also involve PKR activation [7], it also raised the possibility that K1 may inhibit NF-κB in a PKR-independent function. To further query if K1 indeed possesses an alternative strategy to antagonize NF-κB, we used two strategies to uncouple PKR and NF-κB activation; we expressed K1 independently of infection and used reagents that minimized PKR activation. Using these systems, data revealed that K1 localized to the nucleus and prevented CBP/p300-induced RelA acetylation and RelA-CBP interactions.

2.2 Materials and Methods

Cells and plasmids

Human embryonic kidney 293T (293T) cells and human cervical carcinoma (HeLa) cells were obtained from the American Type Culture Collection (ATCC). HeLa cells in which >95% of PKR was knocked down (PKR^{KD}) were obtained from Dr. Charles Samuel (Department of Molecular, Cellular and Developmental Biology, University of California Santa Barbara) and were characterized previously [72]. Cells were cultured in Eagle's minimal essential media supplemented with 10% FBS, 2mM L-glutamine, 100 U/mL penicillin and 100 μg/mL streptomycin.

Plasmid pHA-K1 consists of a hemagglutinin epitope-tagged *K1L* gene inserted into the pCI expression vector [68]. A plasmid encoding an IκBα dominant negative (DN) (pIκBαDN) was provided by Dr. Dean Ballard (Vanderbilt University) [52]. pV5-M2 plasmid expresses a V5 epitope-tagged M2 protein [22]. Plasmids pNF-κB*luc*, pIL-8*luc* and pIRF3*luc* encode the firefly luciferase gene under the control of a synthetic NF-κB promoter (Promega), the IL-8 promoter [14] or four copies of the PRDIII promoter sequence specific for IRF3 [48], respectively. Plasmid pRL-null encodes a promoter-less sea pansy luciferase gene (Promega). Plasmid pMyD88 was obtained from Dr. Richard Tapping (Department of Microbiology, University of Illinois). $pcFLIP_L$ was provided by J. Cohen (National Institutes of Health). Plasmid TBK1 was a kind gift of S. Balachandran (Fox Chase Center). Plasmid pGFP-RelA was provided by Dr. Lin Feng-Chen (Department of Biochemistry, University of Illinois) [11]. A plasmid encoding an FLAG-tagged version of CBP protein (pFLAG-CBP) was obtained from Dr. David P. Lebrun (Queen's University) [31]. Plasmid HA-p300 was obtained from Dr. Den Rock

(Department of Pathobiology, University of Illinois) [15]. All plasmids were transfected into cells using the TransIT reagent (Mirus) following manufacturer's instructions.

Luciferase assays

A dual-reporter luciferase assay was performed to quantify NF-κB or IRF3 activation in transfected cells using previously published protocols [21, 48, 49, 56]. Briefly, subconfluent cellular monolayers of 293T or HeLa cells in 12-well plates were transfected with 112.5 ng pNF-κB*luc* or pIL-8*luc* [14] or pIRF3 [21], 12.5 ng pRL-null and 1000 ng pCI, pIκBαDN, pFLAG-cFLIP$_L$ or pHA-K1. At 24 h later, cells were incubated in regular medium or medium containing tumor necrosis factor-α (TNF) (10 ng/mL; Roche) or phorbol 12-myristate 13-acetate (PMA) (50 ng/mL; Sigma) for the indicated times. In some cases, NF-κB or IRF3 activation was instead triggered by co-transfection of cells with plasmids containing MyD88 or TBK1 genes, respectively. All transfections were performed in triplicate. Cells were lysed in 1x passive lysis buffer (PLB; Promega) and lysates were analyzed for firefly and sea pansy luciferase activities. For each lysate, the ratio of firefly luciferase activity to sea pansy luciferase activity was calculated to correct for differences in transfection efficiencies. The triplicates were averaged. The resultant values were used to compare the expression of the firefly luciferase gene in stimulated cells to that present in unstimulated, pCI-transfected cells, whose value was set to one. Values are shown as mean ± S.D. The Student's *t*-test was used to determine the statistical significance of inhibition of luciferase activity by K1 or dominant-negative IκBα proteins versus unstimulated, pCI-transfected cells. Statistically significant inhibition of luciferase activity is indicated by asterisks (*$P < 0.05$).

Protein expression levels in lysates from luciferase assays were analyzed by immunoblotting. Briefly, 30 μg of protein from each lysate was separated by using SDS-PAGE and transferred to PVDF membranes. Membranes were probed with mouse monoclonal anti-HA antibody (1:1,000; Sigma-Aldrich) or anti-PKR (1:1,000; Santa Cruz) and then HRP-conjugated goat anti-mouse IgG (1:5,000; Thermo Scientific) to detect K1 protein expression levels. Antibody-antigen reactions were detected by using chemilluminescence reagents (Thermo Scientific) and autoradiography.

Quantitative reverse transcriptase PCR (RT-qPCR)

Transcription of the *IL-8*, *IκBα*, *IL-6* and *β-actin* genes in the presence or absence of K1 protein expression was evaluated by RT-qPCR. 293T or HeLa cells were seeded in 6-well plates at $5x10^5$ or $1x10^5$ cells/well, respectively. Cells were transfected with the amounts of plasmids indicated in the figure legends in triplicate. After 24 h, cells were incubated for 4 h (293T) or 2 h (HeLa) with medium lacking or containing 20 ng/mL TNF. Alternatively, cells were co-transfected with pGFP-RelA (500 ng) and pHA-p300 (500 ng) and 1000 ng pCI or pHA-K1 for 24 h prior to collection instead of using TNF as a stimulator of NF-κB activation. Total RNA was extracted from cells using the RNeasy Mini kit (QIAGEN) following manufacturer's instructions. 500 ng of RNA from each sample was incubated with oligo-dT and the M-MuLV Reverse Transcriptase (New England BioLabs). The reaction was incubated at 42°C for 60 min, and then terminated by heating at 85°C for 5 min. The resultant cDNA was diluted 1:5 in DNase and RNase free water. Then, two μl of diluted cDNA were used for quantitative PCR, using a Mastercycler realplex EP (Eppendorf) and SoFast EvaGreen Super Mix (BioRad) per

manufacturer's instructions. qPCR was performed using the following program: 95°C for 2 min; 40 cycles of 95°C for 5 s, 55°C for 10 s. Changes in expression level of each gene were calculated by the $2^{(-\Delta\Delta C(T))}$ method [34]. For normalization, β-actin mRNA quantities for each cDNA sample were measured, and then each value was normalized to that of unstimulated, pCI-transfected cells. Data are presented as means ± S.D. from a minimum of three independent experiments. The Student's *t*-test was used to determine statistically significant differences in mRNA expression levels as compared to unstimulated, pCI-transfected cells. The following designed primers were used to detect β-Actin cDNA: (5'-AGTTGCGTTACACCCTTTCT-3') and (5'-ACCTTCACCGTTCCAGTTT-3'). Primers designed to detect IL-8 cDNA were (5'-CCAAGGGCCAAGAGAATATC-3') and (5'-GAGGTAAGATGGTGGCTAATAC-3'). Primers designed to detect IκBα cDNA were (5'-ATCAGCCCTCATTTTGTTGC-3') and (5'-ACCACTGGGGTCAGTCACTC-3'). Primers (5'-TGAGAGTAGTGAGGAACAAGC-3') and (5'-CATTTGTGGTTGGGTCAGG-3') were used to detect IL-6 cDNA.

Immunoblotting

Protein concentration of lysates (including lysates used for luciferase activity assays) was determined by bicinchoninic (BCA) assay (Pierce) with the exception of experiments in which cytoplasmic and nuclear fractions were assayed. In this case, the 660 nm protein assay (Pierce) was used instead of the BCA assay. Regardless, for each experimental sample, an equal amount of protein from each lysate was electrophoretically separated using SDS-PAGE. Proteins were transferred to PVDF membranes, and

membranes were blocked in 5% (w/v) milk in Tris-Buffered Saline and Tween 20 (TBST; 150 mM NaCl, 50 mM Tris base, 0.05% Tween 20) for at least 30 min at room temperature. Membranes were incubated in the primary and secondary antibodies listed below. Antibody reactions on membranes were detected by using chemiluminescence reagents (Amersham and Thermo Scientific) and autoradiography.

For the detection of IκBα protein levels, subconfluent cellular monolayers of 293T HeLa or PKR^{KD} cells in 6-well plates were transfected with 2000 ng of either pCI or pHA-K1. At 24 h later, supernatants were aspirated and cells were incubated in fresh medium either lacking or containing TNF (10 ng/mL; Roche) for 15 or 30 min. Next, cellular monolayers were dislodged using trypsinization, and cells were collected by centrifugation. Cellular pellets were suspended in cytoplasmic extract (CE) buffer containing HALT protease inhibitors for 15 min [45, 56]. Lysates were centrifuged and clarified supernatants were removed to fresh tubes. Ten μg of cytoplasmically-extracted protein from each sample was evaluated for IκBα protein levels by using immunoblotting, in which immunoblots were incubated with rabbit monoclonal anti-IκBα antibody (1:2,500; Cell Signaling) and then HRP-conjugated goat anti-rabbit IgG (1:10,000; CalBiotech). Blots were re-probed with rabbit monoclonal anti-β-actin antibody (1:5,000; Sigma) and then HRP-conjugated goat anti-rabbit IgG (1:10,000; CalBiotech). An additional, identical set of immunoblotted lysates was used to detect K1 protein expression, in which PVDF membranes containing 30 μg of protein from each sample were incubated with mouse monoclonal anti-HA antibody (1:1,000; Sigma-Aldrich) and then HRP-conjugated goat anti-mouse IgG (1:5,000; Thermo Scientific). Acetylation of the RelA protein at residue 310 was detected as follows. 1×10^5 HeLa cells were

transfected with 250 or 500 ng of pGFP-RelA and pFLAG-CPB or pCI. In addition, cells were co-transfected with 1000 ng of pCI or pHA-K1. At 24 h later cellular monolayers were dislodged by trypsinization and collected by centrifugation (18,000 rcf x 1 min). Cellular pellets were resuspended and lysed in Acetyl Lysis Buffer (ALB; 25 mM Tris-HCl pH 7.5, 250 mM NaCl, 1% NP-40, 1 mM EDTA) for 20 min on ice. Lysates were centrifuged (18,000 rcf x 10 min) and clarified supernatants were transferred to new tubes. Samples were analyzed by immunoblotting, in which membranes were incubated with rabbit monoclonal anti-acetyl NF-κB RelA (Lys310) antibody (1:1,000; Cell Signaling). The blot was reprobed with rabbit polyclonal anti-RelA antiserum (1:1,000; Santa Cruz) to detect unmodified RelA. A duplicate blot was probed with anti-HA antiserum to detect K1 protein expression and actin. CPB was detected in a separate blot using anti-CPB (1,1000; Cell Signaling). To detect RelA-CBP interactions, PKR^{KD} cells were transfected with 250 or 500 ng of pGFP-RelA and pFLAG-CPB or pCI. In addition, cells were co-transfected with 1000 ng of pCI, pHA-K1 or pV5-M2 plasmids using Trans-IT transfection reagent. At 24 h post-transfection, cells from 3 wells were lysed in 300 µl ALB. A portion of each clarified lysate was removed to a new tube and used to probe protein expression in cellular lysates. The remaining clarified lysates were incubated with anti-CBP antibodies (Cell Signaling) for 6 h. Then protein G –Sepharose beads (Life Technologies) were added to the mixture and incubated overnight at 4C. Next, beads were washed in large volumes of ALB. Beads were mixed with 2x sample buffer containing 2-mercaptoethanol and boiled for 5 min. A portion of each immunoprecipitation reaction was separated by SDS-PAGE. Proteins were transferred electrophoretically to PVDF membranes and membranes were probed with the indicated

antiserum described above. The M2 protein was detected using anti-V5 antibody (1:1,000; Millipore).

Cytoplasmic and nuclear fractionations

1 x 10^6 293T cells were transfected with 1500 ng of either pCI, pIκBαDN or pHA-K1. At 24 h after transfection, cells were incubated with medium lacking or containing TNF (20 ng/mL) for 15 or 30 min. Cellular monolayers were detached by trypsinization, collected by centrifugation and processed as described in a previous publication [56]. Cells were suspended in 50 µl CE buffer and incubated on ice for 15 min. Lysates were centrifuged at 1,000 rcf for 5 min, and clarified supernatants were collected to new tubes. The remaining pellet was washed in 200 µl CE and centrifuged (1,000 rcf for 5 min) twice. The nuclei-containing pellet was resuspended in 30 µl of nuclear extract (NE) buffer (20 mM HEPES, 0.4M NaCl, 1 mM EDTA pH 8.0, 1 mM EGTA pH 8.0, 25% glycerol) and incubated for 20 min on ice, vortexing samples every 10 min. Samples were centrifuged for 10 min at 18,000 rcf. Supernatants (nuclear extracts) were collected and stored at -80°C. Both cytoplasmic and nuclear extracts were evaluated by immunoblotting for the following proteins: tubulin (mouse monoclonal anti-tubulin antibody (1:5,000; Abcam), PARP (rabbit polyclonal anti-PARP-1 antibody; 1:1,000 Santa Cruz), RelA (rabbit polyclonal anti-RelA antibody (1:5,000; Santa Cruz) or K1 (mouse monoclonal anti-HA antibody; 1:1,000; Sigma-Aldrich).

NF-κB-oligonucleotide (TransAM) binding assay

To study NF-κB-DNA interactions, 293T cells were transfected with 1500 ng of pCI, pIκBαDN, or pHA-K1. After 24 h, cells were incubated with medium lacking or containing 20 ng/mL TNF for 30 or 60 min. Next, nuclei were isolated and nuclear extracted proteins were generated as described above. Five μg of nuclear extract was evaluated for the DNA binding activity of NF-κB by using the TransAM NF-κB RelA DNA-binding ELISA kit (Active Motif) following the manufacturer's instructions. Nuclear extracts were added to a 96-well plate coated with immobilized oligonucleotides containing an NF-κB consensus site (5'-GGGACTTTCC-3'). Wells were washed and then incubated with a solution containing a primary antibody recognizing the RelA subunit of the NF-κB heterodimer. This antibody only recognizes the transcriptionally active form of RelA when complexed with DNA. Wells were washed and incubated with solution containing an HRP-conjugated secondary antibody. Wells were washed again and incubated with a developer solution provided with the kit. Reactions were analyzed by spectrophotometry at a wavelength of 450 nm. In addition, some wells had an excess amount of immobilized oligonucleotides containing either the regular (wild-type) or mutated NF-κB consensus sequence to evaluate non-specific binding of NF-κB in this system. Data shown are a representative experiment of at least 3 independent experiments, and each experiment was performed with 3 technical triplicates.

2.3 Results

The K1 protein inhibits NF-κB activation independently of virus infection

To examine if K1 inhibited NF-κB via a PKR-independent mechanism, K1 was expressed ectopically in cells as a strategy to uncouple PKR activation and NF-κB activation. NF-κB transcriptional action was evaluated by using luciferase reporter assays. We used pNF-κB*luc*, a plasmid that contains five copies of a NF-κB consensus binding site to activate the transcription of the firefly luciferase reporter gene [56], Fig. 1(a) and 1(b), or pIL-8*luc*, a plasmid in which the cellular IL-8 promoter was used to control the firefly luciferase reporter gene [14], as shown in Fig. 1(c). Controls included cells co-transfected with empty vector (pCI) or with a plasmid expressing a dominant negative IκBα molecule, a protein that cannot be phosphorylated by IKK and thus remains associated with NF-κB to prevent NF-κB activation [64].

Figures 1(a) and 1(b) showed that K1 inhibited NF-κB activation induced by either TNF or MyD88 over-expression respectively, albeit to a lesser extent than the dominant negative IκBα molecule. Because TNF and MyD88-induced NF-κB signal transduction pathways overlap from the point of IKK activation and downwards, this implied that K1 may be inhibiting an event occurring post-IKK activation. K1 was stably expressed in cells for the duration of the experiments, and K1 expression itself did not activate NF-κB. K1 also inhibited reporter activity of a luciferase gene controlled by the cellular IL-8 promoter, a promoter that contains an NF-κB binding site. as shown in Figure 1(c). An additional luciferase assay was performed in which activation of the IRF3 transcription factor was examined by over-expressing TBK1 [21]. As shown in Figure 1(d), the presence of K1 did not inhibit IRF3 activation, showing that K1 specifically

targets NF-κB activation. The $cFLIP_L$ protein, which is known to inhibit IRF3 activation [21], was expressed in parallel to show that conditions were conducive for activating and detecting IRF3 transcriptional activation.

RT-qPCR was used to evaluate the transcription of the NF-κB-regulated interleukin-8 (IL-8) and interleukin-6 (IL-6) genes, as shown in Fig. 1(e) - 1(g), as an alternative measure of NF-κB activation. We were interested in examining IL-6 gene expression because Myskiw et al. reported that induction of IL-6 gene expression is PKR-independent during virus infection [43], thus providing another opportunity to examine PKR-independent NF-κB activation. TNF stimulated the transcription of the IL-8 and IL-6 genes, as expected. In contrast, IL-8 and IL-6 mRNA levels were significantly lower in K1-expressing 293T and HeLa cells, as shown in Figs. 1(e) and 1(f), respectively. IL-8 and IL-6 gene expression was also reduced in cells expressing the dominant negative form of IκBα, as expected. IL-8 mRNA levels were also lower in HeLa cells, although this decrease was not statistically significant, Fig. 1(g). These data demonstrated that ectopically expressed K1 inhibited NF-κB activation under different conditions and in more than one cell type.

The K1 protein inhibits NF-κB activation in a PKR-independent manner

To further test the possibility that K1 possesses a PKR-independent NF-κB inhibitory function, we compared NF-κB activation in normal HeLa cells or a HeLa cell line derivative (PKR^{KD}) that reduces PKR protein levels by 95% [72]. Similar to data in Fig. 1(d), K1 inhibited TNF-induced NF-κB activation in normal HeLa cells. This same inhibition was observed in PKR^{KD} cells, as shown in Fig. 2(b). We noticed that TNF

stimulation of luciferase activity was lower in PKR^{KD} versus parental HeLa cells, and this is consistent with one report showing that PKR plays a role in the TNFR1-NF-κB signaling pathway [63].

PMA was used as an alternative stimulator of NF-κB in Figs. 2(c) and 2(d) because it activates NF-κB independently of PKR [73]. We have confirmed PKR protein levels are reduced in PKR^{KD} cells as compared to HeLa cells in Fig. 2(e), similar to ours and others' observations [69, 72]. Indeed, PMA-induced luciferase activity levels were similar in HeLa and PKR^{KD} cells demonstrating that the absence of PKR did not alter cellular responsiveness to PMA. Importantly, K1 continued to antagonize PMA-induced NF-κB activation to similar extents in both cell lines. While, in some cases, K1 protein levels were slightly lower in stimulated versus unstimulated cells, K1 still inhibited luciferase activity. These data suggest that K1 inhibits NF-κB activation in a PKR-independent mechanism.

IκBα degradation occurs in the presence of K1

To characterize the portion of the NF-κB pathway that K1 was blocking, we initially examined the effect of K1 on IκBα degradation (Figure 3). Observations in Figures 1 and 2 suggested that using TNF to stimulate NF-κB would minimize PKR activation, and this system continued to be used. It is well-known that TNF-TNFR1 interactions trigger IκBα degradation rapidly in several cell lines [25]. This same temporal degradation was observed in pCI-transfected cells (Figure 3). Interestingly, K1 did not block IκBα degradation in all three cell lines tested. This phenotype was surprising because a 2004 publication from our lab shows K1 prevents IκBα degradation

during virus infection [56]. Data in Figure 3, in addition to the data in Figures 1 and 2, strongly implied that K1 possessed an additional mechanism to inhibit NF-κB activation, and that this mechanism occurred after IκBα degradation.

NF-κB translocates to the nucleus in the presence of K1

IκBα degradation unmasks the nuclear localization sequence (NLS) of RelA, now allowing NF-κB to translocate to the nucleus [25]. Since K1 did not prevent IκBα degradation, a logical question was to ask if K1 prevented NF-κB nuclear trans-location. In this case, a cellular fractionation assay separating cytoplasmic and nuclear localized proteins was used to query if K1 affected NF-κB nuclear translocation. There was a visible increase in nuclear-localized RelA in TNF-treated versus unstimulated pCI-transfected cells (Figure 4). This translocation event was inhibited when a dominant negative IκBα was over-expressed, an expected result because dominant-negative IκBα remains bound to NF-κB to inhibit RelA nuclear translocation [13]. However, K1 did not inhibit NF-κB migration to the nucleus. RelA-containing band densities were similar in nuclear extracts from pCI- versus pHA-K1-transfected cells. This implies that K1 does not inhibit NF-κB nuclear translocation.

The localization of K1 also was examined. K1 was predicted to be a cytoplasmic protein because it has no obvious NLS signals. However, K1 proteins were observed in similar amounts in the cytoplasmic and nuclear extracts (Figure 4). Amounts of K1 did not visibly change when cells were stimulated (Figure 4). This suggested that K1 was not migrating into the nucleus as part of an NF-κB complex. These same extracts were also probed with antiserum recognizing β-tubulin and PARP proteins to demonstrate

successful separation of nuclear from cytoplasmic proteins. Note that the expression of a dominant negative IκBα molecule greatly reduced RelA/p65 nuclear translocation. This was expected because the dominant negative IκBα cannot be phosphorylated and degraded. This also demonstrated that K1's inability to inhibit RelA nuclear translocation is not due to transfection inefficiency because all cells were transfected simultaneously and using the same protocol.

K1 allows NF-κB to interact with an oligonucleotide containing NF-κB binding sites

Data from Figure 4 suggested that the antagonistic mechanism of K1 could be associated with K1's nuclear localization. In the nucleus, NF-κB binds to a conserved DNA sequence present in the promoter of its target genes. The TransAM assay is one method to detect and quantitatively measure transcriptionally active NF-κB-DNA interactions (Figure 5). As expected, TNF treatment significantly increased NF-κB-DNA interactions, as demonstrated by the increase in values for the assay. This event was blocked in cells over-expressing a dominant-negative form of IκBα. However, K1 did not inhibit NF-κB DNA interactions. This signal was specific for NF-κB because the signal decreased if an excess of oligonucleotides containing wild-type NF-κB consensus sites was present (WT competitor), but not when an excess of oligonucleotides with mutant NF-κB binding sites (mutant competitor) were present. Note that these controls, where excess WT or mutant competitor nucleotides were present, only were added to lysates from pCI-transfected cells that received 30 min TNF treatment.

K1 inhibits CBP/p300-mediated NF-κB activation and prevents RelA acetylation

The above data suggested that K1 allowed NF-κB to enter into the nucleus and interact with its promoter but inhibited NF-κB transcriptional activation. One explanation for this pattern would be if K1 inhibited RelA acetylation, a post-translational modification required for NF-κB activation. This modification is performed by the CBP/p300 family of proteins [23]. To test this hypothesis, we first asked if K1 could inhibit NF-κB activation triggered by over-expression of RelA and p300, conditions known to induce NF-κB activation [23]. K1 inhibited NF-κB activation, as measured by expression of the NF-κB regulated IL-8 and IκBα genes, as shown in Figs. 6 (a) and 6 (b) respectively. These data support the hypothesis that K1 acts at or downstream of RelA acetylation.

CBP, like its p300 ortholog, binds to and acetylates RelA at lysine 310 [42]. This can occur either before or after NF-κB interacts with κB binding sites in a promoter [42]. To ask if K1 prevented this post-translational modification, RelA and CBP were over-expressed to trigger and detect RelA acetylation [10]. This approach was chosen because it has proven difficult by us and others to detect acetylation of endogenous RelA [10]. As expected, acetylation at lysine 310 was observed in pCI-transfected cells, as shown in Figure 6 (c). However, this acetylation was greatly reduced in K1-expressing cells. This was observed in both HeLa (Fig. 6 c) and PKR^{KD} cells (Fig. 6 d). It was also observed that K1 protein levels slightly decreased when increased amounts of plasmids RelA and CBP were present. Nevertheless, K1 still inhibited RelA acetylation. Thus, data in Figure 6 support the hypothesis that K1 targets RelA acetylation to prevent NF-κB activation in a PKR-independent mechanism.

One possibility for this lack of RelA acetylation would be due to a lack of CBP-RelA interactions in K1-expressing cells. To test this possibility PKR^{KD} cells were examined for RelA-CBP interactions using co-immunoprecipitations, using the same conditions in Figure 6 (c). Results are shown in Figure 6 (d). In vector-transfected cells, RelA-CBP interactions were detected when RelA and CBP were over-expressed. This interaction was greatly reduced when the K1 protein was present. This was a specific property of K1 because the expression of another poxviral NF-κB inhibitory protein (M2) did not inhibit this interaction and did not inhibit RelA acetylation (Fig. 6 e)[22]. M2 is not expected to inhibit RelA-CBP interactions because M2 interferes with MEK-directed phosphorylation of ERK2, a kinase that targets the IKK complex for NF-κB activation [22], thus acting on a signal transduction step prior to RelA-CBP interactions. Multiple attempts were made to co-immunoprecipitate K1 with RelA or with CBP under several different conditions. However, under no conditions tested could we reproducibly detect such interactions.

2.4 Discussion

Several pieces of data indicate that K1 inhibits NF-κB activation in a PKR-independent manner. K1 retained its NF-κB inhibitory function when using stimuli that do not trigger PKR activation (e.g., PMA or co-expression of RelA and CBP/p300) or using a cell line with dramatically decreased PKR levels. Since K1 allowed IκBα degradation and NF-κB nuclear translocation, it was likely that K1 prevented a signal transduction event that occurs after these events. There are two lines of evidence that K1 targets RelA acetylation. First, K1 inhibited RelA/p300-induced luciferase reporter gene

expression. Second, K1 inhibited p300-induced acetylation of RelA. It was also observed that RelA-CBP co-immunoprecipitations no longer occurred in the presence of K1, suggesting that K1 prevents interactions of proteins necessary for NF-κB activation. Unfortunately, we could not reliably detect K1-RelA or K1-CBP interactions in eukaryotic cells by co-immunoprecipitations. Thus, we cannot rule out the possibility that K1 may act indirectly to prevent RelA-CBP interactions.

Interestingly, K1 did not prevent NF-κB from binding to oligonucleotides containing κB-binding sites. Originally, it was thought that CBP/p300 interacts with NF-κB prior to NF-κB binding to its consensus DNA sequence. However, a recent publication from Mukherjee et al. shows that there is a higher preponderance of promoters constitutively loaded with CBP/p300 [42]. One such gene found to be controlled by this latter mechanism is IκBα, a gene we examined here. Thus, one model based on these data is that K1 allows NF-κB to bind to its promoter sequence, but then prevents p300/CBP from interacting with NF-κB. Mukherjee did not report whether the IL-8 gene, an additional gene we examined, was controlled in a similar manner. Thus, whether K1 acts in a similar manner or via a different mechanism remains the focus of future studies.

K1 possesses 9 ankyrin repeat domains (ARDs) [33]. These 33-residue repeats are important for mediating protein-protein interactions in other ARD-containing proteins [32, 40]. Two viral ARD-containing proteins that inhibit NF-κB are African Swine Fever Virus (ASFV) A238 and cowpox CP77 proteins [9, 50], and they bind to RelA. However, two lines of evidence suggest K1 does not interact with RelA. First, we did not observe increase nuclear K1 protein levels in TNF-treated cells, implying that K1 does not enter

the nucleus as an NF-κB binding partners. Second, we do not consistently observe K1-RelA co-immunoprecipitations in pHA-K1-transfected cells. It should be noted that the Orf poxvirus 002 protein also inhibits RelA acetylation by binding to RelA [15]. However, Orf 002 lacks ARDs, suggesting that K1 and Orf 002 share functional similarities despite lacking similarity at the amino acid level [15].

Along with K1, there are other viral ARD proteins (vankyrins) encoded by poxviruses, herpesviruses and polydnaviruses [3, 17, 27]. Most of the poxvirus vankyrins also possess an additional F-box motif [27] (referred to as a PRANC domain) [27]. This F-box motif allows these poxviral ARDs to bind to Skp1, a member of the E3 SCF ubiquitin ligase complex. This occurs for multiple proteins encoded by ectromelia virus (EVM002, EVM005, EVM154 and EVM165) [5, 65], Orf virus (OV008, OV123, OV126, OV128, OV129) [59], myxoma virus (M-T5, M148, M149, M150) [67], vaccinia virus 68k [60], fowlpox virus FPV014 [6], monkeypox virus 003 [39], variola virus G1R [39], and cowpox virus proteins CP77 [9] and CPXV006 [39]. For the ectromelia virus proteins with PRANC domains, this interaction with Skp1 is sufficient to antagonize the normal ubiquitination function of the SCF E3 ligase complex and inhibit IκBα degradation [5]. K1 is unique in that it does not possess a partial or full F-box motif. This implies that K1 cannot interfere with IκBα ubiquitination, a hypothesis supported by the observation that K1 allowed IκBα degradation. Interestingly, the variola virus G1R, cowpox virus 006, ectromelia EVM002, and monkeypox virus 003 ANK/F-box proteins also bind to and cleave p105 to prevent formation of the RelA/p50 complex [39]. It is unlikely that K1 targets p105 processing because NF-κB still binds to an oligonucleotide

containing κB binding sites (Fig. 5), suggesting that a functional RelA/p50 complex is in the nucleus.

Here, we show that K1 inhibits RelA acetylation and RelA-CBP interactions, suggesting that K1 performs its inhibitory function in the nucleus. VACV encodes multiple inhibitors of NF-κB including M2, A46, A52, K7, B14, N1, C4, A49 and E3 [4, 12, 16, 19, 22, 35, 43, 53, 56]. Most of these proteins act prior to NF-κB nuclear translocation. For example, M2, A46, A52, K7 and E3 proteins inhibit cytoplasmic proteins that stimulate IKK [4, 22, 43, 44, 53]. B14 binds to cytoplasmic IKK and inhibits its activation [12]. N1 has also been reported to interact with the IKK complex [16]. However, this interaction has been disputed [12]. Similarly, C4 acts at a step at or downstream of IKK activation but prior to NF-kB nuclear translocation [19]. A49 prevents IκBα ubiquitination and degradation by binding to cytoplasmic βTcRP [35]. Thus, K1 is the first VACV protein to act in the nucleus to prevent NF-κB activation. K1 is unique also because the other known NF-κB inhibitory proteins expressed by VACV do not possess ARDs [58]. It should be noted that Sumner et al. reported that an as-yet-unidentified early VACV protein inhibits an NF-κB signal transduction event that occurs post-RelA nuclear translocation [62]. The construct used for their studies (vv811ΔA49) lacks *K1L*, suggesting that K1 may not be the sole VACV protein that has antagonistic function in the nucleus.

The sub-cellular location of K1 was studied here for the first time. It was present in both the cytoplasm and nucleus of unstimulated and stimulated cells. Because K1 is a small protein (31 kDa), it may be able to enter the nucleus by diffusion [66]. No obvious nuclear localization sequence (NLS) is present in K1. Two other ARD-containing

proteins (myxoma virus M150 protein and cellular IκBα) use an ARD repeat to localize to the nucleus [8]. Thus, a similar mechanism for K1 may be present, which is a future direction for our research.

K1 was identified as a host range gene over 30 years ago [18, 47]. Other functions have been ascribed to K1, including binding to the VACV C10 protein [36], ACAP2 [38], and SAMD9 [57]. K1 also inhibits PKR activation [68, 69], and inhibits a cellular factor whose expression is controlled by IRF1 [37]. These functions map to different regions of K1. For example, K1 residues 47, 51, 82, 83 and 85 are important for vaccinia virus replication in HeLa cells, a cell line where either K1 or C7 is sufficient for virus replication [33, 38]. A mutant K1 that no longer allowed virus replication (mutations at residues 82, 83, 85; S2C#2) still interacted with ACAP2, showing that these two molecular functions of K1 were not related to each other [38]. A future direction of our work is to identify the K1 region responsible for RelA acetylation as a means to better understand how K1 inhibits RelA activation.

The ARD is one of the most abundant motifs in nature [40], and these motifs are the basis for protein-protein interactions that control a variety of cellular signal transduction pathways and functions. ARDs are 33-residues in length, comprising two short α-helices which are connected by β-turns [40]. Sequential ARDs in proteins then stack together. Unlike enzymes, ARD-containing proteins do not recognize specific sequences in their target proteins. Instead, their ability to bind to a certain protein is due to the orientation of ARDs that, when stacked together, form a surface that exposes a binding site unique for its target protein [32]. The solving of the crystal structure of K1 revealed novel aspects of this viral ARD in contrast to cellular ARD proteins [33].

Namely, the residues critical for K1's host range function are exposed on the convex surface of its ANK repeats [33]. This makes K1 unusual; all other ARDs use residues in the concave surface to interact with binding partners. DARPINS (new design ANK repeat proteins) are being explored as a novel alternative strategy to monoclonal antibodies to treat diseases such as measles and HIV [20, 54]. DARPINs are an attractive alternative to antibodies as they provide several advantages including absence of aggregation, high stability, smaller size and simpler architecture, low cost production [61]. Thus, the continued exploration of ARDs like K1 may provide a rational basis for improving DARPINS.

2.5 Figures

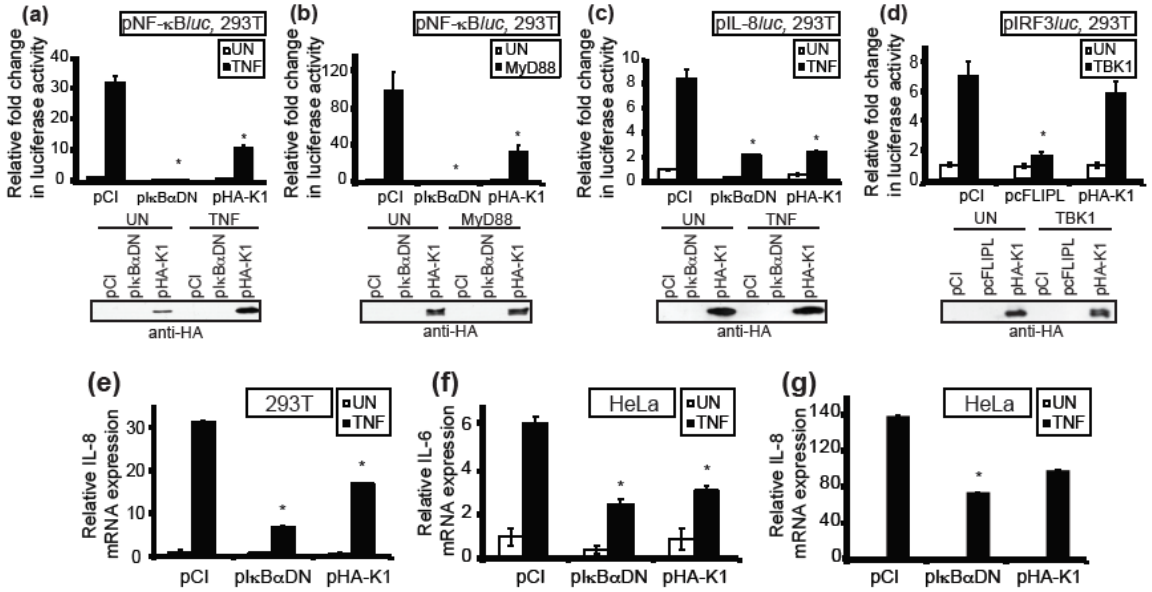

Figure 2.1 The K1 protein inhibits NF-κB activation when expressed independently of infection. (a-d) Luciferase activity detecting NF-κB or IRF3 activation in 293T cells transiently co-transfected with 1000 ng of either empty vector (pCI), pIκBαDN, pHA-K1 or pcFLIP$_L$. Cells were also co-transfected with 12.5 ng pRL-null and 112.5 ng of (a, b) pNF-κB*luc*, (c) pIL8*luc* or (d) pIRF3*luc*. (b) Cells were co-transfected with an additional 500 ng pCI or pMyD88. At 24 h post-transfection, cells were incubated in regular medium (UN) or medium containing 10 ng/mL TNF for 2 h. Cellular lysates were evaluated for luciferase activities. (d) Luciferase activity detecting IRF3 activation in 293T cells transiently co-transfected with 1000 ng of either empty vector (pCI), pcFLIP$_L$ or pHA-K1. In this case, cells were also co-transfected with the reporter plasmids above and 500 ng pCI or pTBK for 24 h [21]. Results are presented as the fold-induction of luciferase activity relative to those of unstimulated, pCI-transfected cells. Lysates were also examined for HA-tagged K1 protein expression. Quantitative RT-PCR analysis of IL-8, IL-6 and β-actin mRNA from (e) 293T or (f, g) HeLa cells that were transfected for 24 h with 1500 ng pCI, pHA-K1 or pIκBαDN and then treated with 20 ng/mL TNF for (e) 4 h, (f) 1 h or (g) 2 h. Results are presented as IL-8 or IL-6 cDNA relative to β-actin cDNA for each sample, and recorded as relative to those of untreated, pCI-transfected cells. These experiments are a representative of experiments performed at least three times. *$P < 0.05$, compared with unstimulated, pCI-transfected cells.

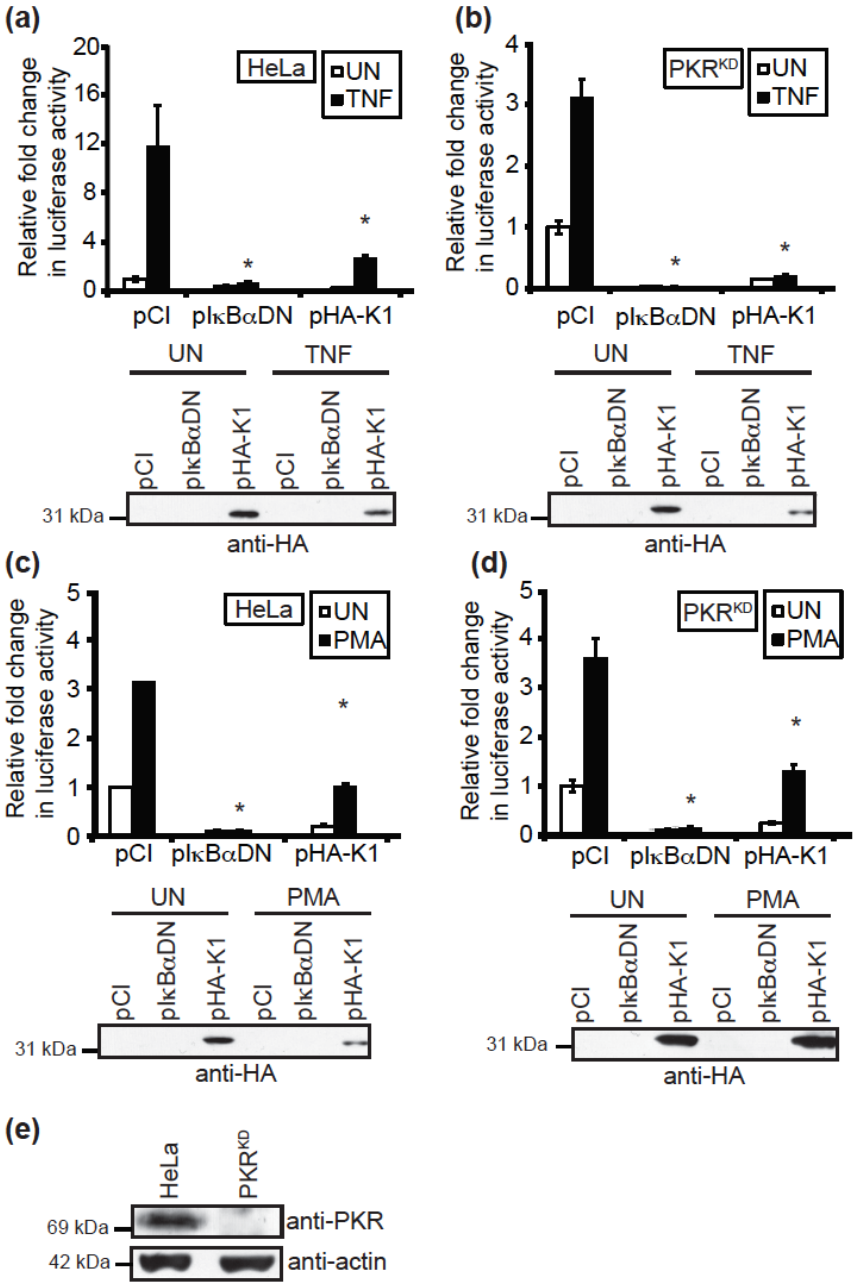

Figure 2.2 K1 inhibits NF-κB activation in a PKR-independent manner. HeLa or PKR^{KD} cells were transfected for 24 h with luciferase reporter plasmids (125 ng pNF-κB*luc*, 12.5 ng pRL-null) and 1000 ng pCI, pIκBαDN or pHA-K1. Next, cells were incubated in regular medium (UN) or medium containing (a) and (b) 10 ng/mL TNF for 2 h or (c) and (d) 50 ng/mL PMA for 8 h. Results are presented as fold-induction of luciferase activity relative to those of untreated, pCI-transfected cells. Lysates were also examined for HA-K1 protein expression. (e) PKR protein levels in HeLa and PKR^{KD} cell lysates. These experiments are a representative of experiments performed at least three times. *$P < 0.05$, compared with unstimulated, pCI-transfected cells.

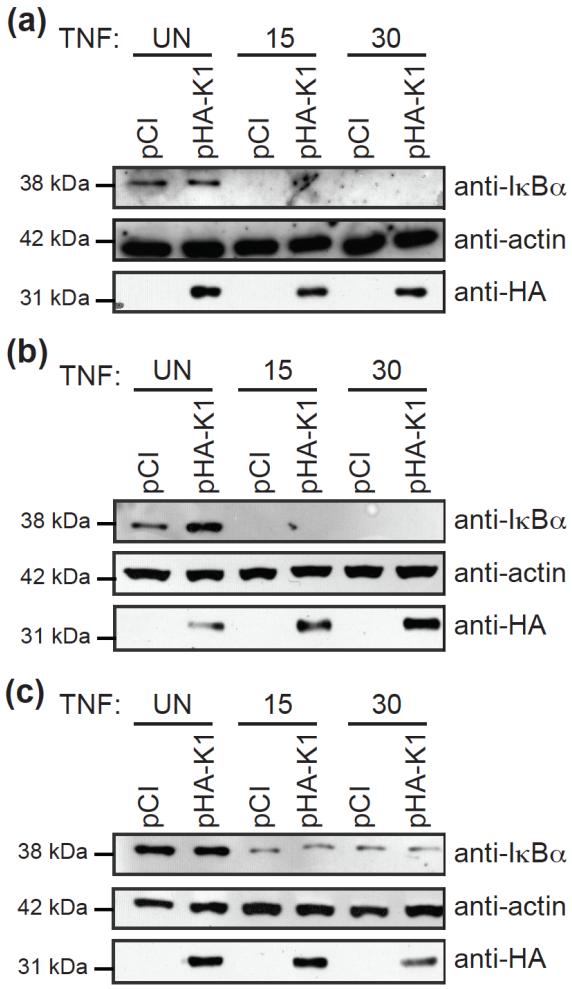

Figure 2.3 IκBα degradation occurs in the presence of K1. (a) 293T (b) HeLa or (c) PKR^{KD} cells were transfected with 2000 ng of pCI or pHA-K1 for 24 h prior to incubation with regular medium (UN) or medium containing 10 ng/mL TNF for 15 or 30 min. Cellular lysates were separated by SDS-PAGE and then transferred to PVDF membranes. Membranes were probed with anti-IκBα antibodies, and then the same blots were re-probed with anti-β-actin antiserum. A separated set of immunoblotted proteins was used to detect HA-K1 protein levels. These experiments are a representative of experiments performed at least three times.

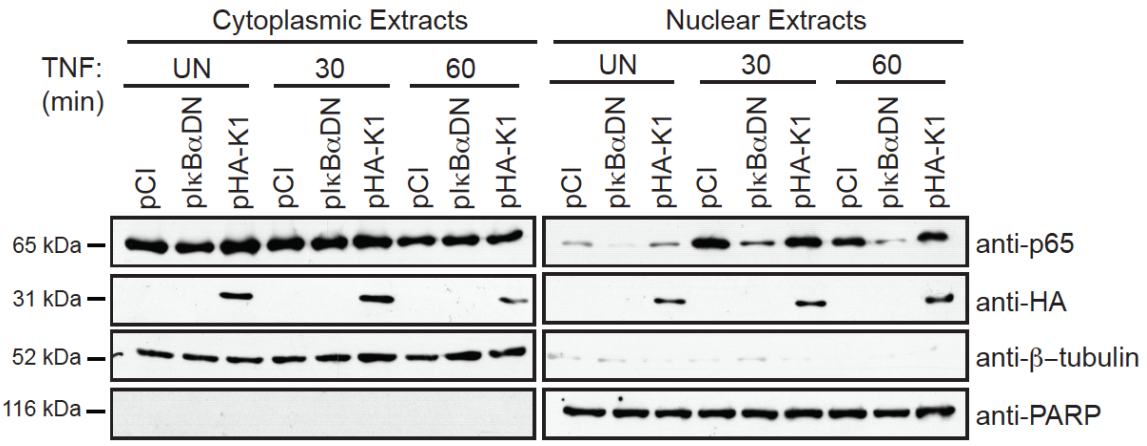

Figure 2.4 NF-κB translocation to the nucleus occurs in the presence of K1. 293T cells were transfected for 24 h with 1500 ng pCI, pIκBαDN or pHA-K1. Cells were incubated in medium either lacking (UN) or containing TNF (20 ng/mL) for 30 or 60 min, and then lysed in a manner that separated cytoplasmic from nuclear proteins. A portion of extracts containing cytoplasmic or nuclear proteins was probed for the presence of the RelA subunit of the NF-κB heterodimer by using immunoblotting. The same samples were also probed for the presence of K1 proteins by immunoblotting. Each sample was also probed with anti-β-tubulin and anti-PARP antibodies to serve as markers of cytoplasmic content and nuclear content, respectively. These experiments are a representative of experiments performed at least three times.

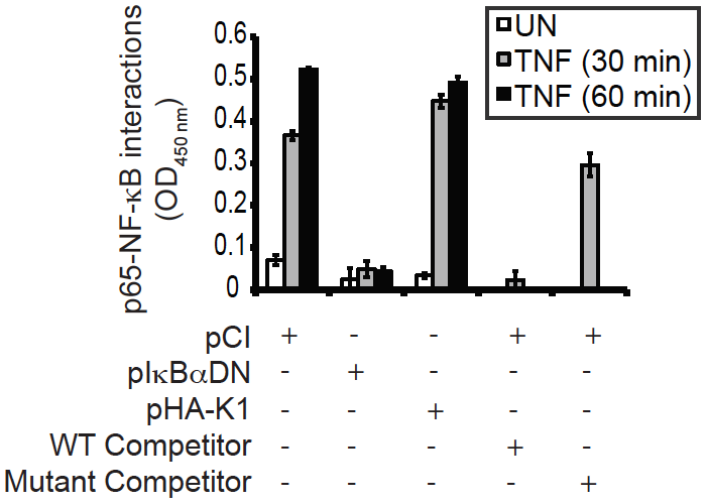

Figure 2.5 The K1 protein allows NF-κB-DNA interactions. ELISA-based analysis of the binding activity of nuclearly-localized NF-κB in 293T cells transfected with pCI, pIκBαDN or pHA-K1. At 24 h post-transfection, cells remained either unstimulated (UN) or stimulated with 20 ng/mL TNF for 30 or 60 min. Cells were lysed and nuclei were isolated. Proteins from isolated nuclei were incubated in 96-well plates containing immobilized oligonucleotides containing consensus NF-κB binding sites. For the extracts collected from pCI-transfected cells after 30 min TNF treatment, extracts were incubated with an excess of oligonucleotides containing a wild type NF-κB consensus sequence (WT competitor) or a mutated consensus sequence (Mutant Competitor) to confirm the specificity of the assay. These oligonucleotides were not added to extracts from cells treated for 60 min with TNF. Regardless, all wells were subsequently incubated with a primary antibody specific for the active form of RelA and an HRP-conjugated secondary antibody. Reactions were quantified by using spectroscopy. Data represent the optical density (OD) average of 3 replicates. These experiments are a representative of experiments performed at least three times.

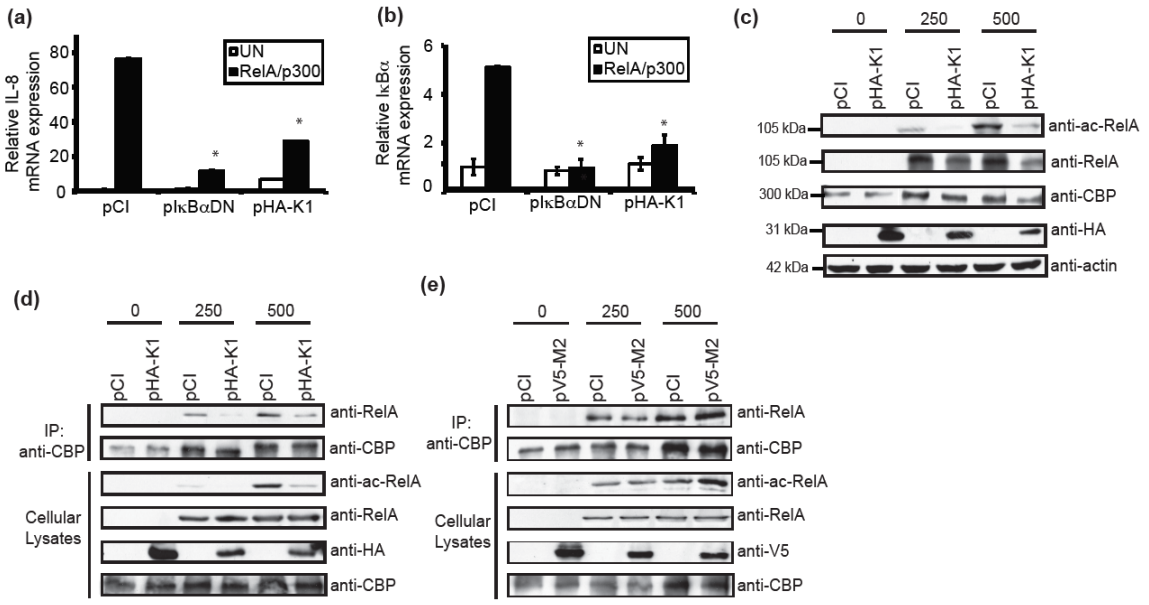

Figure 2.6 The K1 protein inhibits p300/CBP-mediated NF-κB activation and RelA acetylation and RelA-CBP interactions. (a and b) Quantitative RT-PCR (qPCR) analysis of IL-8, IκBα and β-actin mRNA. HeLa cells were co-transfected with 500 ng pCI, pGFP-RelA and pHA-p300 and 1000 ng pCI, pIκBαDN or pHA-K1. At 24h post-transfection, mRNA from lysed cells was reverse-transcribed to cDNA and cDNA was analyzed by using qPCR. Results are presented as (a) IL-8 or (b) IκBα cDNA relative to β-actin cDNA expression for each sample, and recorded as relative to those of unstimulated, pCI-transfected cells. $*P < 0.05$, compared with unstimulated cells transfected with pCI. (c) HeLa or (d and e) PKR^{KD} cell lines were transfected with pCI or 250 or 500 ng pGFP-RelA and pFLAG-CBP and co-transfected with 1000 ng pCI, pHA-K1 or pV5-M2. (c - e) Lysates were probed for the acetyl-RelA (ac-RelA) subunit of NF-κB. The same blots were reprobed with anti-RelA antiserums. A separated set of immunoblotted proteins was used to examine CBP and K1 or M2. (d and e) Co-immunoprecipitation of CBP and RelA. Cells were lysed in ALB and clarified lysates were incubated with anti-CPB antibody and protein G-sepahrose beads. A portion of each lysate prior to immunoprecipitations was saved and used to detect protein expression levels. Beads were washed and then subjected to immunoblotting. Blots were probed with anti-RelA. These experiments are a representative of experiments performed at least three times.

2.6 References

1. Aravalli, R.N., S. Hu, and J.R. Lokensgard, *Inhibition of toll-like receptor signaling in primary murine microglia.* J Neuroimmune Pharmacol, 2008. **3**(1): p. 5-11.

2. Bhatt, D. and S. Ghosh, *Regulation of the NF-kappaB-Mediated Transcription of Inflammatory Genes.* Front Immunol, 2014. **5**: p. 71.

3. Bitra, K., R.J. Suderman, and M.R. Strand, *Polydnavirus Ank proteins bind NF-kappaB homodimers and inhibit processing of Relish.* PLoS Pathog, 2012. **8**(5): p. e1002722.

4. Bowie, A., et al., *A46R and A52R from vaccinia virus are antagonists of host IL-1 and toll-like receptor signaling.* Proc Natl Acad Sci U S A, 2000. **97**(18): p. 10162-7.

5. Burles, K., N. van Buuren, and M. Barry, *Ectromelia virus encodes a family of Ankyrin/F-box proteins that regulate NFkappaB.* Virology, 2014. **468-470**: p. 351-62.

6. Buttigieg, K., et al., *Genetic screen of a library of chimeric poxviruses identifies an ankyrin repeat protein involved in resistance to the avian type I interferon response.* J Virol, 2013. **87**(9): p. 5028-40.

7. Cabanski, M., et al., *PKR regulates TLR2/TLR4-dependent signaling in murine alveolar macrophages.* Am J Respir Cell Mol Biol, 2008. **38**(1): p. 26-31.

8. Camus-Bouclainville, C., et al., *A Virulence Factor of Myxoma Virus Colocalizes with NF- B in the Nucleus and Interferes with Inflammation.* Journal of Virology, 2004. **78**(5): p. 2510-2516.

9. Chang, S.J., et al., *Poxvirus host range protein CP77 contains an F-box-like domain that is necessary to suppress NF-kappaB activation by tumor necrosis factor alpha but is independent of its host range function.* J Virol, 2009. **83**(9): p. 4140-52.

10. Chen, J. and L.F. Chen, *Methods to detect NF-kappaB acetylation and methylation.* Methods Mol Biol, 2015. **1280**: p. 395-409.

11. Chen, L., et al., *Duration of nuclear NF-kappaB action regulated by reversible acetylation.* Science, 2001. **293**(5535): p. 1653-7.

12. Chen, R.A., et al., *Inhibition of IkappaB kinase by vaccinia virus virulence factor B14.* PLoS Pathog, 2008. **4**(2): p. e22.

13. Chen, Z., et al., *Signal-induced site-specific phosphorylation targets I kappa B alpha to the ubiquitin-proteasome pathway.* Genes Dev, 1995. **9**(13): p. 1586-97.

14. da Silva Correia, J. and R.J. Ulevitch, *MD-2 and TLR4 N-linked glycosylations are important for a functional lipopolysaccharide receptor.* J Biol Chem, 2002. **277**(3): p. 1845-54.

15. Diel, D.G., et al., *A nuclear inhibitor of NF-kappaB encoded by a poxvirus.* J Virol, 2011. **85**(1): p. 264-75.

16. DiPerna, G., et al., *Poxvirus protein N1L targets the I-kappaB kinase complex, inhibits signaling to NF-kappaB by the tumor necrosis factor superfamily of receptors, and inhibits NF-kappaB and IRF3 signaling by toll-like receptors.* J Biol Chem, 2004. **279**(35): p. 36570-8.

17. Dreyfus, D.H., et al., *Analysis of an ankyrin-like region in Epstein Barr Virus encoded (EBV) BZLF-1 (ZEBRA) protein: implications for interactions with NF-kappaB and p53.* Virol J, 2011. **8**: p. 422.

18. Drillien, R., F. Koehren, and A. Kirn, *Host range deletion mutant of vaccinia virus defective in human cells.* Virology, 1981. **111**(2): p. 488-99.

19. Ember, S.W., et al., *Vaccinia virus protein C4 inhibits NF-kappaB activation and promotes virus virulence.* J Gen Virol, 2012. **93**(Pt 10): p. 2098-108.

20. Friedrich, K., et al., *DARPin-targeting of measles virus: unique bispecificity, effective oncolysis, and enhanced safety.* Mol Ther, 2013. **21**(4): p. 849-59.

21. Gates, L.T. and J.L. Shisler, *cFLIPL Interrupts IRF3-CBP-DNA Interactions To Inhibit IRF3-Driven Transcription.* J Immunol, 2016. **197**(3): p. 923-33.

22. Gedey, R., et al., *Poxviral regulation of the host NF-kappaB response: the vaccinia virus M2L protein inhibits induction of NF-kappaB activation via an ERK2 pathway in virus-infected human embryonic kidney cells.* J Virol, 2006. **80**(17): p. 8676-85.

23. Gerritsen, M.E., et al., *CREB-binding protein/p300 are transcriptional coactivators of p65.* Proc Natl Acad Sci U S A, 1997. **94**(7): p. 2927-32.

24. Gilbert, S.C., *Clinical development of Modified Vaccinia virus Ankara vaccines.* Vaccine, 2013. **31**(39): p. 4241-6.

25. Hayden, M.S. and S. Ghosh, *Regulation of NF-kappaB by TNF family cytokines.* Semin Immunol, 2014. **26**(3): p. 253-66.

26. Hayden, M.S. and S. Ghosh, *Shared principles in NF-kappaB signaling.* Cell, 2008. **132**(3): p. 344-62.

27. Herbert, M.H., C.J. Squire, and A.A. Mercer, *Poxviral ankyrin proteins.* Viruses, 2015. **7**(2): p. 709-38.

28. Hinz, M., S.C. Arslan, and C. Scheidereit, *It takes two to tango: IkappaBs, the multifunctional partners of NF-kappaB.* Immunol Rev, 2012. **246**(1): p. 59-76.

29. Hinz, M. and C. Scheidereit, *The IkappaB kinase complex in NF-kappaB regulation and beyond.* EMBO Rep, 2014. **15**(1): p. 46-61.

30. Huang, B., et al., *Posttranslational modifications of NF-kappaB: another layer of regulation for NF-kappaB signaling pathway.* Cell Signal, 2010. **22**(9): p. 1282-90.

31. Hyndman, B.D., et al., *E2A proteins enhance the histone acetyltransferase activity of the transcriptional co-activators CBP and p300.* Biochim Biophys Acta, 2012. **1819**(5): p. 446-53.

32. Li, J., A. Mahajan, and M.D. Tsai, *Ankyrin repeat: a unique motif mediating protein-protein interactions.* Biochemistry, 2006. **45**(51): p. 15168-78.

33. Li, Y., et al., *Structure function studies of vaccinia virus host range protein k1 reveal a novel functional surface for ankyrin repeat proteins.* J Virol, 2010. **84**(7): p. 3331-8.

34. Livak, K.J. and T.D. Schmittgen, *Analysis of relative gene expression data using real-time quantitative PCR and the 2(-Delta Delta C(T)) Method.* Methods, 2001. **25**(4): p. 402-8.

35. Mansur, D.S., et al., *Poxvirus targeting of E3 ligase beta-TrCP by molecular mimicry: a mechanism to inhibit NF-kappaB activation and promote immune evasion and virulence.* PLoS Pathog, 2013. **9**(2): p. e1003183.

36. McCraith, S., et al., *Genome-wide analysis of vaccinia virus protein-protein interactions.* Proc Natl Acad Sci U S A, 2000. **97**(9): p. 4879-84.

37. Meng, X., et al., *C7L family of poxvirus host range genes inhibits antiviral activities induced by type I interferons and interferon regulatory factor 1.* J Virol, 2012. **86**(8): p. 4538-47.

38. Meng, X. and Y. Xiang, *Vaccinia virus K1L protein supports viral replication in human and rabbit cells through a cell-type-specific set of its ankyrin repeat residues that are distinct from its binding site for ACAP2.* Virology, 2006. **353**(1): p. 220-33.

39. Mohamed, M.R., et al., *Proteomic screening of variola virus reveals a unique NF-kappaB inhibitor that is highly conserved among pathogenic orthopoxviruses.* Proc Natl Acad Sci U S A, 2009. **106**(22): p. 9045-50.

40. Mosavi, L.K., et al., *The ankyrin repeat as molecular architecture for protein recognition.* Protein Sci, 2004. **13**(6): p. 1435-48.

41. Moss, B., *Poxviridae* 6th ed. Fields Virology, ed. P.M.H. David M. Knipe. Vol. 2. 2013: Lippincott williams & Wilkins.

42. Mukherjee, S.P., et al., *Analysis of the RelA:CBP/p300 interaction reveals its involvement in NF-kappaB-driven transcription.* PLoS Biol, 2013. **11**(9): p. e1001647.

43. Myskiw, C., et al., *Vaccinia virus E3 suppresses expression of diverse cytokines through inhibition of the PKR, NF-kappaB, and IRF3 pathways.* J Virol, 2009. **83**(13): p. 6757-68.

44. Oda, S., M. Schroder, and A.R. Khan, *Structural basis for targeting of human RNA helicase DDX3 by poxvirus protein K7.* Structure, 2009. **17**(11): p. 1528-37.

45. Oie, K.L. and D.J. Pickup, *Cowpox virus and other members of the orthopoxvirus genus interfere with the regulation of NF-kappaB activation.* Virology, 2001. **288**(1): p. 175-87.

46. Orphanides, G., T. Lagrange, and D. Reinberg, *The general transcription factors of RNA polymerase II.* Genes Dev, 1996. **10**(21): p. 2657-83.

47. Perkus, M.E., et al., *Insertion and deletion mutants of vaccinia virus.* Virology, 1986. **152**(2): p. 285-97.

48. Randall, C.M., et al., *Inhibition of interferon gene activation by death-effector domain-containing proteins from the molluscum contagiosum virus.* Proc Natl Acad Sci U S A, 2014. **111**(2): p. E265-72.

49. Randall, C.M., J.A. Jokela, and J.L. Shisler, *The MC159 Protein from the Molluscum Contagiosum Poxvirus Inhibits NF-kappaB Activation by Interacting with the IkappaB Kinase Complex.* Journal of immunology, 2012. **188**(5): p. 2371-9.

50. Revilla, Y., *Inhibition of Nuclear Factor kappa B Activation by a Virus-encoded Ikappa B-like Protein.* Journal of Biological Chemistry, 1998. **273**(9): p. 5405-5411.

51. Sanchez-Sampedro, L., et al., *The evolution of poxvirus vaccines.* Viruses, 2015. **7**(4): p. 1726-803.

52. Scherer, D.C., et al., *Signal-induced degradation of I kappa B alpha requires site-specific ubiquitination.* Proc Natl Acad Sci U S A, 1995. **92**(24): p. 11259-63.

53. Schroder, M., M. Baran, and A.G. Bowie, *Viral targeting of DEAD box protein 3 reveals its role in TBK1/IKKepsilon-mediated IRF activation.* Embo j, 2008. **27**(15): p. 2147-57.

54. Schweizer, A., et al., *CD4-specific designed ankyrin repeat proteins are novel potent HIV entry inhibitors with unique characteristics.* PLoS Pathog, 2008. **4**(7): p. e1000109.

55. Sette, A., et al., *Definition of epitopes and antigens recognized by vaccinia specific immune responses: their conservation in variola virus sequences, and use as a model system to study complex pathogens.* Vaccine, 2009. **27 Suppl 6**: p. G21-6.

56. Shisler, J.L. and X.L. Jin, *The vaccinia virus K1L gene product inhibits host NF-kappaB activation by preventing IkappaBalpha degradation.* J Virol, 2004. **78**(7): p. 3553-60.

57. Sivan, G., et al., *Identification of Restriction Factors by Human Genome-Wide RNA Interference Screening of Viral Host Range Mutants Exemplified by Discovery of SAMD9 and WDR6 as Inhibitors of the Vaccinia Virus K1L-C7L-Mutant.* MBio, 2015. **6**(4): p. e01122.

58. Smith, G.L., et al., *Vaccinia virus immune evasion: mechanisms, virulence and immunogenicity.* J Gen Virol, 2013. **94**(Pt 11): p. 2367-92.

59. Sonnberg, S., et al., *Poxvirus ankyrin repeat proteins are a unique class of F-box proteins that associate with cellular SCF1 ubiquitin ligase complexes.* Proc Natl Acad Sci U S A, 2008. **105**(31): p. 10955-60.

60. Sperling, K.M., et al., *The highly conserved orthopoxvirus 68k ankyrin-like protein is part of a cellular SCF ubiquitin ligase complex.* Virology, 2008. **374**(2): p. 234-9.

61. Stumpp, M.T. and P. Amstutz, *DARPins: a true alternative to antibodies.* Curr Opin Drug Discov Devel, 2007. **10**(2): p. 153-9.

62. Sumner, R.P., et al., *Vaccinia virus inhibits NF-kappaB-dependent gene expression downstream of p65 translocation.* J Virol, 2014. **88**(6): p. 3092-102.

63. Takada, Y., et al., *Genetic deletion of PKR abrogates TNF-induced activation of IkappaBalpha kinase, JNK, Akt and cell proliferation but potentiates p44/p42 MAPK and p38 MAPK activation.* Oncogene, 2007. **26**(8): p. 1201-12.

64. Van Antwerp, D.J. and I.M. Verma, *Signal-induced degradation of I(kappa)B(alpha): association with NF-kappaB and the PEST sequence in I(kappa)B(alpha) are not required.* Mol Cell Biol, 1996. **16**(11): p. 6037-45.

65. van Buuren, N., et al., *Ectromelia virus encodes a novel family of F-box proteins that interact with the SCF complex.* J Virol, 2008. **82**(20): p. 9917-27.

66. Wang, R. and M.G. Brattain, *The maximal size of protein to diffuse through the nuclear pore is larger than 60kDa.* FEBS Lett, 2007. **581**(17): p. 3164-70.

67. Werden, S.J., et al., *The myxoma virus m-t5 ankyrin repeat host range protein is a novel adaptor that coordinately links the cellular signaling pathways mediated by Akt and Skp1 in virus-infected cells.* J Virol, 2009. **83**(23): p. 12068-83.

68. Willis, K.L., J.O. Langland, and J.L. Shisler, *Viral dsRNAs from vaccinia virus early or intermediate gene transcripts possess PKR activating function, resulting in NF-{kappa}B activation, when the K1 protein is absent or mutated.* J Biol Chem, 2011.

69. Willis, K.L., et al., *The effect of the vaccinia K1 protein on the PKR-eIF2alpha pathway in RK13 and HeLa cells.* Virology, 2009. **394**(1): p. 73-81.

70. Yim, H.C. and B.R. Williams, *Protein kinase R and the inflammasome.* J Interferon Cytokine Res, 2014. **34**(6): p. 447-54.

71. Zamanian-Daryoush, M., et al., *NF-kappaB activation by double-stranded-RNA-activated protein kinase (PKR) is mediated through NF-kappaB-inducing kinase and IkappaB kinase.* Mol Cell Biol, 2000. **20**(4): p. 1278-90.

72. Zhang, P., B.L. Jacobs, and C.E. Samuel, *Loss of protein kinase PKR expression in human HeLa cells complements the vaccinia virus E3L deletion mutant phenotype by restoration of viral protein synthesis.* J Virol, 2008. **82**(2): p. 840-8.

73. Zhou, Y., et al., *Double-stranded RNA-dependent protein kinase (PKR) is downregulated by phorbol ester.* FEBS J, 2005. **272**(7): p. 1568-76.

Chapter 3: Deletion of the *K1L* gene results in a vaccinia virus that is less pathogenic due to muted innate immune responses, yet still elicits protective immunity

3.1 Introduction

Vaccinia virus (VACV) is a large, double-stranded DNA virus that encodes nearly 200 genes [45]. VACV was used as the vaccine to eradicate smallpox. The continued study of VACV remains important because there are reports of VACV infections in animals and humans [15, 33, 58]. Moreover, VACV derivatives are now being used as vectors for vaccines against other infectious diseases and as oncolytic virotherapy [54].

The vaccinia K1 protein is an intracellular 31-kDa protein encoded by the *K1L* gene. *K1L* was initially described as a host range factor because its expression is required for VACV replication in rabbit and hamster cell lines [19, 48]. It is now known that K1 possesses other functions that antagonize the immune response. K1 is known to antagonize NF-κB [10, 57], PKR [76, 77], IRF1 [42] and type I IFN [44] signal transduction pathways. There are several cellular and viral binding partners of K1, including the vaccinia C10 protein [41], and the cellular ACAP2 [8] and SAMD9 proteins [59]. However, it is not clear how such interactions may aid in K1 immune evasion. K1 possesses 9 ankyrin repeat domains (ARDs), motifs that mediate protein-protein interactions [34]. While poxviruses encode multiple ARD proteins [29], K1 lacks a C-terminal F-box present in nearly all other poxvirus ARDs [29]. This suggests that K1 may have physiological properties unique from other poxviral ARDs.

Despite this vast knowledge of K1, only one publication examines the role of K1 in pathogenesis [38]. Liu *et al*. show that deletion of the *K1L* gene attenuates VACV strain TianTan as measured by weight loss and neurovirulence in intradermal and

intracranial routes of infection [38]. Unfortunately, the parental strain used by Liu *et al*. lacked additional genes involved in vaccinia virus immune evasion (*A53R*, *C12L*) or morphogenesis (*A33L*) [38], making it difficult to assess the specific contributions of K1 to VACV pathogenesis.

To fill this gap in knowledge, the contribution of the *K1L* gene to viral pathogenicity was examined here by deleting only the *K1L* gene (vΔK1L) from VACV western reserve (WR) strain, the strain that is most often used for pathogenesis studies [60]. We show here that a virus lacking the *K1L* gene was less pathogenic than the parental VACV strain WR (designated vK1L) when using either the intranasal (IN) or intradermal (ID) ear pinnae inoculation models of infection [72, 75]. The ID model of infection was then further investigated because it is argued that, in humans and in mice, intradermal infection of the skin comes closest to the most relevant natural route of infection with VACV [33]. Interestingly, vΔK1L replicated to the same extent as vK1L, suggesting that pathogenicity was not due to diminished viral loads. Instead, the decreased pathogenicity of vΔK1L correlated with a diminished leukocyte infiltration and muted immune gene expression to infection in ears, as measured by flow cytometry and RT-qPCR, respectively. These results suggested that the decreased pathogenicity of vΔK1L was due to a muted immune response, which in turn strengthens the concept that immunopathology plays a role in poxvirus-induced diseases. Despite this muted response by components of the innate immune response, vΔK1L infection still induced VACV-specific $CD8^+$ T cells and protected against a lethal VACV challenge. Thus, vΔK1L had a decreased pathogenicity that nevertheless stimulated protective immune responses. vΔK1L may be a valuable tool to further understand the relationship between viral

pathogenesis, viral modulation of innate immunity and stimulation of protective immune responses.

3.2 Materials and Methods

Viruses and cells

Vaccinia virus strain Western Reserve (referred to as vK1L in this manuscript) and vΔK1L were obtained from Dr. Bernard Moss (Laboratory of Viral Disease, National Institutes of Health). vΔK1L was described previously; it is a Western Reserve (WR) virus in which the *K1L* gene was replaced with the *E. coli gpt* gene by homologous recombination [57]. vK1Lrev is a recombinant virus in which the WR *K1L* gene was re-inserted into vΔK1L at its natural locus. To create vK1Lrev, a DNA amplicon containing the entire *K1L* gene and flanking regions was PCR amplified from WR DNA using oligonucleotide primers (5'-GGGATATTAAGTGCATAGCC-3') and (5'-CCGGAAGATCGCTATCG-3'). vK1Lrev was generated by homologous recombination, in which the *K1L* gene replaced the E. coli *gpt* gene. RK13 cells, which are non-permissive for vΔK1L infection [68], were infected with vΔK1L and then transfected with the K1L-containing amplicon. Thus, only recombinant viruses now stably expressing the *K1L* gene are expected to replicate in RK13 cells [63]. Inoculated cellular monolayers were incubated for 48 h and progeny viruses were isolated by plaque picking and subjected to four rounds of purification. The correct insertion of *K1L* was verified by using PCR analysis of purified viral genomes from recombinant viruses, using two primer sets (5'-CGGTTCCCATGATGAACGTAG-3') and (5'-CCCATAGAACATCAGTCTCC-3') and (5'-CATGCCGTCATGCTTAATG-3') and

(5'-TCACGCCATAACTACCACG-3'). In addition, verification of the presence of *K1L* gene in vK1Lrev viruses were PCR amplified using (5'-GGGATATTAAGTGCATAGCC-3') and (5'-CCGGAAGATCGCTATCG-3'), and the resultant amplicon was sequence analyzed. vΔK1LΔC7L, which lacks both the *K1L* and *C7L* genes, was obtained from Dr. Yan Xiang (University of Texas Health Science Center)[43].

Vero, BSC-1, mouse embryo fibroblasts (MEFs) and RK13 cells were cultured in Eagle's minimal essential media (MEM) supplemented with 10% FBS and 2mM L-glutamine. Virus medium (MEM supplemented with 2.5% FBS) was used for virus absorption phases and for virus infections. Viruses used for inoculation of mice were purified by sucrose density gradient centrifugation.

In vitro growth curves

One-step and multi-step growth curves were performed as follows. Confluent MEF cellular monolayers were infected with vK1L, vΔK1L, vK1Lrev or vΔK1LΔC7L at a multiplicity of infection (MOI) of 0.01 or 10 PFU/cell. After the initial absorption phase, cellular monolayers were washed three times to remove unattached viruses. At the indicated times post-infection, cellular supernatants were removed to a new tube. Supernatants were subjected to centrifugation (800 x g for 10 min at 4°C) and cell-free supernatants were transferred to new tubes. Cellular monolayers were collected by scraping into 1 ml virus medium. Samples were centrifuged at 800 x g for 10 min at 4°C. Cellular pellets were resuspended in 1 ml of virus medium. For all samples, cells or supernatants were lysed by freeze-thawing three times. Samples were sonicated to

release virions from cellular debris. Cellular lysates or supernatants were serially diluted, and 0.5 ml of each dilution was inoculated onto Vero cell monolayers in duplicate. At 48 h later, plaques were visualized by staining cellular monolayers with a crystal violet dye-based solution. Data are expressed as the mean titer per sample +/- SEM.

Murine intranasal and intradermal models of infection

Female BALB/c and C57BL/6 mice (6-8 weeks old) were purchased from The Jackson Laboratory (Bar Harbor, ME) and housed in AAALAC-approved ABL-2 facilities at the University of Illinois at Urbana-Champaign (UIUC). All animal experiments and procedures were approved by the Institutional Animal Care and Use Committee at the UIUC.

For intranasal (IN) inoculations, BALB/c mice (n = 5 per group) were anesthetized by isofluorane (5% in O_2) inhalation using a vaporizer unit (Vetland, Louisville, KY). Mice were inoculated with 10^4 or 10^5 PFU in 20 μl (10 μl per nostril) of vK1L, vΔK1L, vK1Lrev or PBS. Mice were weighed and monitored for signs of illness daily as a means to evaluate severity of infection [69]. Weight data were expressed as the percentage of the mean of each individual animal's weight loss from day 0. Mice that lost more than 25% of their original weight were euthanized. A clinical score for each mouse was assigned daily, based on a metric published by Berhanu et al [6] to assess sickness. Briefly, the scoring was: 0 = normal; 1 = slightly ruffled fur; 2 = significantly ruffled fur; 3 = score 2 combined with hunched posture and/or conjunctivitis; 4 = score 3 combined with difficulty breathing, socializing and/or moving; and 5 = death. Clinical scores are expressed as the mean of each group.

For intradermal (ID) inoculations, anesthetized C57BL/6 mice (n = 5 per group) were inoculated ID in the left ear dorsal pinna with 10^4 PFU of vK1L, vΔK1L, or vK1Lrev in a 10 μl volume using a Hamilton syringe (Reno, NV) and 27-gauge needle as described previously [71, 72]. Infected ears were examined daily for the next 21 days for the presence of lesions. The lesion size was measured by using a 0.01 mm digital caliper (Neiko Tools, Homewood, IL). Lesion size is expressed as the mean of the group +/- SEM.

In some cases, ID-inoculated mice were challenged with a lethal dose of vaccinia virus as a model for protective vaccination [32]. Here, C57BL/6 mice (n = 5 per group) were inoculated ID as described above with PBS or 10^4 PFU of vK1L or vΔK1L. At 30 days post-infection, mice were inoculated IN with vK1L (5×10^6 PFU) in a 20 μl volume, and mice were weighed daily for 7 days post-infection. Weight data were expressed as the percentage of the mean of each individual animal's weight loss from day 0. Mice that lost more than 25% of their original weight were euthanized.

Virus titers in tissues

To assess virus replication in organs after IN inoculations, organs (brains, lungs, spleens) were harvested at 2, 4 and 6 d post infection (pi)(n = 5 mice per experimental group). Organs were flash-frozen in liquid nitrogen. Whole organs were thawed on ice, weighed, and then homogenized in 0.5 ml of virus medium using a 1 ml Dounce homogenizer (Wheaton, Millville NJ). Homogenates were subjected to three freeze-thaw cycles and sonicated. Lysates were serially diluted and 0.5 ml of a dilution was used to inoculate Vero cellular monolayers in duplicate. At 48 h later, viral titers were detected

by plaque assays. Virus titers are expressed as the amount of infectious virus per gram of tissue.

To determine virus replication during ID infections, ears were harvested at 1, 3, 5, 8, or 11 d post-infection (n = 5 mice per experimental group) and flash frozen in liquid nitrogen. Ears were thawed on ice, weighed and placed in 2 ml RB sample tubes (Qiagen, Valencia, CA) with 0.5 ml of virus media and a sterile 7 mm stainless steel bead (Qiagen, Valencia, CA). Samples were subjected to two homogenization rounds at 50 Hz for 3 min using a TissueLyser LT (Qiagen, Valencia, CA). Lysates were serially diluted, and 0.5 ml of a dilution was used to inoculate Vero cellular monolayers in duplicate. At 48 h later, viral titers were detected by plaque assays. Virus titers were expressed as the amount of infectious virus per gram of tissue.

RT-qPCR analysis of host genes from infected ears

Left ears were inoculated ID with vK1L, vΔK1L, vK1Lrev or PBS (n = 4 mice per group) as described above. Ears were collected at 1, 3 or 5 d post-infection and flash frozen in liquid nitrogen. Each frozen ear was cut into two equal parts, and each piece was placed into a sterile tube that previously was incubated in a dry ice/ethanol bath for 15 min to minimize RNA degradation. Each tube also contained a sterile 7 mm stainless steel bead (Qiagen, Valencia, CA). Next, tubes were placed in the TissueLyser LT (Qiagen, Valencia, CA) for 2 min at room temperature prior to adding 0.6 ml of RLT lysis buffer containing 1% 2-mercaptoethanol to each tube. Samples were homogenized using the TissueLyser LT at 50 Hz for 3 min at room temperature. Tubes were then mixed by inverting, and subjected to another round of homogenization. Homogenates

from each ear half were combined into one tube and centrifuged at 18,000 x g for 3 min. Supernatants were transferred to new tubes and one volume of 70% ethanol was added. Total RNA was extracted from samples using the Qiagen RNeasy kit (Qiagen, Valencia, CA). RNA was quantified and the integrity of the RNA was assessed by using a 48 capillary Fragment Analyzer (Advanced Analytical Technologies, Ankeny, IA).

Two μg of RNA from each ear sample was reverse transcribed to cDNA as follows. Briefly, total RNA was incubated with 0.5 μg of oligo dT primer (IDT, Coralville, IA) and (M-MulV) Reverse Transcriptase (New England BioLabs, Ipswitch, MA) at 70° C for 5 min, followed by a 5 min incubation at 4°C, as per manufacturer's instructions. cDNA was submitted to the Carver Biotechnology Center at the University of Illinois at Urbana-Champaign for further analyses. Briefly, all cDNA samples underwent standard target amplification, in which 1.25 μl of cDNA was incubated with 2.5 μl 2X TaqMan PreAmp Master Mix (Thermo Fisher) and 0.5 μl 0.2X TaqMan primer probe mix (Thermo Fisher). The primer probes used are as follows: *ccl4* (Mm00443111_m1), *cxcl2* (Mm00436450_m1), *cxcl5* (Mm00436451_g1), *ccl2 (*Mm00441242_m1), *ccl5* (Mm01302427_m1), *cxcl9* (Mm00434946_m1), *cxcl10* (Mm00445235_m1), *cxcl1* (Mm04207460_m1), *il1b* (Mm00434228_m1), *il6* (Mm00446190_m1), *il10* (Mm01288386_m1), *il7* (Mm01295803_m1), *tnf* (Mm00443258_m1), *ifng* (Mm01168134_m1), *ifna4* (Mm00833969_s1), *ifnb* (Mm00439552_s1), *isg15* (Mm01705338_s1), *Rnase1* (Mm00712008_m1), *mx1* (Mm00487796_m1), *eif2ak2* (Mm01235643_m1), *krt6a* (Mm00833464_g1), *krt16* (Mm01306670_g1), *nfkb2* (Mm00479807_m1), *nfkbia* (Mm00477798_m1), *gapdh* (Mm99999915_g1). Reactions were incubated at 95°C for 10 min, followed by 14 cycles

of 95°C for 15 sec and 60°C for 4 min using the MJ Research Tetrad thermal cycler (MJ Research, Waltham, MA). A portion of each reaction was then incubated with TaqMan FAM-MGB probes specific for each mouse gene shown in Table 1 (Thermo Fisher Scientific). Aliquots (5 μl) of each sample were loaded onto a Fluidigm 48.48 Dynamic Array integrated fluidic circuit (IFC) chip (Fluidigm) according to manufacturer's directions. qPCR was performed in a Biomark HD Real-Time PCR (Fluidigm) using the following thermal conditions: 70°C for 30 min, 25°C for 10 min, 95°C for 1 min, followed by 35 cycles of 96°C for 5 sec and 60°C for 20 sec.

Analysis of data was performed using Fluidigm Real Time PCR Analysis version 4.1.3. The averaged mRNA expression (fold-induction) per group was quantified by calculating the $2^{-\Delta\Delta CT}$ value for each ear and then averaging these values, with values from time-matched mice inoculated with PBS as the calibrator for each day, and GAPDH or HPRT1 (data not shown) as the reference gene. Values were compared between ears infected with vK1L versus vΔK1L, or PBS versus vK1L, or PBS versus vΔK1L, or PBS versus vK1Lrev.

Ultrasound analysis of ID-inoculated mouse ears

C57BL/6 mice were inoculated ID with vK1L, vΔK1L or PBS or not inoculated as described above. All mice were anesthetized using isofluorane and ears were imaged with the VisualSonics Vevo2100 (VisualSonics, Toronto, CA) high-frequency ultrasonic imaging system, using the MS-550S linear array, in dorsal recumbency at the days indicated post-infection. The Vevo2100 acquired the raw radio-frequency (RF) image data from which (off-line) B-mode images were processed from each ear, and from those images, the ear thicknesses were estimated. Also from each B-mode image, a Field of

Interest (FOI; pink line in Fig. 6A) was manually segmented to denote the region where the backscatter coefficient (BSC) was estimated and represented as a color-coded BSC image. The BSC is a quantitative ultrasound (QUS) measure of the B-mode echo strength. To generate the BSC image, the FOI was divided into 75%-overlapped sub-Regions of Interest (sub-ROIs) with dimensions 193 μm x 193 μm (equivalent to 4 x 4 wavelengths at 32 MHz). For each sub-ROI a BSC value was estimated using the reference phantom technique [37, 78], thus yielding a BSC versus ultrasonic frequency curve. Each sub-ROI's BSC value was generated by averaging BSC over the frequency range from 25 to 43 MHz, denoted BSC (25-43 MHz), with a color then assigned to each BSC (25-43 MHz) value. To represent each ear with a single BSC value, all the sub-ROI BSC image values within the FOI were averaged (averaged over space, spatial average); these single BSC values were averaged and then graphically represented. The thickness of the ear was selected from the spatially calibrated BSC image (Fig. 6A) for which the pixel dimension was known (68 x 68 pixels = 1 mm x 1 mm). The number of pixels was estimated in the region of the BSC image that depicted the thickest measure of the color-coded image.

Histopathology

C57BL/6 mice were inoculated ID with vK1L, vΔK1L or PBS or not inoculated as described above. Mice (n = 3 per group) were euthanized on days 3, 4, or 5 post-infection. Ears were collected and fixed in 10% neutral buffered formalin. Three sections of each ear were taken from the inoculation site and routinely processed, paraffin-

embedded, sectioned, deparaffinized and stained with hematoxylin and eosin. Representative microscopic images are shown.

Analysis of immune cell infiltration in infected ears

Female C57BL/6 mice were inoculated ID in the left ear with vK1Lrev, vΔK1L or PBS as described above (n = 7 for vK1L, n = 7 for vΔK1L; n = 10 for PBS). Mice were euthanized on day 5 post-infection. Each inoculated ear was collected and the dorsal and ventral sheets were separated with forceps, and incubated with type I collagenase (3 mg/mL; Worthington Biochemicals, Lakewood, NJ) and deoxyribonuclease I (1.25 U/mL; Worthington Biochemicals, Lakewood, NJ) for 1 hr at 37° C. Each sample was then passed through a 70 μm nylon cell strainer to produce single cell suspensions. Cells from each ear were counted via trypan blue exclusion to determine total number of cells per ear and to ensure cellular viability. Because so few immune cells were present from each PBS-inoculated ear, cells from PBS-inoculated ears were combined to have enough cells for sufficient analyses. For the rest of the ears, there were sufficient immune cells, and cells from each ear were kept separate. The pooled cells from PBS-inoculated ears or cells from each infected ear were incubated with Fc-block (Biolegend, San Diego, CA) for 15 min, and then incubated in a solution of antibodies in the presence of Fc-block and 10% mouse serum (Jackson ImmunoResearch, West Grove, PA) for 1 hr. Antibodies were CD45-eFluor450 (clone 30-F11; 1:400; eBioscience, Waltham, MA), CD11b-PE (clone M1/70; 1:200; BioLegend, San Diego, CA), CD11c-Alexa488 (clone N418; 1:100; BioLegend), Ly6C-Alexa700 (clone AL-21; 1:200; BD Bioscience, San Jose, CA) and Ly6G-PECy7 (clone 1A8; 1:200; BD Bioscience). All sample acquisition and

compensation was performed using a BD LSRII flow cytometer (BD Bioscience). Data were analyzed with FCS Express Software (DeNovo Software, Version 5, Glendale, CA). Events were gated on live cells using forward vs. side scatter. Dead cells were excluded on the basis of atypical fluorescence. Fluorescence minus one (FMO) was used to aid in gating of appropriate cellular populations. Leukocytes were identified as $CD45^+$. We defined tissue-protective monocytes as $CD45^+CD11b^+CD11c^-LyC6^+Ly6G^+$. Inflammatory monocytes were defined as $CD45^+CD11b^+CD11c^-LyC6^+Ly6G^-$ cells. $CD45^+CD11c^+$ cells were also investigated, and these cells include dendritic cells, NK cells and activated T cells. To account for the fact that there were different number of total cellular infiltrates obtained from PBS- vs. vK1Lrev- vs. vΔK1L-infected ears, the percent populations of different immune cells were then multiplied by the number of total cells per ear to obtain total number of each immune cell population examined per ear. Data were expressed as the mean number of cells +/- SEM per ear.

Detection of VACV-specific, IFN-γ expressing $CD8^+$ T cells

C57BL/6 mice were inoculated ID with vK1L, vΔK1L or PBS (n = 5 mice per experimental group) as described above. At 10 d post-infection, mice were euthanized and spleens and livers were harvested. Single-cell suspension of spleens and lymph nodes were prepared as follows. Spleens were forced through a 70 μM nylon mesh (Thermo Fisher Scientific, Waltham, MA) and then erythrocytes were removed by treating sample with ACK red cell lysis buffer. Lymph nodes were homogenized by using a BioMasher II disposable microtube homogenizer (Research Products International, Mt. Prospect, IL).

Single cell suspensions (10^6 cells) of spleens or lymph nodes from each animal were kept separate, and cells from each spleen or lymph node were either unstimulated or stimulated with VACV-specific peptide (TSYKFESV; $B8R_{20-27}$ epitope) for 4 hours in the presence of Brefeldin A (5 μg/mL; Sigma, St. Louis, MO). Using this approach, only $CD8^+$ T cells recognizing VACV peptides would become activated. Then, cells were stained with FITC-conjugated anti-CD8 antibody (clone 53-6.7; 1:100; BioLegend) in Cell Staining Buffer (BioLegend, San Diego, CA) for 30 min on ice to stimulate VACV-specific T cells. Next, samples were fixed for 20 min at room temperature and permeabilized on ice in fixation and intracellular staining permeabilization buffer (BioLegend, San Diego, CA), respectively. Cells were stained for intracellular IFN-γ as a marker of T cell activation by incubating fixed cells with Alexa 647-conjugated anti-IFN-γ (clone XMG1.2; 1:100; BioLegend, San Diego, CA) overnight at 4° C. Samples were washed in permeabilization buffer. Flow cytometry was performed with a BD Accuri C6 cytometer (BD Bioscience, San Jose, CA), and data was analyzed with FCS Express Software (DeNovo Software, Version 5, Glendale, CA). Events were gated for live lymphocytes on forward versus side scatter. Dead cells were excluded on the basis of atypical fluorescence. Data were expressed as the percentage of $IFN\gamma^+CD8^+$ T cells, cells that are considered VACV-specific and activated, out of all $CD8^+$ T cells. In addition, data were expressed as the total number of $IFN\gamma^+CD8^+$ T cells per lymph node or spleen.

Statistical analysis

To determine statistically significant differences between weight loss and lesion sizes during vK1L and vΔK1L infection, two-way ANOVA followed by Tukey's

multiple comparisons test was performed. For viral replication in the lungs, brain and spleen, the non-parametric Kruskal-Wallis test followed by Dunn's multiple comparison test was used to determine statistically significant difference between vK1L and vΔK1L. To determine statistical significant differences in immune cell infiltration between vK1Lrev and vΔK1L one-way ANOVA or Kruskal-Wallis test followed by Tukey's or Dunn's multiple comparison tests, respectively, was performed. For the analyses of RT-qPCR assays, one-way ANOVA was used to determine if there were statistically significant differences between ears infected with vK1L versus vΔK1L, or PBS versus vK1L, or PBS versus vΔK1L, or PBS versus vK1Lrev. To determine if there were statistically significant differences in T cell responses between vK1L and vΔK1L a one-way ANOVA followed by Tukey's multiple comparisons test was performed. All analyses were executed using GraphPad Prism software (La Jolla, California).

3.3 Results

The K1 protein is not essential for replication in mouse cells in vitro

The goal here was to identify the contribution of *K1L* to viral pathogenesis in a mouse model of infection. A vaccinia virus deleted for the *K1L* gene (vΔK1L) replicates to the same extent as wild-type vaccinia virus (vK1L) in several human and non-human primate cell lines [48, 68] but is compromised when replicating in a hamster and a rabbit cell line (e.g. BHK-21 and RK13)[51, 68]. However, it is not known if *K1L* is a host range factor in mouse cells.

Since the goal was to determine the contribution of *K1L* on virus pathogenicity in a mouse model of infection, an important question to ask is if the *K1L* gene is required

for virus replication in mouse cells. To answer this question, virus growth was characterized in mouse embryo fibroblasts (MEFs)(Figure 1). MEFs were infected with a high MOI (10 PFU/cell) to examine a virus replication during a one-step growth curve or a low MOI (0.01 PFU/cell) to examine virus replication and spread during a multi-step growth curve. Infectious viruses present in either cells or cell-free supernatants were quantified by using plaque assays (Figure 1). In all cases, vΔK1L replicated to the same levels as vK1L using either one-step (Figures 1A and 1B) or multi-step growth curve assays (Figures 1C and 1D). A revertant virus in which the *K1L* gene was stably re-inserted into vΔK1L (vK1Lrev) was also tested. As expected, this virus had growth properties similar to vK1L (Fig. 1). For all experiments, an additional virus lacking both the K1L and C7L genes (vΔK1LΔC7L) was examined as a control. vΔK1LΔC7L does not replicate in the murine NIH 3T3 cell line [42]. In a similar manner, this same virus replicated to lower levels than viruses containing C7L in MEFs (Figure 1). In summary, these data suggest that *K1L* is not a host range factor for murine cells.

The K1L gene contributes to pathogenicity in an intranasal mouse model

Liu *et al.* report that the deletion of *K1L* from vaccinia virus strain TianTan (VTTΔK1L) decreases virus pathogenicity [38]. However, it is difficult to appreciate the full impact of the *K1L* gene on pathogenicity using this virus background because VTTΔK1L has different properties than vΔK1L: VTTΔK1L replicates poorly in HeLa cells [38] while the WR-based vΔK1L does not [48, 68]. This may be due to the fact that the parental and *K1L*-less construct used by Liu *et al.* lacked three additional genes involved in vaccinia virus immune evasion (*A53R*, *C12L*) and morphogenesis (*A33L*)

[38], which may have unknown effects on virus pathogenicity. To overcome this problem, our approach was to use a WR strain of vaccinia virus in which only the *K1L* gene was absent (vΔK1L). This allowed the examination of the pathogenic effect of the *K1L* gene without the confounding effects of the absence of other virus genes. WR was chosen as the vaccinia virus strain for study because it is most frequently used for pathogenesis studies in mice [60].

For wild-type vaccinia virus (vK1L), intranasal (IN) inoculation provides a system to evaluate viral pathogenesis in which weight loss and clinical signs of illness indicate the relative pathogenicity of a virus [1, 53]. Typically, mice are inoculated with 10^4 PFU of wild-type VACV (vK1L) and examined daily. Under such conditions, vK1L caused weight loss and clinical signs of illness similar to results reported by Alcami and Smith (Figure 2A)[1]. In contrast, vΔK1L-infected mice lost less weight (Figure 2A). Statistically significant differences in weight between vK1L and vΔK1L were observed on days 5-7 pi. Additionally, vΔK1L-infected mice, but not vK1L-infected mice returned to their original weight by 14 d pi, suggesting that mice fully recovered from vΔK1L infection. The re-insertion of *K1L* into vΔK1L (vK1Lrev) resulted in a virus with a pathogenicity similar to vK1L, indicating that the *K1L* gene was responsible for this decreased pathogenicity (Figure 2A). When data were charted as a Kaplan-Meir survival curve, all mice infected with vK1L or vK1Lrev were euthanized due to weight loss by 8 days pi (Figure 2B). In contrast, all vΔK1L-infected mice survived.

Signs of illness were also examined daily and quantified based on a 5-point scoring system that is used determine the extent of sickness caused by a poxvirus [2, 6]. Notably, there was a 2-day delay before illness onset in mice infected with a virus devoid

of *K1L* versus K1L-containing viruses. In addition, the signs of clinical illness were decreased in vΔK1L-infected mice as compared to mice infected with *K1L*-containing viruses (Figure 2C). As expected, mice inoculated with PBS showed no signs of weight loss or illness at any time point. Together these data suggest that a virus devoid of the *K1L* gene is less pathogenic than its wild-type parental virus.

This experiment was repeated using more stringent conditions, namely a 10-fold higher dose (10^5 PFU) of virus (Figures 2D-F). Again, vΔK1L was less pathogenic than *K1L*-containing viruses. Several differences were noticed when comparing the weights of vΔK1L-infected mice receiving 10^5 versus 10^4 PFU (Figure 2D). First, mice receiving 10^5 PFU vΔK1L lost more weight at earlier times pi as compared to those inoculated with 10^4 PFU. Second, vΔK1L-infected mice did not return to their original weights by 14 days pi. In addition, one vΔK1L-infected mouse was euthanized due to weight loss (Figures 2D and 2E). These differences are likely due to the fact that an increased dose of virus increases the pathogenic effects of a virus [2]. Indeed, when mice received the higher inoculum of 10^5 PFU, signs of illness occurred earlier in all mice. However, signs of illness were significantly reduced in mice infected with vΔK1L versus *K1L*-containing viruses (Figure 2F). Thus, data from Figure 2 show that *K1L* itself is a virulence factor in an IN model of infection. In summary, data from Figure 2 show that vΔK1L has decreased pathogenicity as compared to wild-type vaccinia virus.

K1L contributes to virus replication in vivo

Often, a decrease in virus pathogenicity correlates with decreased virus replication in mouse organs [5, 13, 20, 21, 40, 66]. Data in Figure 3 showed that this

trend also occurred for vΔK1L in the IN infection route. For example, vΔK1L titers in lungs were approximately 10-fold lower than vK1L on day 2 pi, and approximately 100-fold lower than vK1L on days 4 and 6 pi (Fig 3A).

During an IN infection, WR initially replicates in the lungs. Next, VACV disseminates to the brains, and then spreads to distal organs such as the spleen and ovaries [2, 53]. Because vΔK1L titers were decreased in the lungs, it was not surprising that vΔK1L titers also were lower than vK1L in the brains (Figure 3B). Note that only one mouse brain had detectable vK1L or vK1Lrev titers on day 2 pi, while two mouse brains possessed vΔK1L viruses (Figure 3B). This was expected because VACV routinely is not detected in mouse brains until 3 days pi [53]. By day 6 pi, all mouse brains had detectable titers of vK1L or vK1Lrev. However, vΔK1L titers were 200-fold lower as compared to vK1L. No viruses were detected in spleens at 2 days pi (Fig. 3C), reflective of the fact that wild-type VACV is only detectable in spleens as early as 3 days pi [53]. Thus, it was not surprising that no viruses were detected in spleens at 2 days pi (Fig. 3C). While all virus titers increased rapidly by day 4 pi (Figure 3C), vΔK1L titers were approximately 100-fold lower than vK1L titers. All virus titers were lower in spleens by day 6 pi and this is similar to patterns observed by others [1, 53]. Thus, in the IN model of infection, the reduced pathogenicity of vΔK1L correlated with a decrease in vΔK1L virus replication.

The K1 protein contributes to pathogenicity in an intradermal model of infection

The intradermal (ID) inoculation of a mouse ear pinna provides a second model to evaluate vΔK1L pathogenicity [36, 72]. The ID infection model has many strengths to

study how VACV modulates host immune response. It closely resembles the scarification route used during smallpox vaccinations, and is most similar to the locale (skin) of infection for other poxviruses including molluscum contagiosum virus and Orf [52, 61]. Here, lesion formation and size is an indicator of pathogenicity [71]. Unlike the IN route of infection, ID inoculation is localized [72]. Thus, there are no generalized clinical signs of illness like those observed during IN infections (e.g. weight loss or fur ruffling), and there is little to no virus detection in distal organs [72]. Figure 4 shows results using this model system. For all viruses tested, gross lesions were observed starting on day seven pi for all viruses. vK1L or vK1rev infection induced the largest lesion at days 12 and 8, respectively (Fig. 4). In contrast, lesions were smaller in vΔK1L-infected ears at all times examined. These differences were statistically significant on days 7-12 and 14-16 pi. Thus, K1 also contributed to pathogenicity for the ID model of infection.

Decreased lesion size is not due to diminished virus replication in the ID infection

Data from the IN model of infection showed that decreased pathogenicity of vΔK1L was associated with its decreased replication in the lungs (Figure 3). Thus, a logical assumption was that virus titers would be lower in vΔK1L-infected ears. Surprisingly, this premise did not hold true; Figure 5 showed that there were no statistically significant differences in virus titers between viruses containing or lacking the *K1L* gene at any time point examined (Figure 5). This included time points where there was no lesion formation (days 1 and 3 pi), just prior to visible lesion formation (day 5 pi), and times where lesions had formed and remained attached to ears (days 8 and 11 pi). These last two time points were chosen to minimize the possibility that, if there were

a decrease in virus titers, it would not be due to a loss of virus encrusted in lesions. These data showed two important trends. First, lesion size did not correlate with virus replication, which was opposite of the results observed in the IN infection model. Second, since vΔK1L replicated to similar levels as vK1L in pinnae, *K1L* was not a host range gene in mouse ear pinnae.

Examination of edema during infection

We continued studies with the ID infection system but not with IN infection system. This is because there are numerous examples of mutant VACV that lack NF-κB antagonists where a decrease in viral pathogenesis correlates with a decrease in virus replication in lungs and other organs (e.g.; ΔA49, ΔC4, ΔE3, ΔK7) [5, 9, 20, 40]. In contrast, there is only one other published example of a mutant VACV that lacks the NF-κB inhibitor B7 (ΔB7R) where viral pathogenesis is not due to virus replication [50]. Thus, the continued study of vΔK1L in ear pinnae would be more likely to uncover novel aspects of virus-host interactions.

The ID model of infection relies on the visual detection of lesion formation to assess virus pathogenicity [72]. ID infection of ears causes inflammation [17, 22, 30, 31]. Thus, we were curious if edema, a classical sign of inflammation, was accelerated or delayed during vΔK1L infection. Immune responses prior to lesion formation use terminal procedures (e.g., histopathology) to examine tissue damage and are semi-quantitative [17, 22, 30, 31]. In contrast, ultrasound imaging successfully quantified inflammation for processes like fatty liver disease [25]. A benefit of this technology is

that it is non-invasive and allows scientists to quantitatively track progression of disease in the same mouse.

We chose to use ultrasound as a means of asking if early signs of inflammation (e.g. edema) were different in infected ears. Ultrasound was used to collect B-mode images for each ear. The region in pink contains ear tissue while the substrate used for ear placement is shown as a gray platform under the ear (Figure 6A, left hand panel). The pink field of interest was then used for quantitative ultrasound backscatter coefficient (BSC) data assessment (Figure 6A, right hand panel). As fluid concentration (edema) increases in an ear, the ultrasonic scattering magnitude decreases [49]. This is quantified as a decrease in ultrasonic backscatter coefficient (BSC), and this change can be quantified using QUS technology [49] and displayed in graphical form (Fig. 6B). The BSC color-coding represents the quantitative magnitude of the gray-scale B-mode echo data. The color-coded scale on the right is in logarithmic units, in which red is related to the highest BSC value and the lowest fluid content, while dark blue is related to the lowest BSC value and the highest fluid content. Increase in fluid content for this study is edema, confirmed by histopathology. Edema is triggered by early inflammatory signaling. The BSC values from each mouse ear were determined, and measurements from each ear were averaged and yielded a mean +/- SEM (Figure 6B)[49].

Uninoculated and PBS-inoculated ears are color-coded in red, implying that there is little to no fluid infiltration (Figure 6A) resulting in high BSC values (Fig. 6B). Infection with vK1L or vΔK1L showed an increase in edema longitudinally, with the most noticeable differences beginning on day 3 pi and continuing until day 5 pi (Figure 6A), and BSC values decreased during these times (Figure 6B). Overall, there was a

statistically significant decrease in BSC between virus-infected ears versus PBS- or uninoculated ears (Fig. 6B) at days 4 and 5 pi. vΔK1L infection result in a slight decrease in BSC values as compared to vK1L, however this was not statistically significant (Fig. 6B). Thus, vΔK1L infection minimally affected edema.

The thickness of each ear was digitally measured as another means of assessing inflammation. The number of pixels was estimated in the region of the BSC image that depicted the thickest measure of the color-coded image. Data are shown in Figure 6C. Thicknesses of vΔK1L-infected ears were similar to vK1L-infected ears on days 1-3 pi. The largest difference in ear thickness between vK1L and vΔK1L infections occurred on day 4 pi, in which there was an approximately 0.2 mm difference in thickness. However, this difference decreased by day 5 pi, where vΔK1L-infected ears were nearly the same thickness as vK1L-infected cells. Thus, while vΔK1L-infected ears were less thick than vK1L-infected ears, these differences in ear thickness appears to be transient.

Some mouse ears used for ultrasound imaging were processed further for histological examination using hematoxylin and eosin (H & E) staining to evaluate tissue morphology (Figure 7). Examination of the architecture of the ear tissue showed that, at day 3 pi, both vΔK1L and vK1L -infection resulted in mild edema. A single mouse of the vK1L-infection group had a small focal region of more pronounced inflammation. By day 4 pi, both vΔK1L- and vK1L-infected ears exhibited similar pinna thickening and this was primarily due to moderate dermal edema. Ear thickening was also due to hyperplasia with ballooning degeneration and pustules in the epidermis. By day 5 pi, microscopic lesion formation was prominent in both vΔK1L- and vK1L-infected ears and lesions were progressed in severity, with some ulceration and crusting. vΔK1L infection

had less extent of the lesions in the pinna (Figure 7). This correlates with differences in lesion sizes shown in Figure 6C. Overall, there was a moderate and transient decrease in edema in vΔK1L infected ears versus vK1L at all times examined. Thus, classical histopathology showed trends similar to quantitative ultrasound imaging, suggesting quantitative ultrasound technology is a new non-invasive technology to detect inflammation.

_v_ΔK1L infection results in decreased immune cell infiltration

Figure 5 showed that, unlike results from the IN infection model, the decreased lesion size observed in vΔK1L-infected ears was not due to decreased viral replication. Another mutant VACV that lacks the B14 NF-κB antagonist VACV (vΔB14R) enhances the infiltration of immune cells as compared to wild-type VACV during an ID infection [11]. This suggested that an enhanced host inflammatory response may contribute to diminished lesion size.

To test if this also was the basis for reduced lesion sizes for vΔK1L-infected ears, we used flow cytometry to detect and quantify immune cell types that are known to infiltrate the ear upon VACV infection [22, 32]. The presence of these innate immune cells was examined at day 5 post-infection. This time point was chosen because viral replication was robust, and it is a time where it is known that these types of innate immune cells would be detectable in infected ears [22]. Results are show in Figure 8.

The first striking result was that there were dramatically less (4.3 times less) cellular infiltrates harvested from vΔK1L-infected versus vK1Lrev-infected ears (Figure 8A). However, the number of infiltrates in vΔK1L-infected ears was 3 times higher than

PBS-inoculated ears. This implied that vΔK1L infection indeed drew some immune cells into the area of infection, but this number was diminished as compared to vK1L-infected ears.

We were then interested in examining the number and types of infiltrating leukocytes in ears. Because the total number of cells varied between the groups of PBS-, vK1Lrev- and vΔK1L-infected ears, we could not represent data as the percent population of total cells. Instead, data in Figures 8B-E were presented as the total number of each cell population per ear to allow for better comparisons. When examining $CD45^+$ (leukocyte) infiltration, there were 4.7 times more $CD45^+$ cells in vK1Lrev- versus vΔK1L-infected ears (Figure 8B). The number of infiltrates in vΔK1L-infected ears was 3 times higher than PBS-inoculated ears, indicating that vΔK1L infection was not inert.

We investigated the relative abundance of three subsets of $CD45^+$ leukocytes that are reported to be detectable in infected ears 5 d pi [22, 32]. Data are shown in Figures 8C-E. These include tissue-protective monocytes; $CD45^+CD11b^+CD11c^-LyC6^+Ly6G^+$) and inflammatory monocytes ($CD45^+CD11b^+CD11c^-LyC6^+Ly6G^-$)[22, 32]. $CD45^+CD11c^+$ cells were also investigated which can include dendritic cells, NK cells and activated T cells. There were dramatic decreases in all three cell types examined in vΔK1L- versus vK1Lrev-infected ears. Again, $CD11c^+$, $LyC6^+Ly6G^+$ and $LyC6^+Ly6G^-$ cell numbers were higher in vΔK1L- versus PBS-inoculated ears, suggesting that vΔK1L infection elicited a moderate infiltration of leukocytes. These data showed a correlation between a reduced lesion size and reduced immune cell infiltrates, implying that infiltrating immune cells may produce molecules that promote immunopathology.

vΔK1L infection results in a muted host immune gene expression profile

In cell culture, vΔK1L infection resulted in an increased transcription of an NF-κB-controlled gene (*TNF)* as compared to vK1L infection [57]. Thus, one hypothesis was that the expression of immune genes under the control of NF-κB (e.g., cytokines and chemokines) would occur earlier and/or to a greater extent in vΔK1L- versus vK1L-infected ears. Results from Figure 8 showed that there was a decrease in infiltration of leukocytes during vΔK1L infection. Since leukocytes migrate to areas expressing chemokines and other cytokines, this raised an alternative hypothesis: that the expression of cytokines and chemokines would be decreased during vΔK1L infection. To test both hypotheses simultaneously, we evaluated the transcription profile of 24 host cell genes at days 1, 3 and 5 pi in ears inoculated ID with either PBS, vK1L, vΔK1L or vK1Lrev using RT-qPCR. These time points were chosen for two reasons. First, it afforded the opportunity to examine if host immune genes were transcribed in vΔK1L-infected ears before vK1L-infected ears. Second, these time points harvested ears prior to lesion formation, therefore minimizing potential RNA loss due to scab formation. Gene expression values from infected mice were normalized to PBS-inoculated mice euthanized on the same day. Statistical analyses were performed comparing PBS- to vK1L-infected or vK1L- to vΔK1L-infected ears.

Results from these studies are shown in Table 1. Several striking trends were observed. First, there was no statistically significant difference in gene expression between vK1L and vΔK1L-inoculated ears at 1 day pi. These results opposed the first hypothesis that, in the absence of an NF-κB antagonist, there would be an increase in the expression of NF-κB controlled host genes during vΔK1L infection.

By day 3 pi, there was a more robust host response to vK1L infection. Notably, there was a statistically significant induction of *Cxcl1* and *Il6* gene expression. *Il10* mRNA levels were also statistically significantly increased, in agreement with data published by Cush *et al* [16]. While not statistically significant, there was a 9-fold increase in *Cxcl10* gene expression in vK1L-infected ears, also in agreement with a previous publication [30]. We observed that vK1Lrev-infected ears showed a slightly more robust response to virus infection in several instances for reasons that remain unclear. For example, *Cxcl5*, *Isg15*, *Mx1*, *Eif2ak2* (PKR) and *Krt6a* mRNA levels were significantly higher in vK1Lrev- as compared to PBS-inoculated mice. Unexpectedly, vΔK1L-infected ears showed a different pattern of host gene expression. Nearly all the mRNAs examined were lower in vΔK1L-infected ears as compared to vK1L-infected ears. Thus, in contrast to what was expected, removal of *K1L* led to a decrease in the expression of anti-viral genes during infection.

vK1L or vK1Lrev infection continued to stimulate host gene transcription at day 5 pi, and this increase was statistically significant as compared to PBS-inoculated ears in most cases. As reported by others, we detected upregulation of *Ccl4*, *Cxcl9*, *Ifng*, *Il1*, *Il6* and *Mx1* in VACV-inoculated ears, suggesting these are important cytokines to detect and resolve VACV infection [17, 30].The exceptions to this trend were for transcription of the *Il7, Tnf, Ifna4, Ifnb, Nfkb2* and *Nfkbia* genes, which were either similar to or lower than values obtained for infections at 1 day pi. Others have also reported the lack of Tnf and type I IFN gene expression during VACV infection [30]. However, IFN gene expression more recently has been detected by other researchers who have optimized RNA purification protocols (Dr. Chris Norbury, personal communication).

When examining vΔK1L-infected ears at day 5 pi, there were several noticeable trends. Most of the host cell transcripts were lower in vΔK1L- versus vK1L-infected ears. This result was surprising because it was the opposite of our original hypothesis. The greatest reduction for expression of the *Ccl4* gene, with a 12.4-fold reduction of mRNA for vΔK1L versus vK1L infected mice, followed by *Ifng* with a 7.6-fold reduction. Other genes in which there was a statistically significant reduction of mRNA levels in vΔK1L- compared to vK1- infected mice also included *Cxcl2* and *Cxcl5* (5.2-fold), *Il1b* (4.6-fold), *Cxcl9* (3.5-fold), *Il10* (3.3-fold), *Rnasel* (2.2-fold) and *ccl2* (2.0-fold). There were several instances in which there were differences in gene expression, but these differences were not statistically significant due to variance among the mice within the groups. These genes included the chemokine *Ccl5 and Cxcl10* genes, the *Il6* gene, the interferon-stimulated *Mx1* and *Isg15* genes, and the keratinocytes stress response genes *Krt6a* and *Krt16*. As mentioned earlier, K1 antagonizes type I IFN [44] and NF-κB [10, 57]. Interestingly, genes encoding a type I IFN (*Ifnb*) or NF-κB-controlled genes (*Nfkbia* and *tnf*) [14, 28, 56, 67] showed no K1L-dependent change in expression. However, other genes at least partially controlled by NF-κB (*Ifna4*, *Il7* and *Nfkb2*) showed significant down-regulation in the absence of *K1L* [35, 39]. For *Nfkb2,* the mRNA was slightly, but significantly higher in vΔK1L- versus vK1L-infected mice. There was only one gene, *Cxcl1*, which mRNA expression was slightly higher in vΔK1L- vs vK1L-infected mice, however this difference was not statistically significant. Thus, there were two conclusions drawn from these data. First, the decreased expression of immune response genes correlated with a decrease in leukocytes infiltration and a smaller lesion size. Second, vΔK1L counterintuitively dampened pro-inflammatory gene

expression. Many of these pro-inflammatory molecules also induce immunopathology. Thus, vΔK1L-induced lesions may be smaller because of the diminished expression of these pro-inflammatory cytokines.

vΔK1L infection activates VACV-specific CD8$^+$ T cells

We observed that vΔK1L infection was less pathogenic. In addition, the infiltration of leukocytes and expression of immune response genes was lower in vΔK1L- versus vK1L-infected mice. We were curious to ask if this decreased host response would also result in a diminished capacity to trigger a protective immune response. To answer this question, we examined vaccinia-specific, activated CD8$^+$ T cells from the spleens and lymph nodes of infected mice (Fig. 9A-D). In spleens, virus infection significantly increased the number of activated (IFN-γ-expressing), vaccinia-specific CD8$^+$ T cells as compared to mice inoculated with PBS. Moreover, the magnitude of response was similar for vK1L or vΔK1L infection (Fig. 9A, 9B). Slightly different results were observed when examining lymph nodes of infected animals. While both viruses induced an increase in the percentage of VACV-specific CD8$^+$ T cell populations, only vΔK1L-infected mice showed a statistically significant increase as compared to PBS. When the absolute number of VACV-specific CD8$^+$ T cells in lymph nodes were evaluated (Fig. 9D), there was a greater number of CD8$^+$ T cells in vΔK1L-infected versus vK1L-infected mice. However, both values were higher than PBS-inoculated mice. Thus, CD8$^+$ T cell responses were similar despite the decrease in initial innate immune responses to vΔK1L infection.

vΔK1L protects against a lethal challenge of vaccinia virus

Since vΔK1L infection raised VACV-specific $CD8^+$ T cell responses equal to or greater than vK1L infection, we predicted that vΔK1L would be an effective vaccine against a lethal vaccinia virus challenge. To test this hypothesis, we used a previously described vaccination model in which mice were inoculated ID with PBS, or 10^4 PFU vK1L or vΔK1L [32]. At day 30 pi, mice were challenged IN with a lethal dose (5 x 10^6 PFU) of vK1L. We choose this dose because others have reported that doses of 10^5 or higher are sufficient to be lethal in the IN model of infection [32, 74]. In addition, Jacobs *et al.* reported that ID vaccination protected mice when mice were challenged with 5 x 10^6 PFU of wild-type vaccinia virus [32]. Weight was recorded daily as a proxy for protection against the challenge (Figure 9E). All PBS-vaccinated mice rapidly lost weight and all mice from this group were euthanized by day 6 pi. vK1L-vaccinated mice were protected from the challenge. Mice did not lose as much weight as PBS-inoculated mice, and mice nearly recovered their original weight by day 14 pi. vΔK1L vaccination also protected mice against a lethal challenge. Interestingly, vΔK1L-vaccinated mice showed slightly less weight loss than vK1L-vaccinated mice, although these differences were not statistically significant. Thus, vΔK1L is a less pathogenic virus that still provides protection against a lethal virus challenge.

3.4 Discussion

We report here that vΔK1L is less pathogenic in two models of infection. We went on to further examine the ID model of infection because results showed that reduced pathogenicity was not due to a decrease in virus replication. Instead, reduced

pathogenicity correlated with decreased innate immune cell infiltration and decreased inflammatory gene expression in ears. It is well-known that the anti-viral immune response can inadvertently damage the host to such a degree that it causes disease [64]. Thus, we propose that there are two underlying mechanisms responsible for smaller vΔK1L-induced lesions. First, the diminished amount of chemokine expression in vΔK1L-infected ears, which is already observed at day 3 pi, probably results in a decrease in infiltrating immune cells, cells which can express damaging cytokines. The second reason is that there are lower amounts of pro-inflammatory cytokine gene expression at days 3 and 5 pi in ears. Since some of these cytokines are known to have immunopathogenic properties, this decreased expression in vΔK1L ears may result in smaller lesions. Despite these decreased innate immune responses, ID inoculation with vΔK1L still stimulates VACV-specific T cell responses and provides protection against a lethal VACV challenge equivalent to its parental virus. This is the first mutant vaccinia virus describing this type of profile.

To the best of our knowledge, our studies are the first to address the effects of *K1L* itself on viral pathogenesis. These data illustrate two important concepts to both the poxvirus and vaccinology fields. First, the antagonistic functions of immune evasion molecules discovered during cell culture-based studies may not necessarily replicate *in vivo*. For example, K1 is well-known as an antagonist of NF-κB [10, 57]. We reported that vΔK1L infection up-regulated one NF-κB controlled host gene (*Tnf*) in comparison to wild-type VACV in cell lines [57]. Thus, our original expectation was that vΔK1L infection would increase NF-κB-controlled host gene transcripts above or earlier than vK1L-infected ear pinnae. However, we observed the opposite result: nearly all host gene

transcripts were decreased in vΔK1L- as compared to vK1L-infected ears at all times examined (Table 1). This implies that results obtained from cell culture models of infection may not mirror results obtained from *in vivo* models of infection. One other report supports this concept: van Buuren *et al.* reported that transcription of the NF-κB controlled *Tnf*, *Il1b* and *Il6* genes were not altered in organs during intranasal infection with an ectromelia virus devoid of the EMV005 NF-κB antagonist [73]. Data here and from van Buuren et al. demonstrate our lack of understanding of how these poxviral NF-κB inhibitors may truly impact viral pathogenesis.

The second important concept is that an inflammatory immune response triggered by wild-type VACV (vK1L) may be in excess of what is required to mount a protective immune response. Several recent publications suggest that limited inflammation is beneficial for $CD8^+$ T cell activation, which requires signals from antigen, costimulation and inflammatory cytokines [26]. Others have suggested that the positive effect of inflammatory signals on T cell activation might compromise the quantity and quality of memory T cells [3]. Recently it was reported that sensing of a robust inflammatory response affects the transition of effector CD8+ T cells to memory T cells [65]. In addition, chronic inflammation can disrupt epithelial integrity, which can affect T cell migration or access to pathogens [65]. Thus, perhaps a VACV lacking *K1L* is one component for an improved vaccine vector.

One must keep in mind that K1 is a multi-functional protein, antagonizing not only NF-κB [10, 57] but also PKR [76, 77], IRF1 [42] and type I IFN [44] signal transduction pathways. Unfortunately, the K1 regions necessary for each function are not yet known. Until such mapping is performed, the specific K1 function that contributes to

VACV pathogenesis remains to be determined. Thus, we cannot rule out that this decrease in inflammatory gene expression during vΔK1L infection may be due to other K1 functions.

VACV virus encodes for at least 10 inhibitors of NF-κB including K1, A46, A49, A52, B14, C4, E3, K7, M2 and N1 [7, 12, 18, 20, 23, 40, 47, 55, 57]. Interestingly, the deletion of a single NF-κB antagonist results in an attenuated infection [4, 5, 9, 20, 27, 40, 62]. It appears that *K1L* is unique amongst other NF-κB antagonists studied to date *in vivo*. For example, viruses lacking B14R (ΔB14R) or N1L (ΔN1L) are each less pathogenic in the ID model of infection [4, 11]. However, ΔB14R and ΔN1L each replicate to a lesser extent than wild-type VACV [4, 11] while vΔK1L replicates equally as well as VACV in the ear pinnae (Figure 5). Interestingly, ΔB14R infection increases macrophage infiltrates in the ear, and this is suggested to be due to an increase in expression of chemokines and cytokines [11]. However, vΔK1L infection is associated with a decrease in immune cell infiltration. These data higlight that these poxviral NF-κB inhibitors are non-redundant *in vivo*, and argue strongly in favor of a sophisticated multi-step system used by VACV to master distinct cellular environments as it infects and is exposed to myriad organ-specific associated immune responses. Inflammatory gene expression profiles similar to the one performed here have identified host responses to infection with wild-type VACV [24, 30]. To the best of our knowledge this is the first study to report a detailed analysis comparing the inflammatory gene response to virus infection in wild-type VACV (vK1L) versus a VACV devoid of an immune evasion gene. We propose that the continued use of RT-qPCR or RNAseq to compare the immune gene expression profile of ears when using mutant VACV that lack different NF-

κB antagonists is one approach that may identify how each VACV immune antagonist uniquely alters the host response to infection *in vivo*.

In agreement with our data, Liu *et al* reported that deletion of the *K1L* gene attenuates VACV strain TianTan, and that T cell responses remain unaffected by removal of *K1L*. Liu et al also observed that humoral responses were decreased when *K1L* was absent [38]. Humoral responses for vΔK1L were not measured here. It is difficult to accurately predict if vΔK1L would give results similar to vTTΔK1L because the parental vector (vTT) lacks several genes other than *K1L* [38, 70]. Nevertheless, we chose to examine only $CD8^+$ T cell responses because others have reported that $CD8^+$ T cells provide protection against VACV intranasal infection even in the absence of $CD4^+$ T cells and B cells [24].

Investigation of VACV immune evasion molecules has identified important strategies viruses use to modulate the immune response. In turn, this information provides a greater understanding of how the host detects, responds to, and eliminates virus infection [60]. VACV continues to be used as a vaccine vector and as an oncolytic therapy. Thus, information about virus-host interactions is also valuable for researchers who optimize current poxvirus-based vaccine vectors. A continuing challenge for researchers is to develop a VACV-based construct that is simultaneously efficacious and safe. VACV, while highly immunogenic, induces unacceptably high rates of morbidity and mortality. Thus, multiple research labs now are modifying VACV to develop vectors that retain immunogenicity and have improved safety profiles [46]. One strategy used by researchers is to alter the expression of the immune evasion genes of a VACV-based vector [54] in an effort to retain VACV immunogenicity and improve safety. We show

here that vΔK1L infection in mouse ear pinnae has a decreased pathogenicity but no loss in its ability to activate an acquired immune response or protect against a lethal VACV challenge. Thus, vΔK1L may be a useful tool to further understand the relationship between viral modulation of innate immunity and development of immune memory, information that has practical applications for vaccine design and optimization.

3.5 Figures and Table

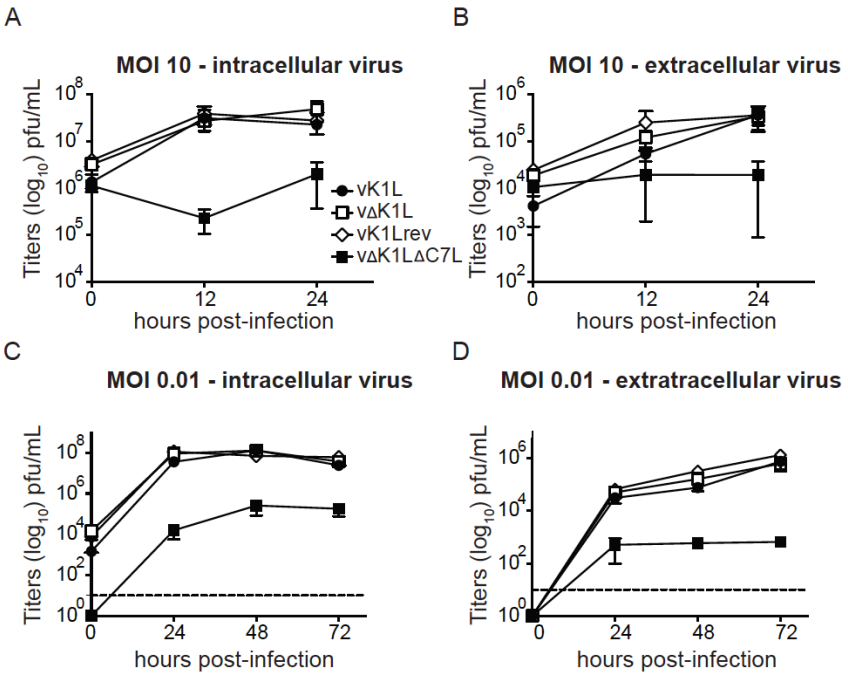

Figure 3.1 *K1L* is not essential for virus replication in *vitro*. Mouse embryonic fibroblasts (MEF) were infected with vK1L, vΔK1L, vK1Lrev or vΔK1LΔC7L at 0.01 or 10 PFU/cell in duplicate. After absorption, cellular monolayers were washed thrice to remove unbound viruses. (A and C) Cells and (B and D) cell-free supernatants were collected separately at the indicated time points. (A and C) Intracellular or (B and D) extracellular virus titers were quantified by plaque assays using Vero cellular monolayers. Data are expressed as the mean titer per sample +/- SEM. Dashed lines represents limit of detection.

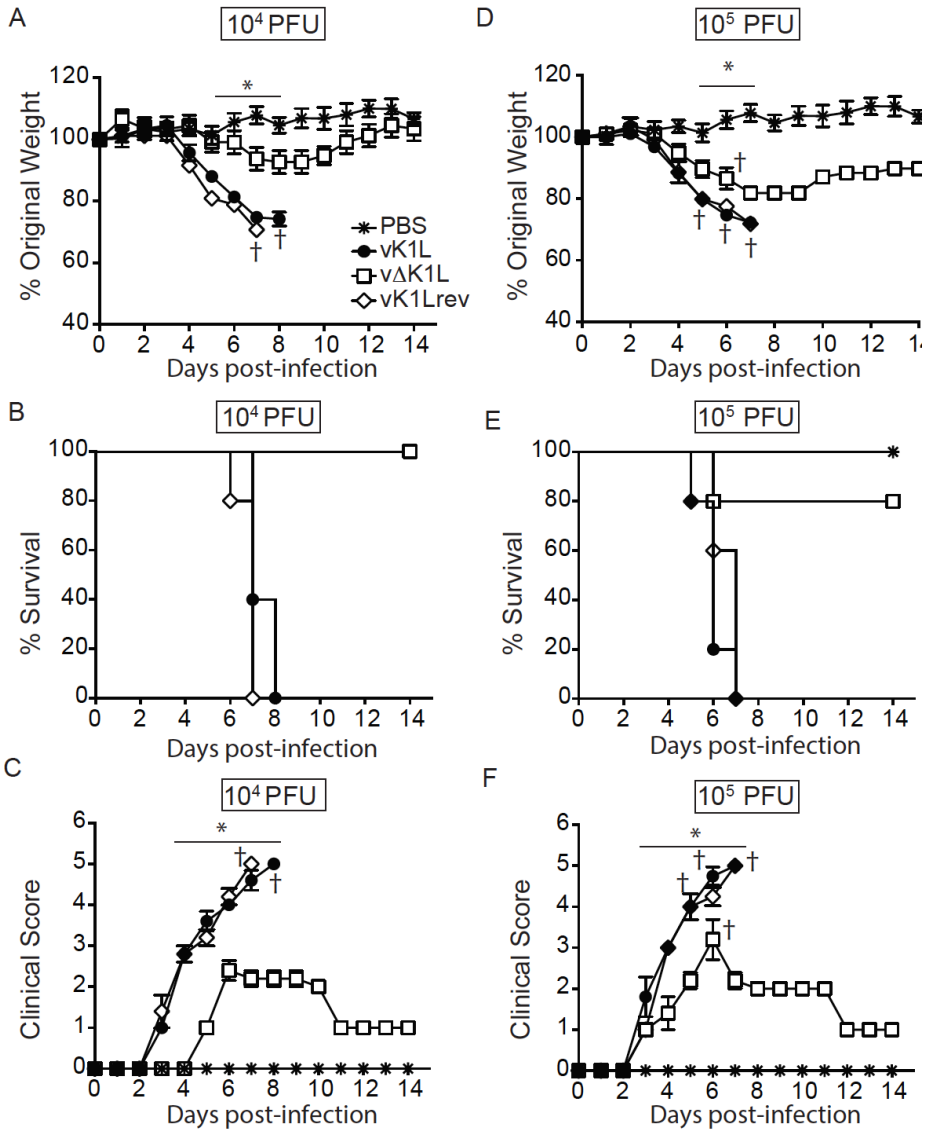

Figure 3.2 A virus lacking *K1L* is less pathogenic when introduced by intranasal inoculation. Female BALB/c mice (n = 5 per group) were inoculated intranasally with (A-C)10^4 or (B-F) 10^5 PFU of vK1L, vΔK1L or vK1Lrev or PBS and monitored for 14 days. (A and D) Mice were weighed daily and data were expressed as the percentage of weight loss from day 0. Mice were euthanized if more than 25% of their original body weight was lost. (B and E) A survival plot was generated based on data from (A and D). (C and F) Clinical signs of illness were monitored daily for 14 days and scored. Statistical significance was determined by two-way ANOVA. Asterisks indicate the days in which the weight loss or signs of illness induced by vΔK1L were statistically different from vK1L ($P < 0.05$).

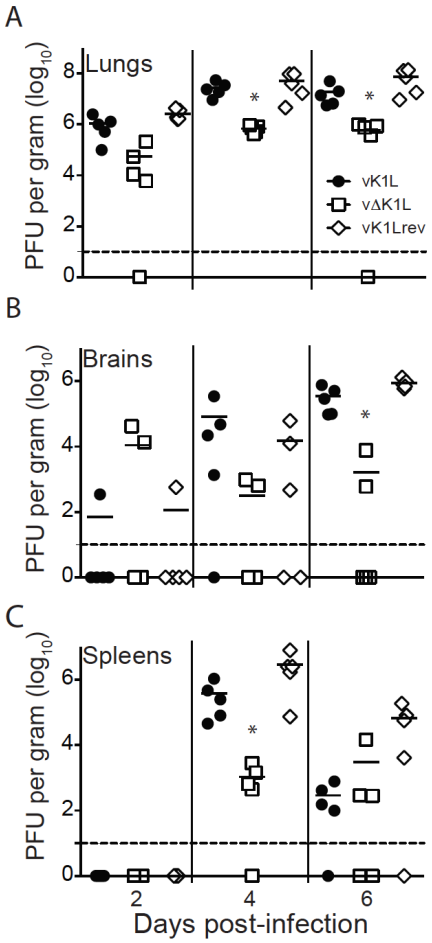

Figure 3.3 vΔK1L virus replication is lower than *K1L*-containing viruses in organs from intranasally-infected mice. Female BALB/c mice (n = 5 per group) were infected intranasally with 10^4 PFU of vK1L, vΔK1L or vK1Lrev. At the indicated times post-infection (A) lungs, (B) brains or (C) spleens were collected, and virus titers were determined by plaque assay on Vero cellular monolayers. Titers are expressed as PFUs per gram of tissue. Each symbol represents the virus titer from an individual animal, and the mean titer is indicated by a line. Statistical significance was determined by Kruskal-Wallis test. Asterisks indicate data points in which titers from vΔK1L-infected mice were statistically different from vK1L ($P < 0.05$). Dashed lines represent the limits of detection.

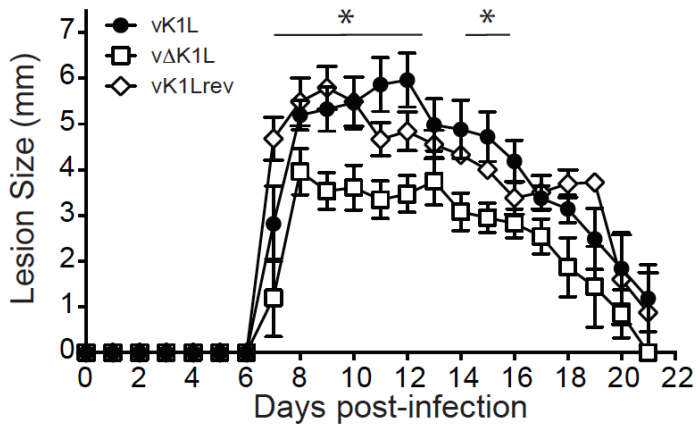

Figure 3.4 ΔK1L is less pathogenic during intradermal infection. C57BL/6 mice (n = 5 per group) were infected intradermally with 10^4 PFU of vK1L, vΔK1L or vK1Lrev in the left ear pinna, and sizes of resulting lesions were measured daily for 21 days. Data are expressed as the mean of lesion sizes ± SEM. Statistical significance was determined by two-way ANOVA. Asterisks indicate the days in which the lesion size caused by vΔK1L was statistically different from vK1L ($P < 0.05$).

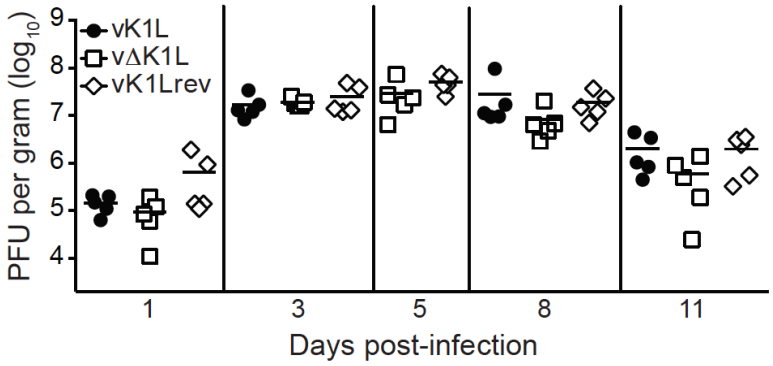

Figure 3.5 Virus replication in ear pinnae of intradermally inoculated mice. C57BL/6 mice (n = 5 per group) were infected with 10^4 PFU of vK1L, vΔK1L or vK1Lrev as indicated. At the indicated days pi, ears were collected, homogenized and lysed, and viral titers of lysates were determined by plaque assay. Data are expressed as the mean titer of virus (PFU) per gram of tissue.

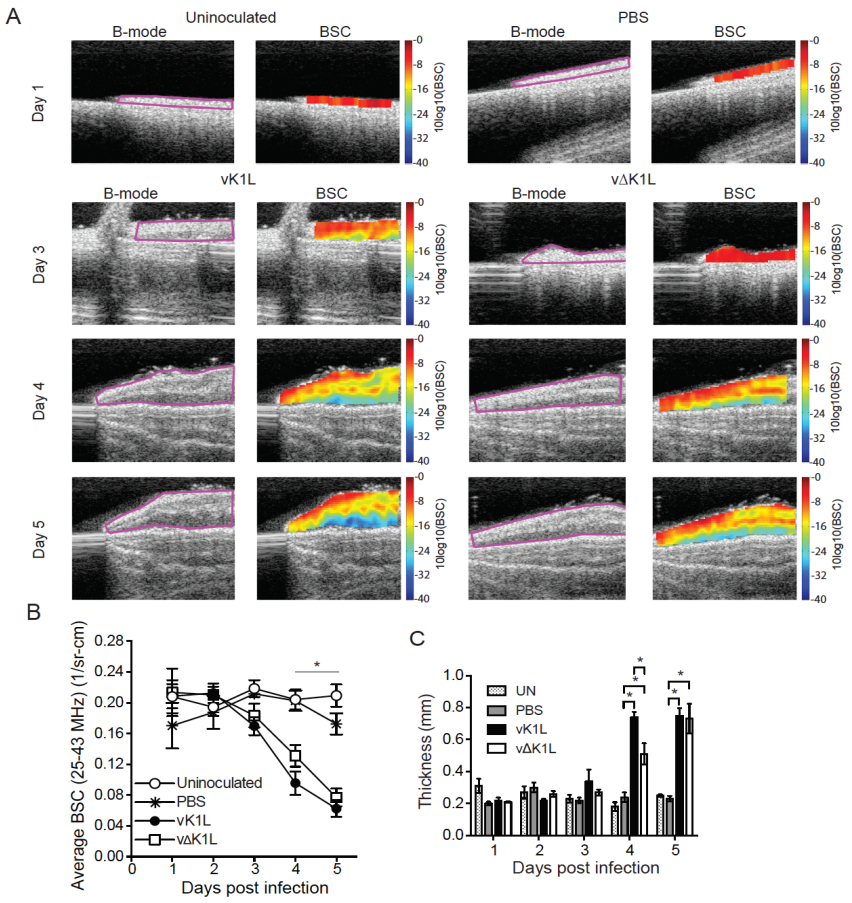

Figure 3.6 Ultrasound imaging and quantitation of edema longitudinally in intradermally-inoculated ears. C57BL/6 mice (day 3, n = 13 mice per experimental group; day 4, n = 10 mice per experimental group; day 5, n = 7 mice per experimental group) were either uninfected (UN) or inoculated ID with PBS or 10^4 PFU vK1L or vΔK1L in the left ear pinna. (A) Mice were anesthetized and B-mode images (B-mode) were collected. The region circled in pink is the field of interest, which contains ear tissue. The field of interest was used for quantitative ultrasonic data (BSC) assessment. The BSC color-coding represents the quantitative magnitude of the gray-scale B-mode echo data. The color-coded scale on the right is in logarithmic units, with red representing the highest magnitude of the BSC, and dark blue representing the lowest magnitude of the BSC. (B) BSC data are quantitatively depicted as a function of time. The BSC values are expressed as the mean +/-SEM. Statistically significant differences between mice inoculated with PBS vs. vK1L was determined by one-way ANOVA and is indicated by one asterisk ($P < 0.05$). (C) The thickness of the ear was selected from the spatially calibrated BSC image (Fig. 6A) for which the pixel dimension was known (68 µm x 68 µm = 1 mm x 1 mm). The number of pixels was estimated in the region of the BSC image that depicted the thickest measure of the color-coded image. Statistically significant differences between inoculated mice were determined by one-way ANOVA and is indicated by an asterisk ($P < 0.05$).

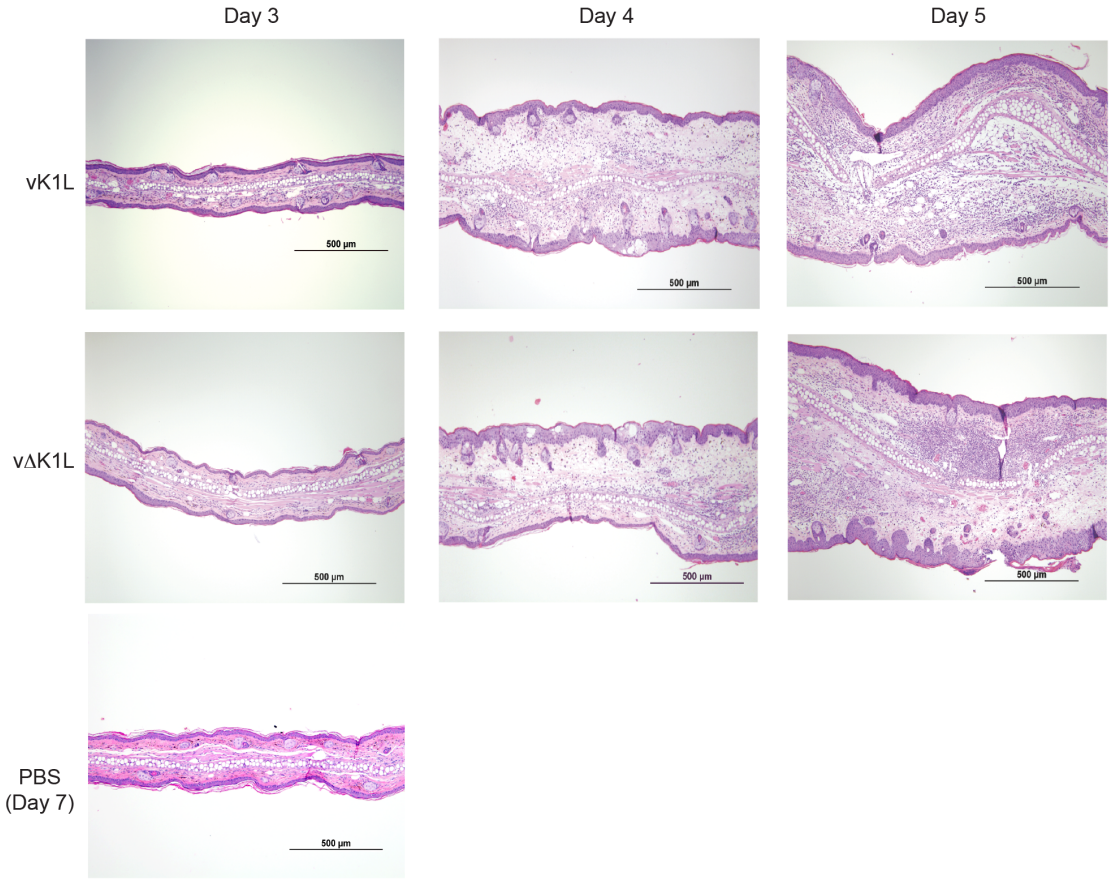

Figure 3.7 Histological analysis of infected ear pinnae. C57BL/6 mice (n = 3 per group) were inoculated with PBS or 10^4 PFU vK1L or vΔK1L. At the days indicated post-infection, ears were collected, fixed in 10% neutral buffered formalin, processed, and stained with hematoxylin and eosin for examination with light microscopy (100X). Representative images of the lesions observed in each group are shown. The bars show the scale of size.

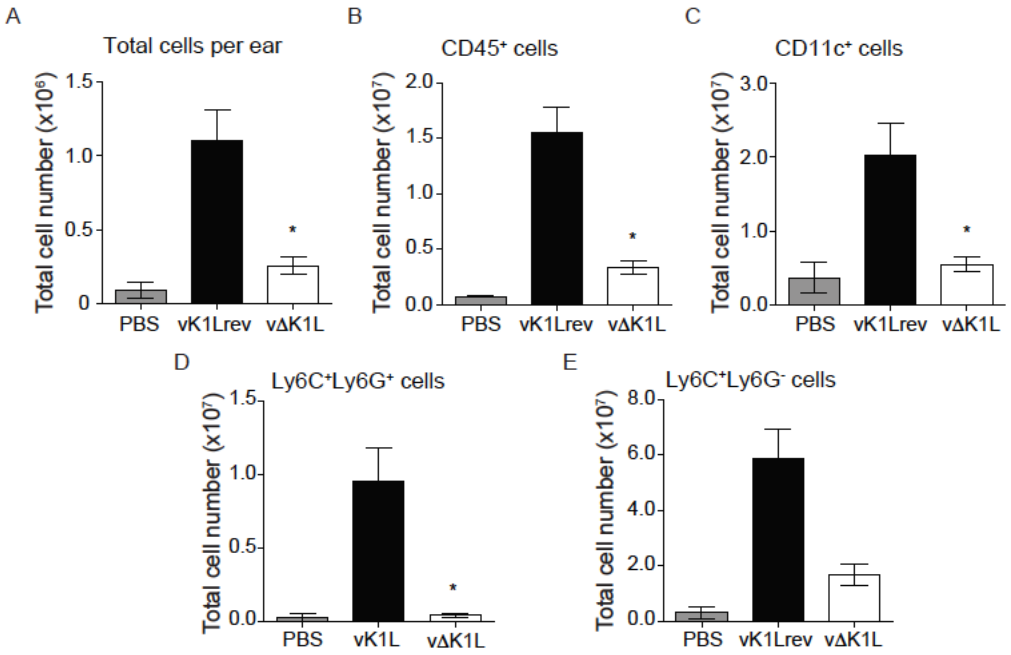

Figure 3.8 vΔK1L infection causes a reduced infiltration of immune cells into ear pinnae. C57BL/6 mice were inoculated in the left ear with PBS (n= 10) or 10^4 PFU vK1Lrev (n = 7) or vΔK1L (n = 7). At 5 d pi, ears were collected and processed. Single cell suspensions were prepared from each ear. Data are expressed as the mean number of cells per ear ± SEM.(A) Mean number of live cells per ear as determined by trypan blue staining. (B-E) Flow cytometry analyses show the mean number of (B) $CD45^+$ cells (C) $CD45^+CD11c^+$, (D) $CD45^+CD11b^+CD11c^-LyC6^+Ly6G^+$ and (E) $CD45^+CD11b^+CD11c^-LyC6^+Ly6G^-$ per ear. Statistical significance was determined by (A-D) Kruskal-Wallis or (E) one-way ANOVA. An asterisk indicates conditions where there was a statistically significant difference between vK1Lrev and vΔK1L ($P < 0.05$).

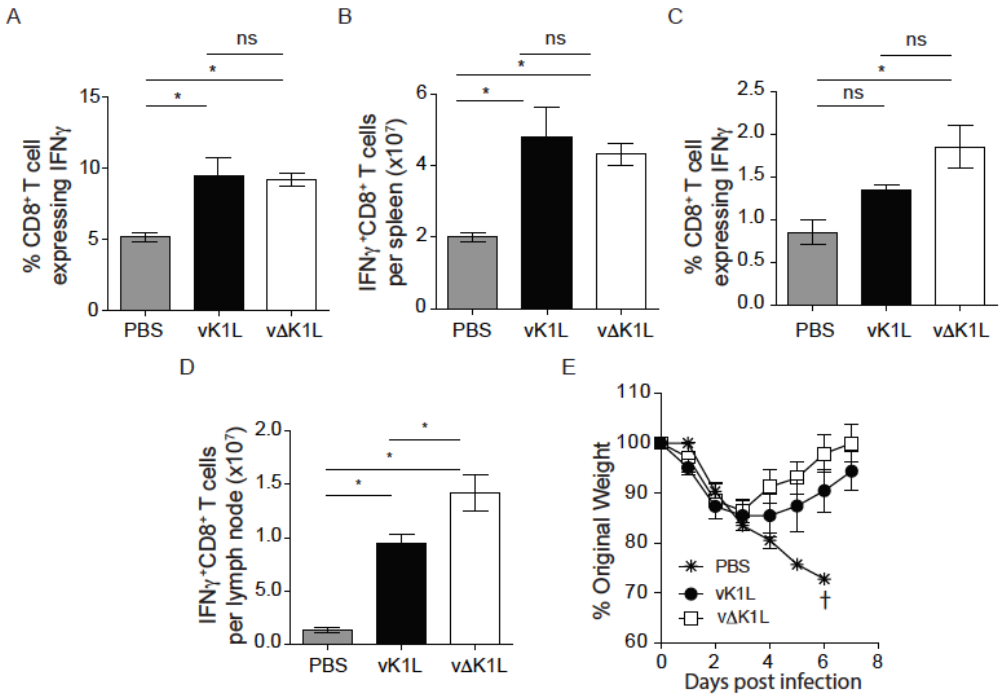

Figure 3.9 vΔK1L infection raises VACV-specific CD8$^+$ T cell responses and protects against a lethal VACV virus challenge. C57BL/6 mice (n=5 mice per group) were inoculated ID with PBS or 10^4 PFU vK1L or vΔK1L. (A-D) At 10 d pi, mice were euthanized, and (A, B) spleens or (C, D) lymph nodes were harvested. Single cell suspensions were prepared from each sample, and incubated with VACV $B8R_{20-27}$ peptide and Brefeldin A. Cells were stained for extracellular CD8 and intracellular IFNγ and activated VACV-specific CD8$^+$ T cells were quantified by using flow cytometry. Data are expressed as the mean ± SEM. (A and C) The percentage of IFNγ$^+$CD8$^+$ T cells out of the total number of CD8$^+$ T cells. (B and D) The total number of IFNγ$^+$CD8$^+$ T cells per organ. Statistical significance was determined by one-way ANOVA. Asterisks indicate conditions where there was a statistically significant increase between vK1L or vΔK1L ($P < 0.05$). ns = not statistically significant. (E) At 30 d pi, mice were inoculated IN with 5 x 10^6 PFU vK1L. Individual animals were weighed daily for the next 7 days. Weight loss is expressed as the percentage +/- SEM of the mean weight of the same group of animals on day 0. Mice were euthanized if more than 25% of their original body weight was lost.

Table 3.1 Gene expression during ID virus infection as detected by RT-qPCR.

	day 1 pi			day 3 pi			day 5 pi		
	vK1L	**vΔK1L**	**vK1Lrev**	**vK1L**	**vΔK1L**	**vK1Lrev**	**vK1L**	**vΔK1L**	**vK1Lrev**
Chemokines									
Ccl4	0.47	0.33	0.54	1.90	0.62	1.98	55.97	**4.51**	49.82
Cxcl2	0.48	0.30	0.53	1.44	0.60	1.15	10.41	**1.99**	8.83
Cxcl5	0.17	0.14	0.18	2.71	**0.44**	8.92	29.76	**5.62**	39.96
Ccl2	0.64	0.80	0.66	4.28	2.00	8.06	12.91	**6.30**	16.27
Ccl5	0.73	0.69	0.75	0.54	0.49	0.89	7.41	1.84	6.84
Cxcl9	1.94	0.87	1.07	3.41	0.95	8.22	307.96	**87.92**	360.41
Cxcl10	0.91	0.52	0.64	9.03	1.02	22.95	302.86	193.49	419.48
Cxcl1	2.68	1.52	2.16	18.23	10.46	26.78	13.95	16.10	20.90
Cytokines									
Il1b	0.35	0.24	0.45	1.57	0.45	1.09	12.47	**2.67**	11.38
Il6	0.46	0.25	0.44	7.11	**1.73**	19.65	49.03	13.44	63.77
Il10	0.54	0.42	0.59	2.28	**0.94**	4.12	9.76	**2.93**	12.76
Il7	1.19	0.96	0.98	0.70	0.99	0.52	0.59	0.73	0.61
Tnf	1.04	0.89	0.91	1.16	0.94	0.97	0.86	0.97	0.78
IFNs									
Ifng	1.45	0.71	1.01	3.40	1.02	7.81	247.88	**32.21**	306.88
Ifna4	1.41	1.40	1.29	0.60	0.85	0.85	0.19	0.51	0.22
Ifnb	1.67	1.41	1.42	1.23	1.02	2.24	0.91	1.20	1.17
ISGs									
Isg15	0.83	0.55	0.87	3.39	0.94	9.27	104.70	36.81	115.28
Rnasel	1.07	0.91	0.91	0.95	0.92	1.23	3.38	**1.52**	3.82
Mx1	0.50	0.51	0.53	3.55	0.99	9.65	116.42	68.74	174.37
Eif2ak2	1.12	0.95	1.10	1.29	1.07	1.56	2.64	1.91	3.02
Keratinocytes stress response									
Krt6a	0.40	0.34	0.45	1.61	**0.54**	2.12	32.94	13.01	37.82
Krt16	0.52	0.47	0.52	2.21	0.87	2.84	15.39	6.54	18.60
NF-κB pathway									
Nfkb2	1.17	1.04	1.02	1.08	1.12	0.93	0.52	**0.93**	0.57
Nfkbia	1.14	0.88	1.05	0.87	1.02	0.71	0.69	0.83	0.72

Data represents the average fold expression level of each gene ($2^{-\Delta\Delta Ct}$) as compared to that in PBS-inoculated ears that were harvested at the same day pi (n = 4 ears per group). Underlined values indicate a statistically significant difference as compared to PBS-inoculated mice ($P < 0.05$). Bolded values indicate statistically significant difference between mice inoculated with vK1L versus vΔK1L ($P < 0.05$).

3.6 References

1. Alcami, A. and G.L. Smith, *A mechanism for the inhibition of fever by a virus.* Proceedings of the National Academy of Sciences of the United States of America, 1996. **93**(20): p. 11029-11034.

2. Alcami, A. and G.L. Smith, *A Soluble Receptor for Interleukin-1-Beta Encoded by Vaccinia Virus - a Novel Mechanism of Virus Modulation of the Host Response to Infection.* Cell, 1992. **71**(1): p. 153-167.

3. Badovinac, V.P., et al., *Accelerated CD8+ T-cell memory and prime-boost response after dendritic-cell vaccination.* Nat Med, 2005. **11**(7): p. 748-56.

4. Bartlett, N., et al., *The vaccinia virus N1L protein is an intracellular homodimer that promotes virulence.* J Gen Virol, 2002. **83**(Pt 8): p. 1965-76.

5. Benfield, C.T., et al., *Vaccinia virus protein K7 is a virulence factor that alters the acute immune response to infection.* J Gen Virol, 2013. **94**(Pt 7): p. 1647-57.

6. Berhanu, A., et al., *ST-246 Inhibits In Vivo Poxvirus Dissemination, Virus Shedding, and Systemic Disease Manifestation.* Antimicrobial Agents and Chemotherapy, 2009. **53**(12): p. 4999-5009.

7. Bowie, A., et al., *A46R and A52R from vaccinia virus are antagonists of host IL-1 and toll-like receptor signaling.* Proc Natl Acad Sci U S A, 2000. **97**(18): p. 10162-7.

8. Bradley, R.R. and M. Terajima, *Vaccinia virus K1L protein mediates host-range function in RK-13 cells via ankyrin repeat and may interact with a cellular GTPase-activating protein.* Virus Res, 2005. **114**(1-2): p. 104-12.

9. Brandt, T.A. and B.L. Jacobs, *Both carboxy- and amino-terminal domains of the vaccinia virus interferon resistance gene, E3L, are required for pathogenesis in a mouse model.* J Virol, 2001. **75**(2): p. 850-6.

10. Bravo Cruz, A.G. and J.L. Shisler, *The vaccinia virus K1 ankyrin repeat protein inhibits NF-kB activation by preventing RelA acetylation.* J Gen Virol, 2016. **97**: p. 2691-2702.

11. Chen, R.A., N. Jacobs, and G.L. Smith, *Vaccinia virus strain Western Reserve protein B14 is an intracellular virulence factor.* J Gen Virol, 2006. **87**(Pt 6): p. 1451-8.

12. Chen, R.A., et al., *Inhibition of IkappaB kinase by vaccinia virus virulence factor B14.* PLoS Pathog, 2008. **4**(2): p. e22.

13. Colamonici, O.R., et al., *Vaccinia virus B18R gene encodes a type I interferon-binding protein that blocks interferon alpha transmembrane signaling.* J Biol Chem, 1995. **270**(27): p. 15974-8.

14. Collart, M.A., P. Baeuerle, and P. Vassalli, *Regulation of tumor necrosis factor alpha transcription in macrophages: involvement of four kappa B-like motifs and of constitutive and inducible forms of NF-kappa B.* Mol Cell Biol, 1990. **10**(4): p. 1498-506.

15. Costa, G.B., et al., *Detection of Vaccinia Virus in Urban Domestic Cats, Brazil.* Emerg Infect Dis, 2017. **23**(2): p. 360-362.

16. Cush, S.S., et al., *Locally Produced IL-10 Limits Cutaneous Vaccinia Virus Spread.* PLoS Pathog, 2016. **12**(3): p. e1005493.

17. Davies, M.L., et al., *MyD88-Dependent Immunity to a Natural Model of Vaccinia Virus Infection Does Not Involve Toll-Like Receptor 2.* Journal of Virology, 2014. **88**(6): p. 3557-3567.

18. DiPerna, G., et al., *Poxvirus protein N1L targets the I-kappaB kinase complex, inhibits signaling to NF-kappaB by the tumor necrosis factor superfamily of receptors, and inhibits NF-kappaB and IRF3 signaling by toll-like receptors.* J Biol Chem, 2004. **279**(35): p. 36570-8.

19. Drillien, R., F. Koehren, and A. Kirn, *Host range deletion mutant of vaccinia virus defective in human cells.* Virology, 1981. **111**(2): p. 488-99.

20. Ember, S.W., et al., *Vaccinia virus protein C4 inhibits NF-kappaB activation and promotes virus virulence.* J Gen Virol, 2012. **93**(Pt 10): p. 2098-108.

21. Ferguson, B.J., et al., *Vaccinia virus protein N2 is a nuclear IRF3 inhibitor that promotes virulence.* J Gen Virol, 2013. **94**(Pt 9): p. 2070-81.

22. Fischer, M.A., et al., *CD11b(+), Ly6G(+) cells produce type I interferon and exhibit tissue protective properties following peripheral virus infection.* PLoS Pathog, 2011. **7**(11): p. e1002374.

23. Gedey, R., et al., *Poxviral regulation of the host NF-kappaB response: the vaccinia virus M2L protein inhibits induction of NF-kappaB activation via an ERK2 pathway in virus-infected human embryonic kidney cells.* J Virol, 2006. **80**(17): p. 8676-85.

24. Goulding, J., et al., *CD8 T cells use IFN-gamma to protect against the lethal effects of a respiratory poxvirus infection.* J Immunol, 2014. **192**(11): p. 5415-25.

25. Han, A.G., et al., *Early detection of fatty liver disease in mice via quantitative ultrasound.* 2014 Ieee International Ultrasonics Symposium (Ius), 2014: p. 2363-2366.

26. Haring, J.S., V.P. Badovinac, and J.T. Harty, *Inflaming the CD8+ T cell response.* Immunity, 2006. **25**(1): p. 19-29.

27. Harte, M.T., et al., *The Poxvirus Protein A52R Targets Toll-like Receptor Signaling Complexes to Suppress Host Defense.* Journal of Experimental Medicine, 2003. **197**(3): p. 343-351.

28. Haskill, S., et al., *Characterization of an immediate-early gene induced in adherent monocytes that encodes I kappa B-like activity.* Cell, 1991. **65**(7): p. 1281-9.

29. Herbert, M.H., C.J. Squire, and A.A. Mercer, *Poxviral ankyrin proteins.* Viruses, 2015. **7**(2): p. 709-38.

30. Hickman, H.D., et al., *CXCR3 chemokine receptor enables local CD8(+) T cell migration for the destruction of virus-infected cells.* Immunity, 2015. **42**(3): p. 524-37.

31. Hickman, H.D., et al., *Anatomically restricted synergistic antiviral activities of innate and adaptive immune cells in the skin.* Cell Host Microbe, 2013. **13**(2): p. 155-68.

32. Jacobs, N., et al., *Intradermal immune response after infection with Vaccinia virus.* J Gen Virol, 2006. **87**(Pt 5): p. 1157-61.

33. Kroon, E.G., et al., *Zoonotic Brazilian Vaccinia virus: from field to therapy.* Antiviral Res, 2011. **92**(2): p. 150-63.

34. Li, Y., et al., *Structure function studies of vaccinia virus host range protein k1 reveal a novel functional surface for ankyrin repeat proteins.* J Virol, 2010. **84**(7): p. 3331-8.

35. Libermann, T.A. and D. Baltimore, *Activation of interleukin-6 gene expression through the NF-kappa B transcription factor.* Mol Cell Biol, 1990. **10**(5): p. 2327-34.

36. Lin, L.C., S.A. Smith, and D.C. Tscharke, *An intradermal model for vaccinia virus pathogenesis in mice.* Methods Mol Biol, 2012. **890**: p. 147-59.

37. Lin, S.C., et al., *Noninvasive Diagnosis of Nonalcoholic Fatty Liver Disease and Quantification of Liver Fat Using a New Quantitative Ultrasound Technique.* Clin Gastroenterol Hepatol, 2015. **13**(7): p. 1337-1345 e6.

38. Liu, Z., et al., *Deletion of C7L and K1L genes leads to significantly decreased virulence of recombinant vaccinia virus TianTan.* PLoS One, 2013. **8**(7): p. e68115.

39. Lombardi, L., et al., *Structural and functional characterization of the promoter regions of the NFKB2 gene.* Nucleic Acids Res, 1995. **23**(12): p. 2328-36.

40. Mansur, D.S., et al., *Poxvirus targeting of E3 ligase beta-TrCP by molecular mimicry: a mechanism to inhibit NF-kappaB activation and promote immune evasion and virulence.* PLoS Pathog, 2013. **9**(2): p. e1003183.

41. McCraith, S., et al., *Genome-wide analysis of vaccinia virus protein-protein interactions.* Proc Natl Acad Sci U S A, 2000. **97**(9): p. 4879-84.

42. Meng, X., et al., *C7L family of poxvirus host range genes inhibits antiviral activities induced by type I interferons and interferon regulatory factor 1.* J Virol, 2012. **86**(8): p. 4538-47.

43. Meng, X. and Y. Xiang, *Vaccinia virus K1L protein supports viral replication in human and rabbit cells through a cell-type-specific set of its ankyrin repeat residues that are distinct from its binding site for ACAP2.* Virology, 2006. **353**(1): p. 220-33.

44. Meng, X.Z., et al., *Vaccinia Virus K1L and C7L Inhibit Antiviral Activities Induced by Type I Interferons.* Journal of Virology, 2009. **83**(20): p. 10627-10636.

45. Moss, B., *Poxviridae* 6th ed. Fields Virology, ed. P.M.H. David M. Knipe. Vol. 2. 2013: Lippincott williams & Wilkins.

46. Moss, B., *Reflections on the early development of poxvirus vectors.* Vaccine, 2013. **31**(39): p. 4220-2.

47. Myskiw, C., et al., *Vaccinia virus E3 suppresses expression of diverse cytokines through inhibition of the PKR, NF-kappaB, and IRF3 pathways.* J Virol, 2009. **83**(13): p. 6757-68.

48. Perkus, M.E., et al., *Vaccinia virus host range genes.* Virology, 1990. **179**(1): p. 276-86.

49. Pohlhammer, J. and W.D. O'Brien, Jr., *Dependence of the ultrasonic scatter coefficient on collagen concentration in mammalian tissues.* J Acoust Soc Am, 1981. **69**(1): p. 283-5.

50. Price, N., et al., *Vaccinia virus gene B7R encodes an 18-kDa protein that is resident in the endoplasmic reticulum and affects virus virulence.* Virology, 2000. **267**(1): p. 65-79.

51. RamseyEwing, A.L. and B. Moss, *Complementation of a vaccinia virus host-range K1L gene deletion by the nonhomologous CP77 gene.* Virology, 1996. **222**(1): p. 75-86.

52. Randall, C.M.H. and J. Shisler, *Molluscum contagiosum virus: persistence pays off.* Future Virology, 2013. **8**(6): p. 561-573.

53. Reading, P.C. and G.L. Smith, *A kinetic analysis of immune mediators in the lungs of mice infected with vaccinia virus and comparison with intradermal infection.* J Gen Virol, 2003. **84**(Pt 8): p. 1973-83.

54. Sanchez-Sampedro, L., et al., *The evolution of poxvirus vaccines.* Viruses, 2015. **7**(4): p. 1726-803.

55. Schroder, M., M. Baran, and A.G. Bowie, *Viral targeting of DEAD box protein 3 reveals its role in TBK1/IKKepsilon-mediated IRF activation.* Embo j, 2008. **27**(15): p. 2147-57.

56. Shakhov, A.N., et al., *Structural analysis of the rabbit TNF locus, containing the genes encoding TNF-beta (lymphotoxin) and TNF-alpha (tumor necrosis factor).* Gene, 1990. **95**(2): p. 215-21.

57. Shisler, J.L. and X.L. Jin, *The vaccinia virus K1L gene product inhibits host NF-kappaB activation by preventing IkappaBalpha degradation.* J Virol, 2004. **78**(7): p. 3553-60.

58. Silva-Fernandes, A.T., et al., *Natural human infections with Vaccinia virus during bovine vaccinia outbreaks.* J Clin Virol, 2009. **44**(4): p. 308-13.

59. Sivan, G., et al., *Identification of Restriction Factors by Human Genome-Wide RNA Interference Screening of Viral Host Range Mutants Exemplified by Discovery of SAMD9 and WDR6 as Inhibitors of the Vaccinia Virus K1L-C7L-Mutant.* MBio, 2015. **6**(4): p. e01122.

60. Smith, G.L., et al., *Vaccinia virus immune evasion: mechanisms, virulence and immunogenicity.* J Gen Virol, 2013. **94**(Pt 11): p. 2367-92.

61. Spyrou, V. and G. Valiakos, *Orf virus infection in sheep or goats.* Vet Microbiol, 2015. **181**(1-2): p. 178-82.

62. Stack, J., et al., *Vaccinia virus protein A46R targets multiple Toll-like-interleukin-1 receptor adaptors and contributes to virulence.* J Exp Med, 2005. **201**(6): p. 1007-18.

63. Staib, C., et al., *Transient host range selection for genetic engineering of modified vaccinia virus Ankara.* Biotechniques, 2000. **28**(6): p. 1137-42, 1144-6, 1148.

64. Stanford, M.M., et al., *Immunopathogenesis of poxvirus infections: forecasting the impending storm.* Immunol Cell Biol, 2007. **85**(2): p. 93-102.

65. Stelekati, E., et al., *Bystander chronic infection negatively impacts development of CD8(+) T cell memory.* Immunity, 2014. **40**(5): p. 801-13.

66. Strnadova, P., et al., *Inhibition of Translation Initiation by Protein 169: A Vaccinia Virus Strategy to Suppress Innate and Adaptive Immunity and Alter Virus Virulence.* PLoS Pathog, 2015. **11**(9): p. e1005151.

67. Sun, S.C., et al., *NF-kappa B controls expression of inhibitor I kappa B alpha: evidence for an inducible autoregulatory pathway.* Science, 1993. **259**(5103): p. 1912-5.

68. Sutter, G., et al., *Stable expression of the vaccinia virus K1L gene in rabbit cells complements the host range defect of a vaccinia virus mutant.* J Virol, 1994. **68**(7): p. 4109-16.

69. Symons, J.A., A. Alcami, and G.L. Smith, *Vaccinia virus encodes a soluble type I interferon receptor of novel structure and broad species specificity.* Cell, 1995. **81**(4): p. 551-60.

70. Tartaglia, J., et al., *Nyvac - a Highly Attenuated Strain of Vaccinia Virus.* Virology, 1992. **188**(1): p. 217-232.

71. Tscharke, D.C., P.C. Reading, and G.L. Smith, *Dermal infection with vaccinia virus reveals roles for virus proteins not seen using other inoculation routes.* J Gen Virol, 2002. **83**(Pt 8): p. 1977-86.

72. Tscharke, D.C. and G.L. Smith, *A model for vaccinia virus pathogenesis and immunity based on intradermal injection of mouse ear pinnae.* J Gen Virol, 1999. **80**: p. 2751-5.

73. van Buuren, N., et al., *EVM005: an ectromelia-encoded protein with dual roles in NF-kappaB inhibition and virulence.* PLoS Pathog, 2014. **10**(8): p. e1004326.

74. Wilcock, D., et al., *The vaccinia virus A4OR gene product is a nonstructural, type II membrane glycoprotein that is expressed at the cell surface.* J Gen Virol, 1999. **80 (Pt 8)**: p. 2137-48.

75. Williamson, J.D., et al., *Biological characterization of recombinant vaccinia viruses in mice infected by the respiratory route.* J Gen Virol, 1990. **71**: p. 2761-7.

76. Willis, K.L., J.O. Langland, and J.L. Shisler, *Viral double-stranded RNAs from vaccinia virus early or intermediate gene transcripts possess PKR activating function, resulting in NF-kappaB activation, when the K1 protein is absent or mutated.* J Biol Chem, 2011. **286**(10): p. 7765-78.

77. Willis, K.L., et al., *The effect of the vaccinia K1 protein on the PKR-eIF2alpha pathway in RK13 and HeLa cells.* Virology, 2009. **394**(1): p. 73-81.

78. Yao, L.X., J.A. Zagzebski, and E.L. Madsen, *Backscatter Coefficient Measurements Using a Reference Phantom to Extract Depth-Dependent Instrumentation Factors.* Ultrasonic Imaging, 1990. **12**(1): p. 58-70.

Chapter 4: The K1 protein is structurally similar to the NF-κB cellular inhibitor, IκBα, and likewise co-immunoprecipitates with NF-κB

4.1 Introduction

The K1 protein was discovered over 30 years ago [5, 7]. Originally, based on structure prediction software SMART, it was thought that K1 consisted of six ankyrin repeat domains (ARDs) [17], motifs known for protein-protein interactions [15]. However, the elucidation of K1's crystal structure revealed that it consists of nine ARDs [16]. In addition, the crystal structure confirmed that K1 does not contain an F-box domain. This is a unique feature of K1 because most other poxviral ARD-containing proteins that are known to inhibit NF-κB activation contain this F-box motif. This implies that the K1 mechanism to inhibit NF-κB activation is likely different than the mechanism used by other poxvirus ARD-containing proteins, which is confirmed in chapter 2.

ARDs are abundant in cellular proteins but are not common in bacterial or viral proteins [1]. Indeed, only three known virus families (*Poxviridae, Asfaviridae and Polydnaviridae*) have genes that encode ARDs. Poxviruses encode multiple viral ARD-containing proteins (vankyrins) [25, 26], and the functions of some of these proteins are known to be involved in functions as diverse as viral replication and virulence. However, many of the poxviral vankyrins still have unknown functions [12].

The cellular IκB proteins are a family of proteins that bind to and inhibit NF-κB activation [13]. IκB proteins possess ARDs, which mediate NF-κB-IκB interactions [14]. A strategy used by poxviruses and other viruses to inhibit NF-κB activation is to encode vankyrins. Each of them employs unique mechanisms to inhibit NF-κB

activation, which provides insights as to how K1 might inhibit NF-κB. For example, the myxoma virus encodes the *M150R* gene, whose product consists of nine ARDs [3]. M150 localizes to the nucleus by using one of its ARDs as a nuclear localization signal, similar to the mechanism employed by IκBα [3]. M150 does not inhibit IκBα degradation or NF-κB nuclear translocation. Instead, it co-localizes with the p65 subunit in the nucleus [3]. The mechanism employed by M150 to inhibit NF-κB activation is not yet completely understood. However, it has been suggested that M150 could interact with the NF-κB subunit RelA and trap NF-κB after entry to the nucleus. Work in this thesis (chapter 2) demonstrated that K1 also localizes to the nucleus. One hypothesis is that similar to the proposed mechanism for M150, K1 traps NF-κB after nuclear translocation and prevents it from interacting with co-activator CBP.

Another example of an IκBα viral homolog is the ARD-containing A238 protein, encoded by the African swine fever virus (ASFV) [23] . A238 allows IκBα degradation, but binds to free RelA to form a biologically inactivate A238-NF-κB heterodimer in the cytoplasm [23]. Moreover, A238 also inhibits post-translational modifications of NF-κB by inhibiting p300 transactivation, thereby diminishing p300-mediated acetylation of RelA [8]. Similarly, we have found that K1 prevents RelA acetylation (chapter 2).

Additionally, cowpox virus encodes the CP77 protein, which blocks NF-κB nuclear translocation and subsequent activation by binding to the p65 subunit through its N-terminal six-ARD region. Similar to the ASFV A238 protein above, CP77 does not block IκBα degradation [4]. The VARV G1R protein family, which includes ECTV 002, MPXV 003, CPXV 006, interacts with NF-κB1/p105 and inhibits NF-κB activation [18].

The function of K1's ARDs remains a subject of investigation in our lab. Determining the contribution of K1's ARDs to NF-κB inhibition was the original scope of my thesis project. Although the effect of removing one or two ARDs still remains unstudied, this chapter describes the tools and advances made to determine the biological relevance of K1's ARDs in NF-κB inhibition.

4.2 Materials and Methods

Cells, plasmids and viruses

Human embryonic kidney 293T (293T) cells and Vero cells were obtained from the American Type Culture Collection (ATCC). Cells were cultured in Eagle's minimal essential media supplemented with 10% FBS, 2mM L-glutamine, 100 U/mL penicillin and 100 μg/mL streptomycin. Virus medium (MEM supplemented with 2.5% FBS) was used for virus absorption phases and virus infections.

Plasmid pHA-K1 consists of a hemagglutinin epitope-tagged *K1L* gene inserted into the pCI expression vector [27]. Plasmids were transfected into cells using the Fugene 6 (Promega) or TransIt (Mirus) reagents following manufacturer's instructions.

Vaccinia virus western reserve strain (vK1L) and modified vaccinia Ankara (MVA) were obtained from Dr. Bernard Moss (Laboratory of Viral Diseases, National Institutes of Health). vΔK1L is a WR virus in which the *K1L* gene was replaced with the *Escherichia coli gpt* gene by homologous recombination. The MVA/K1L virus contains the vaccinia virus western reserve strain *K1L* gene stably inserted into the del III region of MVA, and was a gift from Gerd Sutter (Institute for Molecular Virology, Munich, Germany).

Three-dimensional structure alignment

To compare the protein structures of IκBα and K1, the Flexible structure AlignmenT by Chaining Aligned fragmenT pairs allowing twists (FATCAT) algorithm was used [28]. The three-dimensional structures of both Iκbα and K1 were obtained from the protein data bank website (IκBα; PDB ID: 1 IKN and K1; PDB ID: 3KEA) [14, 16].

Immunoprecipitations

To detect RelA-CBP interactions, subconfluent cellular monolayers of 293T cells in 6-well plates were transfected with 2000 ng of pHA-K1 or pCI using Fugene 6. At 24 h post-transfection, dislodged cells were centrifuged (14,000 rpm for 1 min) and the cellular pellet was resuspended in RIPA buffer (150 mM NaCl, 1% sodium deoxycholate, 1% NP-40, 0.1% SDS, 0.01 M Tris-HCl pH 7.4) for 30 min on ice. Lysates were centrifuged (14,000 rpm for 10 min). A portion of each clarified lysate was removed to a new tube and used to probe protein expression in cellular lysates. Protein concentration of lysates was determined by bicinchoninic (BCA) assay (Pierce). The remaining clarified lysates were placed in a new tube and incubated with 1 μl of anti-RelA antibodies (Santa Cruz; sc-8008 X) for 1 h. Then protein G-Sepharose beads (Life Technologies) were added to the mixture and incubated overnight at 4° C. Next, beads were washed in large volumes of RIPA Buffer. Beads were mixed with 2x sample buffer containing 2-mercaptoethanol and boiled for 5 min. A portion of each immunoprecipitation reaction was separated by SDS-PAGE. Proteins were transferred electrophoretically to PVDF membranes and membranes were blocked in 5% (w/v) milk in Tris-Buffered Saline and Tween 20 (TBST; 150 mM NaCl, 50 mM Tris base, 0.05% Tween 20) for at least 30 min

at room temperature were then incubated with anti-HA antibody (1:1,000; Sigma) and then HRP-conjugated goat anti-mouse IgG (1:5,000; Thermo Scientific). Antibody reactions on membranes were detected by using chemiluminescence reagents (Amersham and Thermo Scientific) and autoradiography.

Luciferase assays

A dual-reporter luciferase assay was performed to quantify NF-κB activation in infected cells using previously published protocols [21, 22, 24]. Subconfluent 293T cellular monolayers were transfected with 112.5 ng pNF-κB*luc* and 12.5 ng pRL-null (Promega). 24 h later, cells were either mock-infected or infected with vK1L, vΔK1L, MVA or MVA/K1L at a multiplicity of infection (MOI) of 10 PFU/cell. At eight hours post-infection, cells were lysed in 1X Passive Lysis Buffer (PLB; Promega) and lysates were analyzed as described previously.

Plasmids construction

(This work was performed by Arielle B Guzman, an undergraduate student working under my supervision)

A panel of recombinant viruses expressing either wild-type K1 or K1 mutants each lacking one or two ARDs (D1-D7) was obtained from Dr. Yan Xiang (University of Texas Health Science Center) [17]. Since these deletion mutants were generated before K1's crystal structured was elucidated, each deletion number does not correspond to the ARD deleted (e.g. D1 does not correspond to a deletion of the ARD 1, but instead ARD 2

is deleted). A schematic of the corresponding ARD deleted in each mutant is shown in Figure 4.3.

To clone each K1 deletion mutant into the pCI mammalian vector, viral genomes were collected. Briefly, confluent monolayers of Vero cells in 6-well plates were infected at an MOI of 5 PFU/cell. At 18 h post-infection, cellular and viral genomes were collected using the DNeasy Blood and Tissue Kit (Qiagen) following manufacturer's instructions.

To insert an HA-tag on the N-terminus, and remove the V5-tag on the C-terminus of each mutant, the wild-type or each mutated *K1L* gene was PCR amplified from collected viral genomes using primers (5'GGTTAGAATTCGCCACCATGGATTATCC ATATGATGTTCCAGATTATGCTGATCT GTCACGAATTAATACTTGG-3') and (5'GTACAGCGGCCGCTCAG TTTTTC TTTACACA ATTGACGTA-3') and Phusion High-Fidelity DNA Polymerase (New England BioLabs). PCR amplicons were purified using PCR Purification Kit (Qiagen) and analyzed by electrophoresis. PCR products and pCI plasmid were cut with EcoRI-HF and NotI-HF restriction enzymes (New England BioLabs) at 37° C for 15 min. Digested products were analyzed by electrophoresis and purified using the QIAquick Gel Extraction Kit (Qiagen). Purified cut PCR product and plasmid were ligated at a 3:1 or 6:1 ratio using T4 DNA ligase (New England BioLabs) at room temperature for 20 min. Insertion of *K1L* gene into pCI was confirmed by double digestion with EcoRI-HF and NotI-HF. Sequence integrity of the *K1L* gene was confirmed by sequencing.

To analyze the expression of each K1 mutant, subconfluent cellular monolayers of 293T cells in 6-well plates were transfected with 1500 ng of pHA-K1WT, pHA-D1,

pHA-D2, pHA-D3, pHA-D4, pHA-D5, pHA-D6, pHA-D7 or pCI using TransIt. At 24 h post-transfection, dislodged cells were centrifuged (14,000 rpm for 1 min) and the cellular pellet was resuspended in CE buffer with HALT for 15 min on ice. Lysates were centrifuged (14,000 rpm for 1 min) and clarified supernatants were removed to fresh tubes. Protein concentration of lysates was determined by BCA assay. Thirty μg of cytoplasmically-extracted protein from each sample was evaluated for K1 protein levels by using immunoblotting, in which immunoblots were incubated with mouse anti-HA antibody. Blots were re-probed with rabbit monoclonal anti-β-actin antibody (1:5,000; Sigma) and then HRP-conjugated goat anti-rabbit IgG (1:10,000; CalBiotech).

4.3 Results

K1 and IκBα are structurally similar

IκBα, the cellular inhibitor of RelA-p50 heterodimers, contains 6 ARDs [14]. Interestingly, the K1 protein also contains ARDs [16]. The amino acid sequences of both K1 and IκBα (specifically the region involved in NF-κB binding) show no significant similarity (data not shown). However, the 3D structures of K1 and IκBα proteins were significantly similar *(P* value of 2.28e-09) as determined by Flexible structure Alignment by Chaining aligned fragment pairs allowing twists (FATCAT), which defines significant similarity by a P value < 0.05 [28]. Both the 3D structure alignment and the aligned amino acid sequences based on the structural alignment are shown in Figure 4.1. In addition, the IκBα residues involved in NF-κB interactions and the corresponding aligned amino acid of the K1 protein are shown in Table 4.1.

The K1 protein co-immunoprecipitates with NF-κB

IκBα inhibits NF-κB activation by binding to NF-κB [11]. I hypothesized that, due to their structural similarity, K1 would also be able to bind to NF-κB. To test this hypothesis, co-immunoprecipitation assays were performed in which endogenous RelA (NF-κB subunit) was pulled down and bound K1 was detected by immunoblotting. Figure 4.2 shows that K1 and RelA co-immunoprecipitated in both unstimulated or TNF-stimulated conditions. However, this co-immunoprecipitation assay needs to be optimized since it was very challenging to repeatedly detect those interactions. This raises the possibility that K1 may bind to another cellular factor such as CBP instead of NF-κB or that a viral protein stabilizes these interactions since these co-IPS were performed independently of infections.

Expression of K1 ARD mutants

The original scope of this thesis was to determine if binding to RelA contributes to K1's NF-κB inhibitory mechanism. If K1-NF-κB interactions are biologically relevant, I rationalized that a mutant that has lost its ability to bind to RelA should then lose its NF-κB inhibitory function. A panel of recombinant viruses each expressing a V5 epitope-tagged mutant K1 protein that lacks one or two ARDs was obtained (Fig 4.3) [17]. I expected to use this panel of mutant viruses to test the biological relevance of K1-NF-κB interactions by testing the ability of each mutant K1 protein to inhibit and bind to NF-κB. However, these viruses could not be used for these purposes because I did not observe NF-κB activation or IκBα degradation in 293T cells infected with vΔK1L (Figure 4.4A and 4.4B, respectively). NF-κB–controlled luciferase activity levels were low in mock-

infected cells or in vK1L- or vΔK1L-infected cells, indicating that NF-κB remained inactive under these conditions (Fig. 4.4B). Some cells were instead infected with MVA, an attenuated strain of vaccinia virus that lacks the *K1L* gene and other immune evasion genes as a positive control [2]. As shown previously, MVA infection stimulated NF-κB in this cell line [24] [20]. In contrast, infection with a recombinant MVA/K1L resulted in inhibition of NF-κB (Fig 4.4B). Taken together the K1 protein is sufficient, but not required to inhibit NF-κB activation in 293T cells.

Data from an IκBα degradation assay complemented results from Figure 4.4A: IκBα degradation was observed by immunoblotting and the intensity of these IκBα-containing bands was similar to the band observed in mock-infected cells, inferring that virus infection itself, regardless of the presence or absence of K1L, did not stimulate NF-κB. Similarly, IκBα remained present when infected cells were incubated with TNF, a cytokine that is an extrinsic stimulator of NF-κB [10], and this is not surprising given that VACV encodes proteins that inhibit NF-κB activation reference. Notably, IκBα was no longer detectable in mock-infected cells that were treated with TNF, showing that 293T cells had the capacity to respond to NF-κB-inducing stimuli. Since K1 is not required to inhibit NF-κB, I could not use this panel of mutant viruses in the 293T cell line to map the K1 region containing NF-κB antagonistic activity.

One alternative to study the effects of removing one ARD in K1's inhibitory function is to express these mutants in an MVA/K1L background. However, results from chapter 2 concluded that viral infections are not suitable to study NF-κB inhibition by K1 due to the cofounding effects of other viral proteins still present in VACV or MVA.

Thus, the best approach to study the role of K1's ARDs in NF-κB inhibition is to express each mutant independently of viral infection. Previous undergraduate students working under my mentoring cloned recombinant V5-tagged *K1L* genes into the pCI mammalian expression vector. However, these plasmids exhibited a poor and inconsistent K1 expression in 293T cells. Since epitope tags can alter protein expression, we created a second set of mutant constructs in which we engineered an HA tag in place of the V5 tag. We chose the HA epitope because an HA-tagged K1 protein expressed from pCI showed consistent expression throughout multiple experiments in chapter 2 of this thesis. Data from Figure 4.5 showed that each HA-tagged K1 mutant protein was expressed in 293T cells. We have noticed that these mutant K1 proteins consistently have decreased expression as compared to wild-type K1 proteins. Interestingly, this decreased expression was also observed during infection [17]. The next goal is to use these proteins in our acetylation assays discussed in chapter 2 as a read-out for which K1 region possesses NF-κB antagonistic function.

4.4 Discussion

Here I show that the K1 protein ARDs are structurally similar to the ARDs in IκBα. In addition, I show that, similar to IκBα, K1 co-immunoprecipitates with NF-κB. However, these interactions were difficult to observe consistently, despite multiple attempts to repeat or optimize assays to detect RelA-K1 interactions.

Despite this lack of reliability, I believe that RelA-K1 interactions might contribute to K1's NF-κB inhibitory mechanism. However, I hypothesize that K1's mechanism is different from the one employed by IκBα. RelA-IκBα interactions mask

RelA nuclear localization signal (NLS) and keep NF-κB inactive in the cytoplasm [14]. Results from chapter 2 show that NF-κB localized to the nucleus in the presence of K1. Thus it is unlikely that K1-RelA interactions mask NF-κB's NLS. In addition to blocking NF-κB nuclear translocation, RelA-IκBα interactions cause a conformational change that induces allosteric inhibition of NF-κB-DNA binding [14]. However, work from chapter 2 does not support a conformational change as a result of RelA-K1 interactions since K1 allows NF-κB to interact with an oligonucleotide containing NF-κB binding sites.

RelA is acetylated by CBP/p300, a post-translational modification that is required for NF-κB full transcriptional activity [6, 19]. For this acetylation to occur CBP/p300-RelA interaction must occur. I have shown that neither acetylation or CBP-RelA interactions occur in the presence of K1 (chapter 2). Thus our current hypothesis is that K1 binds to RelA in the same region that CBP/p300, does preventing CBP-RelA interactions. Interestingly, the ASFV A238 vankyrin also utilizes a CBP/p300-dependent mechanism to inhibit NF-κB activation by preventing the recruitment of CBP/p300 to the enhanceosomes [9]. This raises the possibility that some vankyrins share a similar mechanism to prevent NF-κB activation.

4.5 Figures and Table

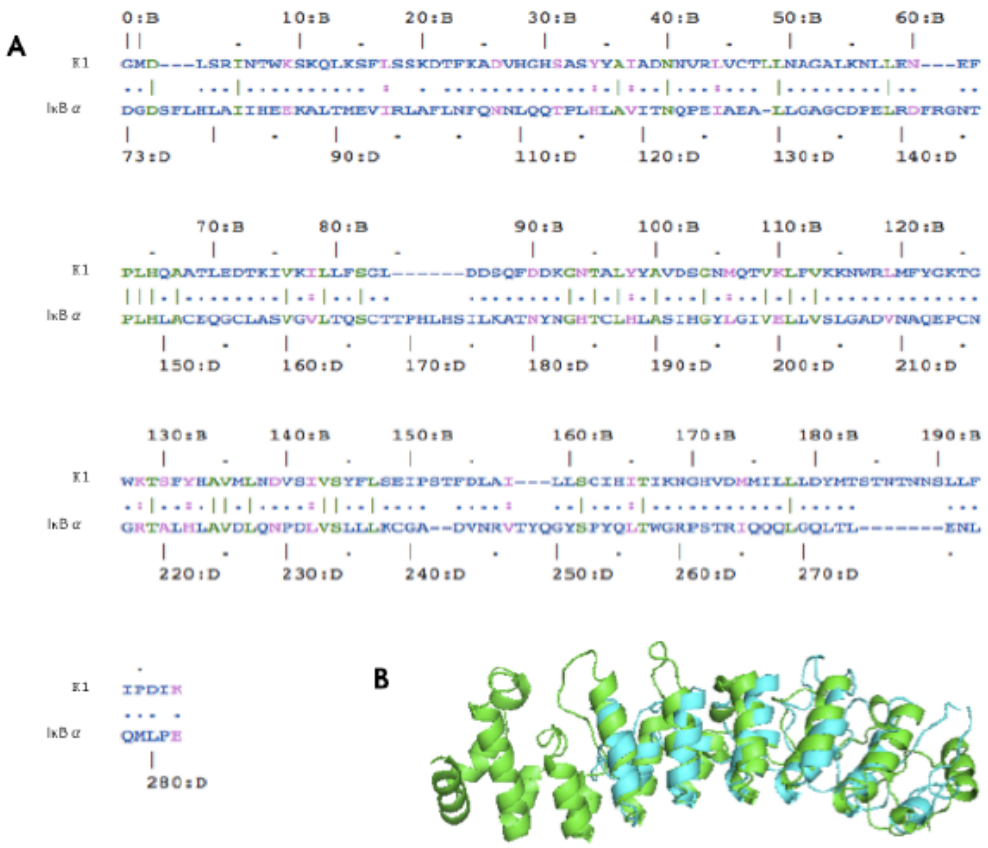

Figure 4.1 The 3D structures of K1 and IκBα are significantly similar. (A) Sequence alignment obtained using Flexible structure AlignmenT by Chaining Aligned fragment pairs allowing Twists (FATCAT). The two structures are significantly similar with a P-value of 2.28e-09. Blue residues: structurally equivalent, but not similar; Pink residues: structurally equivalent, and similar; Green residues: structurally equivalent and identical residues. (B) Graphic representation of the alignment. Green: K1; Blue: IκBα.

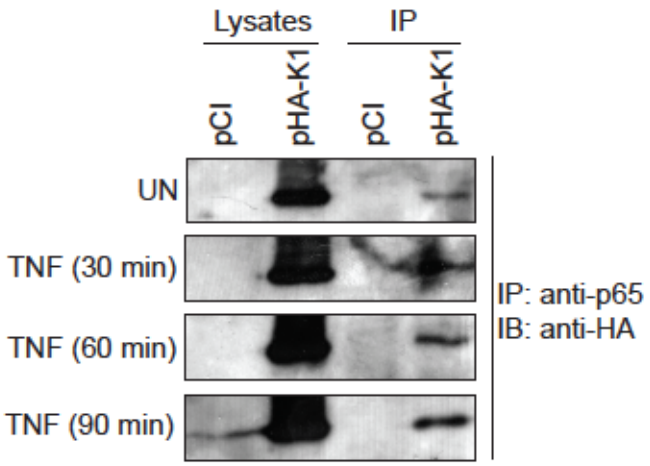

Figure 4.2 The K1 protein immunoprecipitates with NF-κB. 293T cells were transfected with pCI or pHA-K1. At 24 h post-transfection, cells were incubated in medium lacking (UN) or containing TNF (10 ng/mL). Cells were lysed in RIPA buffer at the indicated time. Immunoprecipitation (IP) was performed by incubating lysates with anti-RelA antibody for 1 h and then protein G-sepharose beads were added for overnight incubation. IPs or 30 µg of lysates were subjected to 12 % SDS- PAGE and transferred to PVDF membranes. Blots were incubated with anti-HA antibodies.

Figure 4.3 Schematic of K1 mutants. The wild-type K1 protein possess nine ARDs, each depicted as a purple box (WT). Each mutant (D1-D7) lacks one or two ARDs. The corresponding ARD in each mutant is depicted as a white box.

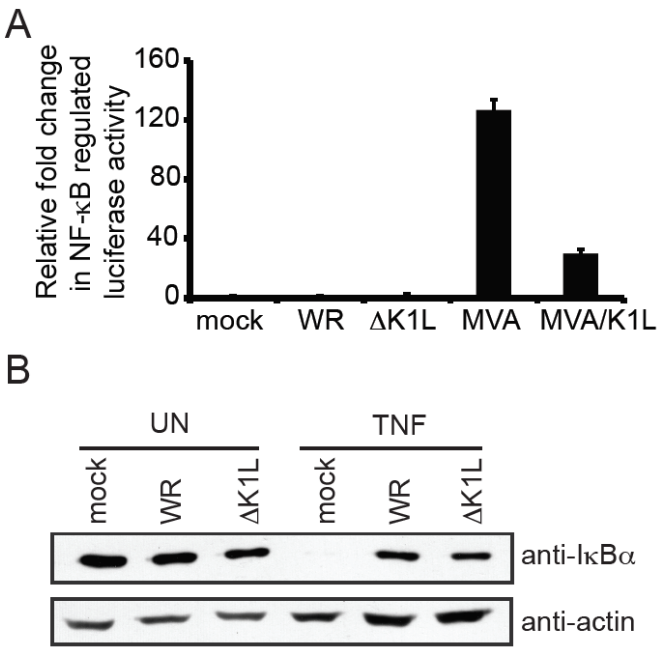

Figure 4.4 The K1 protein is not required to inhibit NF-κB activation in infected 293T cells. (A) 293T cell monolayers were either mock-infected or infected with WR or ΔK1L (MOI = 5). At 3 h pi, cells were incubated in medium lacking (UN) or containing TNF (10 ng/mL) for 20 min. Cells were lysed in CE buffer. Equal amounts of cytoplasmic extracts (15 μg) were separated by 10% SDS-PAGE and transferred to a PVDF membrane. Immunoblots were probed with anti-IκBα antibody and re-probed with anti-actin antibodies. (B) Sub-confluent 293T cellular monolayers were transfected with 112.5 ng pNF-κB*luc* and 12.5 ng pRL-null. At 24 h post-transfection, cells were mock-infected or infected with the indicated viruses (MOI = 10). At 8 h pi, cells were lysed, and firefly and sea pansy luciferase activities were measured. Experiments were performed in triplicate and data show the average luciferase/sea pansy ratio normalized to the value obtained from mock-infected cells, for which the value was set to 1. Error bars represent standard deviation.

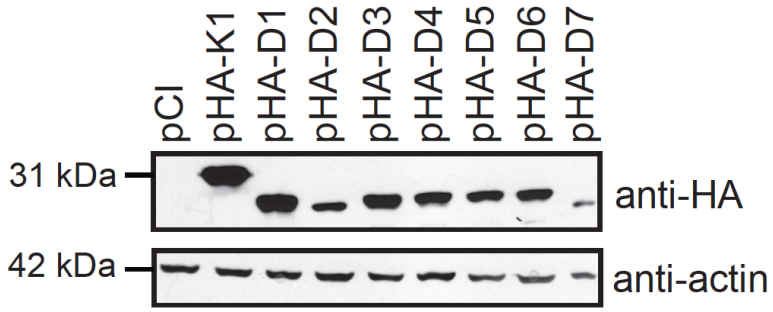

Figure 4.5 Expression of K1 ARD mutants. 293T cells were transfected with 1500 ng of pCI, pHA-K1 or plasmids encoding for K1 mutants (pHA-D1 to pHA-D7). 24 post transfection cells were lysed in CE buffer. Cellular lysates were separated by SDS-PAGE and then transferred to PVDF membranes. Membranes were probed with anti-HA antibodies, and then the same blots were re-probed with anti-β-actin antiserum.

Table 4.1 Comparison of IκBα residues contacting NF-κB with corresponding K1 residues.

Residue in IκBα	Residue in K1	Contact with NF-κB	Similarity
Glu 138	Leu	p50 DD	Structurally equivalent; not similar residues
Leu 150	Gln	RelA NLS	Structurally equivalent; not similar residues
Glu 153	Thr	RelA NLS	Structurally equivalent; not similar residues
Gln 154	Leu	RelA NLS	Structurally equivalent; not similar residues
Tyr 181	Asp	p50 DD	Structurally equivalent; not similar residues
Pro 214	Lys	p50 DD	Structurally equivalent; not similar residues
Cys 215	Thr	p50 DD	Structurally equivalent; not similar residues
Asn 216	Gly	p50 DD	Structurally equivalent; not similar residues
Arg 218	Lys	RelA DD	Structurally equivalent; similar residues
Thr 247	-	p50 DD	-
Tyr 248	-	p50 DD	-
Tyr 251	Leu	RelA DD	Structurally equivalent; not similar residues
Leu 256	Ile	p50 DD, RelA DD	Structurally equivalent; similar residues
Trp 258	Ile	RelA ATD, RelA DD	Structurally equivalent; not similar residues
Arg 260	Asn	RelA DD	Structurally equivalent; not similar residues
Gln 266	Met	RelA ATD	Structurally equivalent; not similar residues
Leu 269	Leu	RelA ATD	structurally equivalent; identical residues
Gln 271	Asp	RelA ATD	Structurally equivalent; not similar residues
Met 279	Pro	RelA DD	Structurally equivalent; not similar residues
Leu 280	Asp	RelA DD	Structurally equivalent; not similar residues
Glu 282	Glu	RelA DD	Structurally equivalent; similar residues

DD: Dimerization domain; NLS: nuclear localization signal; ATD: Amino terminal domain.

4.6 References

1. Al-Khodor, S., et al., *Functional diversity of ankyrin repeats in microbial proteins.* Trends Microbiol, 2010. **18**(3): p. 132-9.

2. Antoine, G., et al., *The complete genomic sequence of the modified vaccinia Ankara strain: comparison with other orthopoxviruses.* Virology, 1998. **244**(2): p. 365-96.

3. Camus-Bouclainville, C., et al., *A Virulence Factor of Myxoma Virus Colocalizes with NF- B in the Nucleus and Interferes with Inflammation.* Journal of Virology, 2004. **78**(5): p. 2510-2516.

4. Chang, S.J., et al., *Poxvirus host range protein CP77 contains an F-box-like domain that is necessary to suppress NF-kappaB activation by tumor necrosis factor alpha but is independent of its host range function.* J Virol, 2009. **83**(9): p. 4140-52.

5. Drillien, R., F. Koehren, and A. Kirn, *Host range deletion mutant of vaccinia virus defective in human cells.* Virology, 1981. **111**(2): p. 488-99.

6. Gerritsen, M.E., et al., *CREB-binding protein/p300 are transcriptional coactivators of p65.* Proc Natl Acad Sci U S A, 1997. **94**(7): p. 2927-32.

7. Gillard, S., et al., *Localization and sequence of a vaccinia virus gene required for multiplication in human cells.* Proc Natl Acad Sci U S A, 1986. **83**(15): p. 5573-7.

8. Granja, A.G., N.D. Perkins, and Y. Revilla, *A238L inhibits NF-ATc2, NF-kappa B, and c-Jun activation through a novel mechanism involving protein kinase C-theta-mediated up-regulation of the amino-terminal transactivation domain of p300.* J Immunol, 2008. **180**(4): p. 2429-42.

9. Granja, A.G., et al., *African swine fever virus blocks the host cell antiviral inflammatory response through a direct inhibition of PKC-theta-mediated p300 transactivation.* J Virol, 2009. **83**(2): p. 969-80.

10. Hayden, M.S. and S. Ghosh, *Regulation of NF-kappaB by TNF family cytokines.* Semin Immunol, 2014. **26**(3): p. 253-66.

11. Hayden, M.S. and S. Ghosh, *Shared principles in NF-kappaB signaling.* Cell, 2008. **132**(3): p. 344-62.

12. Herbert, M.H., C.J. Squire, and A.A. Mercer, *Poxviral ankyrin proteins.* Viruses, 2015. **7**(2): p. 709-38.

13. Hinz, M., S.C. Arslan, and C. Scheidereit, *It takes two to tango: IkappaBs, the multifunctional partners of NF-kappaB.* Immunol Rev, 2012. **246**(1): p. 59-76.

14. Huxford, T., et al., *The crystal structure of the IkappaBalpha/NF-kappaB complex reveals mechanisms of NF-kappaB inactivation.* Cell, 1998. **95**(6): p. 759-70.

15. Li, J., A. Mahajan, and M.D. Tsai, *Ankyrin repeat: a unique motif mediating protein-protein interactions.* Biochemistry, 2006. **45**(51): p. 15168-78.

16. Li, Y., et al., *Structure function studies of vaccinia virus host range protein k1 reveal a novel functional surface for ankyrin repeat proteins.* J Virol, 2010. **84**(7): p. 3331-8.

17. Meng, X. and Y. Xiang, *Vaccinia virus K1L protein supports viral replication in human and rabbit cells through a cell-type-specific set of its ankyrin repeat residues that are distinct from its binding site for ACAP2.* Virology, 2006. **353**(1): p. 220-33.

18. Mohamed, M.R., et al., *Proteomic screening of variola virus reveals a unique NF-kappaB inhibitor that is highly conserved among pathogenic orthopoxviruses.* Proc Natl Acad Sci U S A, 2009. **106**(22): p. 9045-50.

19. Mukherjee, S.P., et al., *Analysis of the RelA:CBP/p300 interaction reveals its involvement in NF-kappaB-driven transcription.* PLoS Biol, 2013. **11**(9): p. e1001647.

20. Oie, K.L. and D.J. Pickup, *Cowpox virus and other members of the orthopoxvirus genus interfere with the regulation of NF-kappaB activation.* Virology, 2001. **288**(1): p. 175-87.

21. Randall, C.M., et al., *Inhibition of interferon gene activation by death-effector domain-containing proteins from the molluscum contagiosum virus.* Proc Natl Acad Sci U S A, 2014. **111**(2): p. E265-72.

22. Randall, C.M., J.A. Jokela, and J.L. Shisler, *The MC159 Protein from the Molluscum Contagiosum Poxvirus Inhibits NF-kappaB Activation by Interacting with the IkappaB Kinase Complex.* Journal of immunology, 2012. **188**(5): p. 2371-9.

23. Revilla, Y., *Inhibition of Nuclear Factor kappa B Activation by a Virus-encoded Ikappa B-like Protein.* Journal of Biological Chemistry, 1998. **273**(9): p. 5405-5411.

24. Shisler, J.L. and X.L. Jin, *The vaccinia virus K1L gene product inhibits host NF-kappaB activation by preventing IkappaBalpha degradation.* J Virol, 2004. **78**(7): p. 3553-60.

25. Sonnberg, S., S.B. Fleming, and A.A. Mercer, *Phylogenetic analysis of the large family of poxvirus ankyrin-repeat proteins reveals orthologue groups within and across chordopoxvirus genera.* J Gen Virol, 2011. **92**(Pt 11): p. 2596-607.

26. Sonnberg, S., et al., *Poxvirus ankyrin repeat proteins are a unique class of F-box proteins that associate with cellular SCF1 ubiquitin ligase complexes.* Proc Natl Acad Sci U S A, 2008. **105**(31): p. 10955-60.

27. Willis, K.L., J.O. Langland, and J.L. Shisler, *Viral double-stranded RNAs from vaccinia virus early or intermediate gene transcripts possess PKR activating function, resulting in NF-kappaB activation, when the K1 protein is absent or mutated.* J Biol Chem, 2011. **286**(10): p. 7765-78.

28. Ye, Y. and A. Godzik, *Flexible structure alignment by chaining aligned fragment pairs allowing twists.* Bioinformatics, 2003. **19 Suppl 2**: p. ii246-55.

Chapter 5: Summary and Future Directions

5.1 Summary

This thesis project describes several novel findings about the anti-inflammatory effects of the K1 protein. Our lab has previously published that the K1 protein inhibits NF-κB activation as an indirect effect of inhibiting the upstream activator PKR. In addition, the effects of lacking the K1 protein on VACV pathogenesis were unknown. Here, I discovered a novel PKR-independent mechanism by which K1 inhibits NF-κB activation. Also, I found that VACV lacking the K1 protein (vΔK1L) is attenuated in two animal models of infection.

The K1 protein is known to inhibit the activation of the dsRNA sensor PKR, and it was originally hypothesized that inhibition of IκBα degradation and subsequent NF-κB activation was solely an effect of PKR inhibition. However, I have found that K1 not only inhibits NF-κB in PKR deficient cells, but also allows NF-κB nuclear translocation and DNA binding, events that occur after IκBα degradation in the NF-κB signaling pathway. These observations suggested a PKR-independent mechanism. Indeed, in this mechanism, K1 prevents NF-κB-CBP interactions and consequently CBP-mediated NF-κB acetylation. This is the first report of a VACV protein inhibiting NF-κB acetylation, one of the most downstream events in NF-κB signaling.

Although K1 has been shown to inhibit multiple anti-viral immune responses, such as NF-κB, PKR, and IFN in cell culture models of infection, no studies have investigated the effects of removing K1 from VACV in viral pathogenesis. I have found that vΔK1L is attenuated in two animal models of infection, IN and ID, measured by

weight loss and lesion size, respectively. In the IN model, I observed that vΔK1L replicated less than wild-type VACV and had limited spread. In contrast, in the ID model, there was no difference in viral replication between wild-type VACV and vΔK1L. However, I saw a decrease in inflammatory gene response in vΔK1L-infected mice as compared to VACV, despite K1's known NF-κB inhibitory function in cell culture. This unexpected result reconfirms that animal models of infection are needed to truly understand the contributions of immune evasion proteins to viral pathogenesis. Although vΔK1L induced a moderate inflammatory gene expression, vΔK1L was protective against a VACV lethal challenge. This suggests that the robust inflammatory gene expression induced by VACV is an excess of what is needed to mount a protective immune response and that our field still has a lack of understanding of how VACV is such a successful vaccine.

5.2 Future Directions

K1's nuclear localization

I have found that the K1 protein localizes to the cytoplasm and nucleus when K1 is expressed either by infection or transfection. It is unclear how K1 localizes to the nucleus because it lacks a classical nuclear localization signal (NLS). However, other ARD-containing proteins such as IκBα and poxviral protein M150 use one of their ARDs as a non-canonical NLS. To investigate this hypothesis, mutants described in Chapter 4 could be utilized to detect changes in K1's sub-cellular localization when it lacks one ARD. Another possibility is that K1 binds to NF-κB and translocates to the nucleus as part of a complex. However, this is unlikely because K1 localizes to the nucleus in

unstimulated cells, where most of the NF-κB population is cytoplasmic. K1 may passively diffuse to the nucleus because K1 is relatively small (32.5 kDa).

How does K1 inhibit NF-κB-CBP interactions?

In chapter 2 I described that K1 prevents NF-κB-CBP interactions to prevent RelA acetylation and NF-κB activation. How NF-κB-CBP interactions are disrupted by K1 still needs to be investigated. I observed that K1 co-immunoprecipitates with NF-κB. Thus, our working hypothesis is that K1 binds to the same region of NF-κB that CBP does and prevents CBP from docking. Mutational analysis of K1-NF-κB and CBP-NF-κB interactions can be used to test this hypothesis. As an additional means to confirm that K1-NF-κB interactions are biologically relevant for K1's NF-κB inhibitory function, the ARD mutants described in chapter 4 could be tested for their ability to bind to and inhibit NF-κB as compared to wild-type K1. I expect that mutants that no longer bind to NF-κB should no longer inhibit NF-κB activation (as measured by RelA acetylation). In addition, mutants that no longer bind to NF-κB should not disrupt NF-κB-CBP interactions to support the hypothesis that K1 and CBP competitively bind to NF-κB. This competitive binding could also be confirmed if the NF-κB region to which K1 binds to is determined. For this, NF-κB (RelA) mutants could be obtained to specifically determine which region K1 binds to, which should be the same region that CBP binds.

It should be noted that luciferase assays, which are the standard means to evaluate NF-κB activation, need to be optimized. During my tenure as a graduate student, there were different luciferase assay conditions in which K1would either inhibit or no longer

inhibit NF-κB activation. Multiple attempts were tried to obtain the same NF-κB inhibitory results by K1. Unfortunately, these attempts were not successful, which could be attributed to changes in the luminometer, transfection reagents and cell line stocks that occurred over the years. However, NF-κB inhibition by K1 was reliably detected via NF-κB acetylation assays, suggesting that these assays may be better than luciferase assays. In addition, as mentioned in chapter 4, the K1-NF-κB co-immunoprecipitation assays need to be optimized since it was very challenging to detect those interactions.

Why is vΔK1L attenuated during an intranasal or intradermal infections?

Chapter 3 describes how the deletion of *K1L* from VACV results in an attenuated infection during an IN and ID inoculation. Our hypothesis was that a virus lacking *K1L* would be deficient in NF-κB inhibition and subsequently greater infiltration of immune cells will occur, which would lead to a faster viral clearance and decreased pathogenesis. However, in the ID model of infection, the opposite result was observed and infection with vΔK1L resulted in a decrease in NF-κB-controlled gene expression.

I recognize that IN and ID infections are very different, one being a systemic infection and the other a highly localized infection, respectively. Thus, there are several future directions for research with respect to IN infection. First, whether NF-κB inflammatory controlled genes are down or upregulated in lungs of vΔK1L-infected mice as compared to wild-type VACV should be determined. The approach utilized to determine the expression of inflammatory genes during an ID infection was Fluidigm, which allowed for the simultaneous quantification of 24 cellular genes. This same approach can be used again with lung tissues. During ID infection I have observed a

decrease in inflammatory gene expression in vΔK1L-infected ears as compared to wild-type VACV-infected ears. However, during IN infection I expect the opposite; an increase in the gene expression of cytokines and chemokines in vΔK1L-infected lungs, which would result in an increase in immune cell infiltration. These immune cells could promote rapid viral clearance and explain the decreased replication of vΔK1L as compared to wild-type VACV, which is not observed during ID infection. The prediction of an opposite effect during ID and IN models could be supported by K1 employing different antagonistic functions (NF-κB or PKR) in each model.

One limitation of our Fluidigm platform is that it has only monitored the transcription of 24 host genes. One goal is to use RNAseq from infected tissues to obtain a global picture of host responses to virus infection. This information could provide a better understanding of how K1L alters the local environment to support viral replication and spread.

Other NF-κB deletion mutant VACVs, such as ΔK7R, have a different infiltration pattern of immune cells to the lungs and ears as compared to wild-type VACV [2]. It will be beneficial to determine if vΔK1L infection leads to more or less infiltration of immune cells via flow cytometry, which could help to understand why vΔK1L infection results in decreased pathogenesis. During ID infection, I hypothesize that there will be less infiltration of immune cells during vΔK1L as compared to wild-type VACV since there is a decreased expression of chemokines during vΔK1L infection. However, as described above, I expect an increase in immune cells infiltration during IN vΔK1L infection.

Does K1 inhibit NF-κB or PKR activation *in vivo*?

K1 is a known inhibitor of anti-viral immune responses such as PKR and NF-κB in cell culture models of infection. Thus, the decreased in NF-κB-regulated genes during vΔK1L intradermal infection was unexpected. However, it remains unknown if it is K1's role as an NF-κB or PKR antagonist that is responsible for this phenotype. To answer this question, I propose two approaches. The first is to examine NF-κB and PKR activation from infected tissues of mice by either: (i) performing immunoblotting from mice tissues to measure acetylation of NF-κB, an event blocked by K1 in cell culture, (ii) *in vivo* luciferase assay imaging or (iii) *ex vivo* luciferase assays. In addition, immunoblotting could also be employed to measure PKR activation during vΔK1L infection.

Second, mutant K1 proteins from chapter 4 that lack either NF-κB or PKR inhibitory function (or both) could be used to determine which of these two K1 functions is important for VACV pathogenesis. First, the inhibitory phenotype of each mutant for PKR and NF-κB activation should be tested *in vitro*. (In addition, the ability of each mutant to inhibit IFN should be determined as this is another K1 function.) Once each mutant is characterized in cell culture, the pathogenicity of viruses expressing mutant K1 proteins that either inhibited only PKR, only NF-κB, or both PKR and NF-κB, could be compare using both the IN and ID models of infection. The ultimate goal would be to correlate virus virulence with one or more of the K1 antagonistic functions.

Why does VACV encode multiple inhibitors of NF-κB?

It is still elusive why VACV encodes more than 10 inhibitors of NF-κB. Since deletion of any of these inhibitors results in an attenuated virus [1-8], each of them must

play a critical role in VACV pathogenesis. I hypothesize that NF-κB inhibition *in vivo* by each inhibitor occurs in a time-dependent and spatially-specific manner. Once the best approach to measure NF-κB activation *in vivo* is determined, a comparison of NF-κB activation at different times and tissues during infection with VACV mutants lacking one NF-κB inhibitor should be performed. I believe that activation of NF-κB would be observed at different times and at different organs during infection with these viruses. This will shed light into the non-redundancy of these NF-κB inhibitors.

5.3 References

1. Bartlett, N., et al., *The vaccinia virus N1L protein is an intracellular homodimer that promotes virulence.* J Gen Virol, 2002. **83**(Pt 8): p. 1965-76.

2. Benfield, C.T., et al., *Vaccinia virus protein K7 is a virulence factor that alters the acute immune response to infection.* J Gen Virol, 2013. **94**(Pt 7): p. 1647-57.

3. Brandt, T.A. and B.L. Jacobs, *Both carboxy- and amino-terminal domains of the vaccinia virus interferon resistance gene, E3L, are required for pathogenesis in a mouse model.* J Virol, 2001. **75**(2): p. 850-6.

4. Chen, R.A., N. Jacobs, and G.L. Smith, *Vaccinia virus strain Western Reserve protein B14 is an intracellular virulence factor.* J Gen Virol, 2006. **87**(Pt 6): p. 1451-8.

5. Ember, S.W., et al., *Vaccinia virus protein C4 inhibits NF-kappaB activation and promotes virus virulence.* J Gen Virol, 2012. **93**(Pt 10): p. 2098-108.

6. Harte, M.T., et al., *The Poxvirus Protein A52R Targets Toll-like Receptor Signaling Complexes to Suppress Host Defense.* Journal of Experimental Medicine, 2003. **197**(3): p. 343-351.

7. Mansur, D.S., et al., *Poxvirus targeting of E3 ligase beta-TrCP by molecular mimicry: a mechanism to inhibit NF-kappaB activation and promote immune evasion and virulence.* PLoS Pathog, 2013. **9**(2): p. e1003183.

8. Stack, J., et al., *Vaccinia virus protein A46R targets multiple Toll-like-interleukin-1 receptor adaptors and contributes to virulence.* J Exp Med, 2005. **201**(6): p. 1007-18.